Investigations on the mechanism of heat-induced programmed cell death mediated by a MazE-MazF like type II toxin-antitoxin system in the cyanobacterium, *Synechocystis* sp. PCC 6803

Thesis submitted to the University of Hyderabad for the award of Doctor of Philosophy

By
Afshan Srikumar
(Regd. No. 11LTPM07)

Department of Biotechnology & Bioinformatics
School of Life Sciences
University of Hyderabad
Hyderabad - 500046
India
June, 2019

University of Hyderabad
(A Central University established in 1974 by act of parliament)
HYDERABAD – 500 046, INDIA

CERTIFICATE

This is to certify that this thesis entitled **"Investigations on the mechanism of heat-induced programmed cell death mediated by a MazE-MazF like type II toxin-antitoxin system in the cyanobacterium, *Synechocystis* sp. PCC 6803"** submitted to the University of Hyderabad by **Ms. Afshan Srikumar** bearing registration number **11LTPM07** for the degree of Doctor of Philosophy, is based on the studies carried out by her under my supervision.

This thesis is free from plagiarism and has not been submitted earlier in part or in full to this or any other University or Institution for the award of any degree or diploma.

The work in this thesis has been:

A. Published in the following journal:

1. **Afshan S**, Pilla S.K, Dokku S, Kopfmann S, Wolfgang R. Hess, Musti J. Swamy, Sue Lin-Chao, J.S.S. Prakash (2017). The Ssl2245-Sll1130 toxin-antitoxin system mediates heat-induced programmed cell death in *Synechocystis* sp. PCC6803. *J. Biol. Chem*. 292(10) : 4222-4234

B. Presented in the following conferences:

1. Poster presentation at "PRS-2017" International conference on photosynthetic research at the University of Hyderabad, Hyderabad India. (International)
2. Oral presentation at "Bioquest-2017" at University of Hyderabad, Hyderabad India. (National)
3. Oral presentation at "Plastid Preview -2015" at University of Essex, Colchester, UK. (International)

4. Poster presentation at International conference “All India microbiologists association-2015” at JNU, Delhi, India. (International)

Further, the student has passed the following courses towards fulfillment of course work requirement for Integrated M.Sc-Ph.D Biotechnology programme.

Course code	Name	Credits	Grades	Pass/Fail
BT 506	Research Methodology	4	B	Pass
BT 507	Scientific Writing	1	A^+	Pass
BT 508	Laboratory training	4	A	Pass
BT 571	Elective-1 (Gene Therapy)	2	B	Pass
BT 572	Elective-2 (Model Genetic Systems)	2	A^+	Pass

Supervisor | **Head, Department of Biotechnology and Biioinformatics** | **Dean, School of Life Sciences**

University of Hyderabad
(A Central University established in 1974 by act of parliament)
HYDERABAD – 500 046, INDIA

DECLARATION

I, **Afshan Srikumar** hereby declare that the work presented in this thesis entitled **"Investigations on the mechanism of heat-induced programmed cell death mediated by a MazE-MazF like type II toxin-antitoxin system in the cyanobacterium, *Synechocystis* sp. PCC 6803"** submitted by me under the guidance and supervision of **Prof. Jogadhenu S. S. Prakash** is an original and independent research work. I also declare that it has not been submitted previously in part or in full to this University or any other University or Institution for the award of any degree or diploma.

Date:

Afshan Srikumar
(Reg. No. 11LTPM07)

CONTENTS

ACKNOWLEDGEMENTS

It has been a long journey filled with a lot of learning, excitement, disappointments, failures, successes and a heap of emotions along the way, and this work would not have been possible without the involvement of many individuals.

First and foremost, I would like to take this opportunity to thank my supervisor, **Prof. J. S. S. Prakash** for his immense faith in me that helped me carry out this research. It was under his able guidance that I could learn so much and gradually progress in my work. I am ever grateful for the opportunity I got to learn several experiments directly under his expertise. He has always been a source of encouragement and support when things did not work out well and was highly appreciative of the progress in my work. He always created a positive environment that helped me give my best that made me what I am today in this field. I will always be indebted to him for making this journey smooth. It is his knowledge and critical assessment that has helped me in shaping my thesis.

I am also grateful to my doctoral committee members, **Prof. Appa Rao Podile** and **Dr. N. Prakash Prabhu** for their suggestions and critical assessment throughout my PhD tenure. I also thank the present and former Deans of School of Life Sciences, **Prof. S. Dayananda**, **Prof. K. V. A. Ramaiah**, **Prof. Pallu Reddanna**, **Prof. A.S. Raghavendra**, **Prof. R.P. Sharma**, **Prof. Aparna Dutta Gupta** and **Prof. M. Ramanadham** and the present and former Heads of Department of Biotechnology and Bioinformatics, **Prof. K. P. M. S. V. Padmashree**, **Prof. J. S. S. Prakash**, **Prof. A.K. Kondapi**, **Prof. Niyaz Ahmed** and **Prof. P. Prakash Babu** for allowing me to use the facilities of the School and the Department.

I thank **Prof. M. J. Swamy**, School of Chemistry and **Prof. Surajit Dhara**, School of Physics for letting me use their facilities and **Mrs. Leena Bhashyam**, Genomics facility, School of Life Sciences for helping me with Microarray experiments.

I express my gratitude to **Prof. Wolfgang Hess**, **Prof. Sue-lin Chao**, **Prof. Iwane Suzuki**, **Prof. M.J. Swamy** and **Prof. Surajit Dhara** for their scientific discussions and valuable suggestions.

I am also grateful to **Dr. Sankara Krishna**, **Dr. Sivarama Krishna**, **Mr. Tejaswi Naidu** , **Dr. Kiran Kumar**, **Dr. Stefan Kopfman** and **Mr. Harish** for helping me in my research work.

I thank the non-teaching staff of Department of Biotechnology, **Mr. Rajsekhar**, **Mr. Rahul**, **Mr. Murali** and **Mr. Sekhar** for helping me with all the official work during my PhD tenure.

I sincerely acknowledge the infrastructural support provided by **UGC-SAP**, **DST-FIST**, **DBT-CREBB**, to the Department of Biotechnology and Bioinformatics as well as the **CSIR** and **DBT**, Govt. of India for the research fellowship.

This journey would not have been fun without my lovely lab mates with whom there are a lot of memories associated. Our lab, **S-53** was almost like our second home, where we spent most of the time all through these years. My heartfelt thanks to all my seniors and friends in the lab, **Dr. Sankarakrishna, Dr. Mahalaxmi, Dr. Subhashini, Dr. Bhavani, Dr. Arun, Mrs. Radharani, Mr. Deepak, Lingaswamy Bantu, Jahnabi, Pankaj, Suraj, Shruti, Somasekhar, Harish, Vignan, Ranjana, Anamya, Shubhangi** and **Ramana Murthy** for their support, which meant a lot to me. I would also like to mention the project students, **Ganesh, Drishti,** and **Neelima,** who worked with me and helped me. I am also thankful to the lab attenders, **Sridhar** and **Manohar** without whom our lab work would never have run smoothly.

Words would never suffice to describe the amount of gratitude and love towards my parents**, Dr. P. S. Srikumar** and **Dr. Shakila Srikumar,** for being the strongest pillars of support all through my life. It is their constant effort, guidance and sacrifices that have led me to this stage in life. It is their inculcation of the value of education and constant assurance that life would be better, kept me going whenever I felt like quitting. I would never be able to thank them enough**.**

A special thanks to my special one, my husband, **Sandeep Kunder** who has closely seen all my highs and lows, celebrated my successes, listened to all my frustrations and helped me get through all my bad situations. Thank you for always being there. I also thank my in-laws for being the most supportive and understanding people throughout my work**.**

Leaving the best to the last, my little baby girl, **Ayra**, who has been the most co-operative baby while I was writing my thesis. Though challenging, her sparkling smile made it all worth it. God has been kind to me with his immense blessings for which I would forever be grateful. Ending this journey here, with the hope of a beautiful future ahead….

To all my family members and friends who constantly asked me “When would you be done with your PhD?” Here comes my answer…..

Afshan Srikumar

Dedicated to my parents and my little one, Ayra……..

LIST OF ABBREVIATIONS

µg	:	microgram
µM	:	micromolar
°C	:	degree centigrade/degree Celsius
AFM	:	Atomic force microscopy
ATP	:	Adenosine triphosphate
Bp	:	base pair (bp)
BSA	:	bovine serum albumin
CD	:	circular dichroism
cDNA	:	complementary DNA
CRISPR	:	Clustered regularly interspersed short palindromic repeats
DEPC	:	diethylpyrocarbonate
DNA	:	deoxy ribonucleic acid
dNTPs	:	deoxy nucleotide triphosphates
DSC	:	Differential scanning microscopy
DTT	:	dithiothreitol
EDF	:	extracellular death factors
EDTA	:	ethylene diamine tetra acetic acid
EF-Tu	:	Elongation factor Tu
g	:	gram
GltX	:	Glutamyl tRNA synthetase
GTP	:	Guanosine triphosphate
h	:	hour(s)
Hepes	:	4-(2-Hydroxyethyl)piperazine-1-ethanesulfonic acid sodium salt, N-(2- Hydroxyethyl) piperazine-N′-(2-ethanesulfonic acid) sodium salt
IgG	:	immunoglobulin G
IPTG	:	isopropyl β-D-thiogalactoside
ITC	:	Isothermal titration calorimetry
kb	:	kilobase pair
kDa	:	kilodalton
L	:	litre
LB	:	Luria-Bertani
M	:	molar
Mb	:	Mega base pair
mg	:	milligram
min	:	minute
ml	:	milliliter
mM	:	millimolar
Ni-NTA	:	nickel-nitroacetic acid agarose
nm	:	nanometers

N-terminal	:	amino terminal
OD	:	optical density
ORF	:	open reading frame
PAGE	:	polyacrylamide gel electrophoresis
PCD	:	programmed cell death
PCR	:	polymerase chain reaction
PMSF	:	phenylmethylsulfonylfluoride
PSK	:	post segregational killing
qRT-PCR	:	quantitative real time PCR
RNA	:	ribonucleic acid
rpm	:	revolutions per minute
RT-PCR	:	reverse transcriptase-polymerase chain reaction
SDS	:	sodium dodecyl sulphate
s	:	seconds
TA	:	toxin-antitoxin
TE	:	Tris-EDTA
Tris	:	tris-(Hydroxymethyl) aminoethane
UNAG	:	Uridine diphosphate-N-acetylglucosamine
V	:	volts

LIST OF FIGURES

LIST OF TABLES

1. INTRODUCTION

1.1 Toxin-Antitoxin (TA) systems

TA systems have been identified as small genetic elements, generally organised as a dicistronic operon, consisting of an antitoxin gene preceeding the toxin gene in most of the cases and have been reported to be present in bacteria as well as in archaea. These genes encode a stable toxin and a comparatively labile or less stable antitoxin, which can either be a protein or RNA. The antitoxin binds to the toxin, forming a TA complex where it neutralizes the function of the toxin (Gerdes *et al*, 2005). Being labile, in order to neutralize the toxin, the antitoxin has to be continuously expressed in the cell, but under various stress conditions the antitoxin has been reported to be degraded by proteolysis and / or regulated at its transcription level (Christensen *et al*, 2001, 2003; Vogel *et al*, 2004). This change in the levels of the antitoxin, frees the toxin from the TA complex and the free toxin thus exerts its inhibitory effect on various essential cellular metabolic pathways, ultimately leading to the death of the cell or causing a bacterial growth arrest (Figure 1.1).

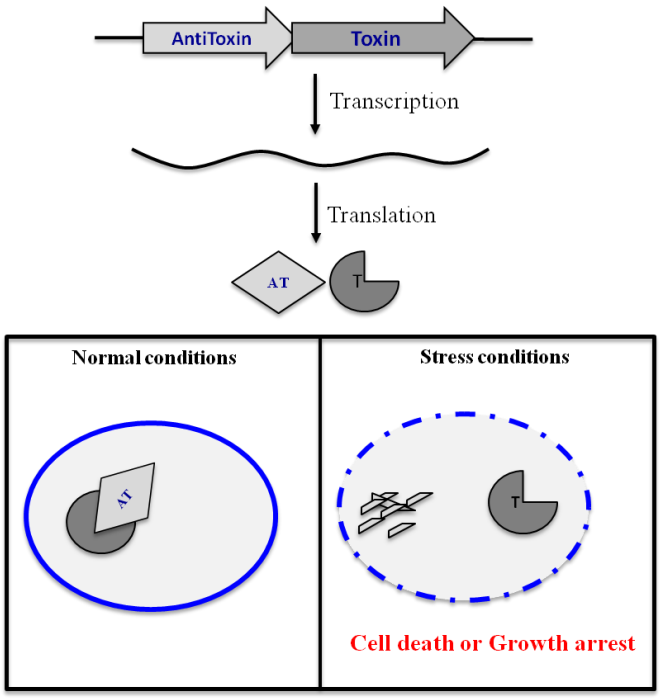

Figure 1.1. Action of TA systems under different conditions. Under normal conditions, the antitoxin binds to the toxin and masks its function, allowing the bacterial cell to grow. However, upon exposure to stress conditions, the labile antitoxin is degraded faster leaving the toxin to function, thereby leading to cell death or growth inhibition.

TA systems were initially identified on bacterial plasmids with a main function of maintaining the plasmid by being involved in the death of the daughter cells that failed to receive a plasmid copy containing the TA operon during cell division (Jaffe *et al*, 1985; Gerdes *et al*, 1986). This precise mechanism of maintaining only the daughter cells that have received the plasmid and eliminating the ones that failed to receive them was carried out by TA systems through a process termed as post-segregational killing (PSK) (Figure 1.2). The first TA system discovered was the *ccdAB* operon (denoting 'coupled cell division') on the *E. coli* mini-F plasmid. This TA system consisted of the CcdB toxin and the CcdA antitoxin proteins. If the plasmid containing this TA operon is lost in the course of segregation during cell division, the toxin:antitoxin complex stoichiometry undergoes a change due to degradation of the labile antitoxin protein, thereby freeing the CcdB toxin from the complex.

This results in execution of function of the CcdB toxin that is involved in targeting cellular replication by poisioning of DNA gyrase, thereby leading to the elimination of daughter cells that failed to receive the plasmid, whose effect is otherwise counteracted by the antitoxin CcdA while in the complex state (Figure 1.2) (Ogura & Hiraga, 1983; Hayes, 2003). Thereafter, the TA systems were termed as 'addiction modules', based on their function to 'addict' the bacterial cells to the TA system, as it's loss was observed to ultimately result in PSK (Gerdes *et al*, 1986; Engelberg-Kulka, 1999) . Later on, homologs of these TA systems were found to be located even on the chromosome in *E. coli* (Masuda *et al*, 1993). Chromosomal TA systems were then identified in several bacterial species, especially found to be abundantly present in bacteria living in changing environments. These TA systems thereby have been proposed to function in helping the bacteria survive under various stress conditions, suggesting their broader roles other than just plasmid maintenance (Gerdes, 2000; Hayes, 2003).

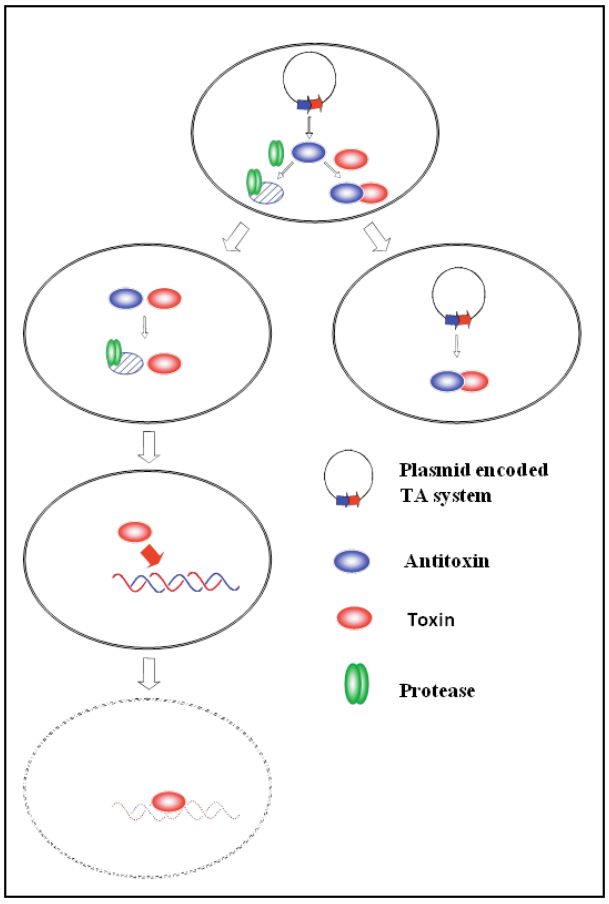

Figure 1.2. TA system in post-segregational killing and plasmid maintenance. After cell division, the daughter cell inheriting the plasmid encoding the TA system is sustained due to the inhibition of the toxin function by the antitoxin. When the daughter cell fails to receive the plasmid encoding the TA system, the labile antitoxin, unable to replenish itself is degraded faster, freeing the toxin. The free toxin results in the death and elimination of the plasmid-free daughter cell (Hayes, 2003).

1.2 Classification of TA systems

The functional antitoxin in the cell can either be RNA or a protein but the toxin is always a protein and based on the mechanism by which toxin neutralization is carried out by the antitoxin, TA systems have been classified into five different types.

1.2.1 Type I TA systems

In this class of TA system, the antitoxin is a small non-coding RNA (sRNA). This antitoxin sRNA is complimentary to the mRNA of the toxin. In most of the cases, the toxin and antitoxin genes of this type of TA system are encoded on opposite strands of DNA. The

antitoxin sRNA binds to the toxin RNA and leads to inhibition of the toxin translation by blocking the Shine-Dalgarno sequence or leads to the degradation of the toxin mRNA via RNase III (Figure 1.3A) (Brielle *et al*, 2016; Brantl & Jahn, 2015). The type I toxin proteins are generally small polypeptides of length >60 amino acids, consisting mostly of hydrophobic peptides and are reported to function by disrupting the bacterial membrane integrity leading to disruption of ATP synthesis and ultimately causing death of the cell (Unoson & Wagner, 2008). One of the well characterized examples of the this TA system is the hok/sok locus discovered on the plasmid R1 (Gerdes *et al*, 1990). This TA locus encodes the Hok (***ho***st ***k***illing) toxin protein and the *sok* (***s***uppression ***o***f ***k***illing) antisense RNA. The Hok toxin is reported to cause irreversible damage to the cell membrane, causing cell death. The function of this toxin is inhibited by the complimentary binding of the *sok* antisense RNA to the *hok* mRNA, thereby preventing its translation. Several other chromosomal type I TA systems were later identified like the tisB/IstR1, shoB/OhsC, symE/SymR and ibs/Sib loci in *E. coli* (Kawano, 2012; Fozo, 2012).

1.2.2 Type II TA systems

In this class of TA system, the antitoxin is a small unstable protein. The toxin-antitoxin proteins in this system are expressed separately from the same operon, where the first gene is the antitoxin, which is followed by the toxin gene with both the genes having at least a few base pairs of overlap at the start and stop codons in almost all of the cases except in the *higBA* operon, where the genes are reversed in order (Gerdes *et al*, 2005). The antitoxin protein forms a complex with the toxin protein, where the antitoxin blocks the catalytic site of the toxin, masking its toxin function under normal conditions. Due to this complex formation, the cells grow normally (Figure 1.3B). The TA protein complex or the antitoxin alone have been reported to act as transcriptional repressors, autoregulating the transcription of their operon by binding to their promoter (Bukowski *et al*, 2011). Upon

exposure to cellular stresses such as amino acid starvation or antibiotic pressure, the transcription of this TA operon has been studied to be repressed, and the antitoxin protein being unstable is degraded by proteases that are stress-induced, like Lon or ClpXP, freeing the toxin from the TA complex, allowing it to exhibit it's toxic function (Sat *et al*, 2001; Hazan *et al*, 2004). The toxins of this TA system have different cellular targets such as DNA gyrase, cellular mRNA, translating ribosomes etc. Some of the well studied examples of this TA system are the *ccdAB*, *mazEF*, *higBA* and *relBE* loci (Bernard & Couturier, 1992; Zhang *et al*, 2003b; Van Melderen & De Bast, 2009).

1.2.3 Type III TA systems

In this class of TA system, the antitoxin is an RNA that binds to the toxin protein, inhibiting the function of the toxin (Figure 1.3C). In the locus arrangement of this TA system, a short palindromic repeat is present in the upstream region of the toxin gene, which forms a transcriptional terminator that can control the relative levels of the toxin and antitoxin RNA and this repeat sequence also consists an upstream tandem array of nucleotide repeats (Fineran *et al*, 2009). The type III toxins function as endoribonucleases that are involved in the antitoxin precursor processing into small RNAs and also in cleaving of several host RNAs. The first type III TA system identified was the *toxIN* locus, located on the plasmid pECA1039 of *Pectobacterium atrosepticum.* ToxN is the toxin protein and ToxI is the antitoxin RNA which consists of repeat sequences of a 36-nucleotide motif (Fineran *et al*, 2009). The ToxIN complex formed consists of three ToxN proteins and three RNA psuedoknots of the ToxI antitoxin, making a hetero-hexameric triangular structure (Blower *et al*, 2011). Another characterized example is the *antiQ-abiQ* locus, located on the plasmid of *Lactococcus lactis* which was found to be similar to the ToxIN TA system both structurally and functionally (Samson *et al*, 2013).

1.2.4 Type IV TA systems

In this type of TA system, the antitoxin is a protein that competes with the toxin protein in binding to the cellular targets of the toxin, thereby indirectly interfering with the binding of the toxin to its targets, inhibiting its ability to function (Figure 1.3D). An example of this TA system is the *yeeUV* locus in *E. coli* that encodes the YeeU antitoxin and the YeeV toxin proteins. The YeeV toxin protein is reported to bind to the bacterial cytoskeletal proteins MreB and FtsZ, blocking their polymerization, thereby leading to growth inhibition. The YeeU antitoxin protein competes with YeeV in binding to MreB and FtsZ, stabilizing and promoting their polymerization (Masuda *et al*, 2012).

1.2.5 Type V TA systems

In this type of TA system, the antitoxin is a protein that cleaves the toxin mRNA, preventing its translation, thereby inhibiting its function (Figure 1.3E). An example of this TA system is the *ghoST* locus in *E. coli* that encodes the GhoS antitoxin protein that cleaves the mRNA of the *ghoT* toxin specifically at the AU rich sites. The GhoT toxin protein was reported to function in damaging the cell membrane, thereby forming ghost cells, which are lysed cells with damaged membranes (Wang *et al*, 2012). It has been studied that under stress conditions, MqsR, a type II toxin has a function in cleaving the *ghoS* antitoxin mRNA, allowing the translation of the GhoT toxin mRNA (Wang *et al*, 2013).

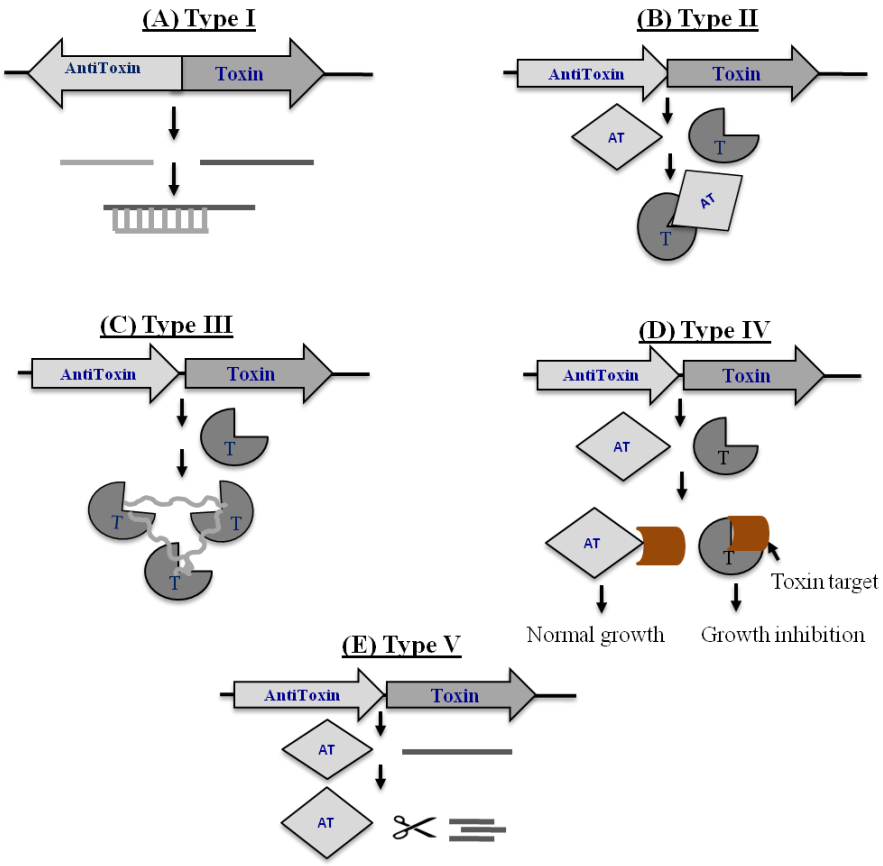

Figure 1.3. Schematic representation of the different types of TA systems. **(A)** In type I TA systems, the antitoxin is a non-coding RNA (—) that is complementary to the mRNA of the toxin (▬), which binds to the toxin mRNA, preventing its translation, thereby allowing the growth of the cell. **(B)** In type II TA systems, the antitoxin protein (◇) binds to and inhibits the function of the toxin protein (◔), allowing the cell to grow normally. **(C)** In type III TA systems, the antitoxin RNA (〰) binds to and masks the function of the toxin protein (◔), allowing cell growth. **(D)** In type IV TA systems, the antitoxin protein (◇) binds to the toxin targets (▬), protecting them from degradation by the toxin protein (◔), thereby letting the cell grow normally. **(E)** In type V TA systems, the antitoxin protein (◇) binds to and degrades the toxin mRNA (▬), thereby preventing its translation and allows normal cell growth.

1.3 Classification of TA families based on the toxin cellular targets

Among the five classified types of TA systems mentioned above, the type II TA systems are the most highly abundant and well characterized. The type II toxins have been classified into the following nine TA families depending on the toxin sequence similarity and the type of their cellular target: CcdAB, RelBE, MazEF, ParDE, HigBA, HipAB, Phd/doc, VapBC and ω-ε-ξ (Van Melderen & De Bast, 2009).

1.3.1 CcdAB TA family

This was the first TA system identified on the mini F plasmid of *E. coli* that is involved in PSK and plasmid maintenance as discussed previously. The *ccd* locus consists of the *ccdA* and *ccdB* genes that code for the CcdA antitoxin and CcdB toxin proteins respectively. The CcdA antitoxin binds to and inhibits the function of the CcdB toxin by forming a hetero-tetramer, consisting of 2 units of CcdA and 2 units of CcdB proteins respectively (Maki *et al*, 1996). The CcdB toxin has been reported to be involved in inhibiting cellular DNA replication by inhibiting DNA gyrase, thereby preventing cell division (Critchlow *et al*, 1997). DNA gyrase therefore became the first identified target of toxins (Bernard & Couturier, 1992). The Tryptophan99 residue of the CcdB toxin has been reported to interact with the Arginine462 residue of the GyrA subunit of DNA gyrase, trapping it in a cleavable complex, eventually leading to the inhibition of DNA replication in the cell (Dao-Thi *et al*, 2005).

1.3.2 RelBE TA family

The *relBE* locus was first identified in the *E. coli* K-12 strain and consists of the relB and relE genes that encode the RelB antitoxin and RelE toxin proteins respectively, where RelB binds to and masks the function of the RelE toxin (Gotfredsen & Gerdes, 1998). The RelB and RelE proteins form a V-shaped hetero-tetrameric non-toxic complex, consisting of 2 units of the RelB antitoxin and 2 units of the RelE toxin proteins respectively (Boggild *et al*, 2012). The RelE toxin is reported to function as a ribosome-dependent endoribonuclease that blocks cellular translation by associating with the ribosomes (Galvani *et al*, 2001). The mechanism of inhibition of cellular translation by RelE involves the binding of RelE to the ribosomal A site and cleavage of the mRNAs between the second and third site in the codon (Neubauer *et al*, 2009; Pedersen *et al*, 2003).

1.3.3 MazEF TA Family

The *mazEF* locus consists of the *mazE* gene upstream of the *mazF* gene and encodes the MazE antitoxin and MazF toxin proteins respectively. The MazE antitoxin binds to and inhibits the function of the MazF toxin (Aizenman *et al*, 1996). The MazE and MazF proteins form a hetero-hexameric complex, consisting of a MazE dimer that is packed between two MazF dimers (Kamada *et al*, 2003). MazF functions as a ribosome-independent endoribonuclease that catalyzes site-specific cleavage of mRNAs, leading to translation inhibition (Christensen *et al*, 2003; Zhang *et al*, 2003b; Muñoz-Gómez *et al*, 2004). It cleaves the mRNAs at the ACA sites and specifically at the 5' side of the residue A (Zhang *et al*, 2005).

1.3.4 ParDE TA family

The *parDE* locus (denoting '*par*titioning') was first identified on the broad host range and low copy number plasmid, RP4/pRK2, specifically in a lot of gram-negative bacteria, later found even on bacterial chromosomes (Roberts & Helinski, 1992). This locus encodes the ParD antitoxin and the ParE toxin proteins where ParD binds to and forms a non-toxic complex with ParE. This non-toxic complex is reported to consist of a dimer of parD which binds to a dimer of ParE, forming a hetero-tetramer (Johnson *et al*, 1996). This TA locus is involved in plasmid maintenance by leading to PSK in the plasmid-free cells. It was earlier reported that the ParE toxin was involved in extensive cell filamentation but its exact target was later identified as DNA gyrase, where it has been studied to inhibit the function of DNA gyrase, leading to blocking of cellular DNA replication (Roberts *et al*, 1994; Jiang *et al*, 2002).

1.3.5 HigBA TA family

The *higBA* locus (denoting '*h*ost *i*nhibition of *g*rowth') was identified on the kanamycin resistance conferring plasmid, Rts1 of *Proteus vulgaris,* and was reported to be involved in PSK at high temperatures of 42ºC (Terawaki, Y., Kakizawa, Y., Takayasu, H., and Yoshikawa, 1968). The operon organisation of this locus is the only exception from the remaining type II TA systems, in that the toxin gene *higB* is arranged upstream of the antitoxin gene *higA* (Tian *et al*, 1996). Under normal conditions, the HigA antitoxin and HigB toxin proteins form a non-toxic complex, where the HigA antitoxin inhibits the function of the HigB toxin. This non-toxic complex has been reported to consist of a dimer of HigA sandwiched between two HigB monomers, forming a hetero-tetramer (Schureck *et al*, 2014). HigB toxin has been reported to target cellular translation by degrading mRNA in a ribosome-depended manner, preferentially recognizing and cleaving the 5'-AAA-3' codon, though codons with a single adenosine residue were also reported to be enough for cleavage by HigB (Hurley & Woychik, 2009).

1.3.6 HipBA TA family

The *hipBA* locus (denoting '*hi*gh *p*ersistence') was identified on the chromosome of *E. coli* K12 strain that encodes the HipB antitoxin and HipA toxin proteins, that bind to each other and form a non-toxic complex under normal conditions, where HipB inhibits the function of HipA (Moyed & Broderick, 1986). The non-toxic complex is reported to consists of HipB and HipA proteins in the ratio of 1:1 (Black *et al*, 1994). The HipA toxin is peculiarly larger than remaining toxin proteins consisting of 440 amino acid residues (Black *et al*, 1991). This locus has been studied to have a major function involving increased persistence of bacteria exposed to antibiotics (Falla & Chopra, 1998). Initially, the HipA toxin was reported to function as a kinase, involved in phosphorylation of the Elongation factor Tu (EF-Tu) leading to translational inhibition and growth arrest (Schumacher *et al*,

2009). Later, the main cellular target of HipA toxin was reported as Glutamyl-tRNA synthetase (GltX) that was phosphorylated at the Serine239 instead of EF-Tu (Germain *et al*, 2013).

1.3.7 Phd/Doc TA family

The *phd/doc* locus (denoting '*p*revent *h*ost *d*eath-*d*eath *o*n *c*uring') was first identified on the *E. coli* plasmidic bacteriophage P1, with a main function associated with plasmid maintenance via lysogeny (Lehnherr *et al*, 1993). This locus encodes the Phd antitoxin and the Doc toxin proteins, where the Phd antitoxin binds to and masks the function of Doc toxin forming a trimeric complex consisting of two units of the Phd antitoxin proteins and one unit of the Doc toxin protein (Garcia-Pino *et al*, 2008; Gazit & Sauer, 1999). The Doc toxin has been reported to function as a kinase, involved in targeting the EF-Tu by phophorylating it at the Threonine382 position, obstructing its binding to the aminoacylated tRNA, ultimately leading to cellular translation inhibition (Castro-Roa *et al*, 2013; Cruz *et al*, 2014).

1.3.8 VapBC TA family

The vapBC locus (denoting '*v*irulence *a*ssociated *p*rotein') was first identified on the virulence plasmid of *Salmonella dublin*. This locus encodes the VapB antitoxin and the VapC toxin proteins, where the VapB antitoxin binds to and inhibits the function of the VapC toxin (Pullinger & Lax, 1992). These proteins have been reported to form mostly a hetero-tetrameric complex, consisting of two units of VapB and two units of VapC in bacteria such as *Mycobacterium tuberculosis* or a hetero-octameric complex, consisting of four units of VapB and four units of VapC proteins in bacteria such as *S. flexneri* (Miallau *et al*, 2009; Dienemann *et al*, 2011). The VapC toxin has a conserved PIN-domain (PilT N-terminal domain) and PIN-domain proteins are studied to have a function in RNA decay, ribosome biogenesis and RNA interference (Anantharaman & Aravind, 2003; Clissold & Ponting, 2000). The VapC toxins from the virulence plasmid pMYSH600 of *Shigella flexneri* 2a and

Salmonella enteric have been reported to function in cleaving the initiator tRNA, $tRNA^{fMet}$ in the anticodon stem-loop, thereby leading to cellular translational inhibition (Winther & Gerdes, 2011).

1.3.9 Omega-epsilon-zeta (ω-ε-ζ) TA family

The ω-ε-ξ TA locus was first identified on the pSM19035 plasmid of *Streptococcal pyogenes* with a function on plasmid maintenance through PSK (Zielenkiewicz & Cegłowski, 2005). This was the first and only TA system identified to consist of three components instead of two. This locus encodes the ε antitoxin and ξ toxin proteins where the ε antitoxin binds to and inhibits the function of the ξ toxin by blocking its ATP/GTP binding site by forming a hetero-tertrameric complex, consisting of two units of the ε antitoxin and two units of the ξ toxin proteins (Meinhart *et al*, 2003). The additional protein encoded by this locus is the ω protein that is studied to function as an auto-repressor, negatively regulating the transcription of the two promoters (*P*ω and *P*ε) of this operon (de la Hoz *et al*, 2000). The ζ toxin is reported to function as a kinase, phosphorylating the precursor of cell wall synthesis in bacteria, uridine diphosphate-N-acetylglucosamine (UNAG), leading to the formation of the inactive UNAG-3P and ultimately leading to the bacterial cell death or growth inhibition (Mutschler *et al*, 2011).

Table 1.1: Different Type II TA families

TA family	Antitoxin	Toxin	Non-toxic TA complex	Toxin Function	Cellular process targeted
CcdAB	CcdA	CcdB	$(CcdA)_2$-$(CcdB)_2$	Inhibition of DNA gyrase	DNA replication
RelBE	RelB	RelE	$(RelB)_2$-$(RelE)_2$	Ribosome-dependent endorbionuclease (cleavage of mRNA)	Translation
MazEF	MazE	MazF	$(MazF)_2$-$(MazE)_2$-$(MazF)_2$	Ribosome-dependent endorbionuclease (cleavage of mRNA, 16S rRNA, 23S RNA)	Translation
ParDE	ParD	ParE	$(ParD)_2$-$(ParE)_2$	Inhibition of DNA gyrase	DNA replication
HigBA	HigA	HigB	$(HigA)_2$-$(HigB)_2$	Ribosome-dependent endorbionuclease (cleavage of mRNA)	Translation
HipBA	HipB	HipA	HipB-HipA	Phosphorylation of GltX	Translation
Phd/Doc	Phd	Doc	$(Phd)_2$-$(Doc)_2$	Phosphorylation of EF-Tu	Translation
VapBC	VapB	VapC	$(VapB)_2$-$(VapC)_2$ / $(VapB)_4$-$(VapC)_4$	Cleavage of $tRNA^{fMet}$	Translation
ω-ε-ζ	ε	ζ	$(\varepsilon)_2$-$(\zeta)_2$	Phosphorylation of UNAG	Poisoning of Cell wall synthesis

Table 1.1. Different Type II TA families with different functions and cellular targets of their respective toxins were compiled. The components of the non-toxic TA complex of each of the TA families have also been denoted.

1.4 Biological functions and benefits of TA systems to bacteria

So far, we have seen how different TA systems are involved in mediating the growth inhibition or death of the cells. But, apart from being beneficial in maintaining the plasmids in the bacterial cells by PSK during cell division, what other benefits can these small genetic modules that are located on the chromosomes, provide the bacteria? We know that bacteria are constantly exposed to various kinds of changes in their surroundings and most of the times, these changes can be a threat to the survival and existence of the bacterial community.

Some of the different biotic or abiotic stresses they are exposed to include: heat, cold, nutrient deprivation, oxidative stress, antibiotic pressure, extreme pH, phage invasion etc. It is interesting to see that several TA systems have been studied to be involved in responses against most of these stresses.

1.4.1 TA systems in stress responses

Among the various types of TA systems described so far, the toxins belonging to the most abundant type II TA systems such as RelE and MazF, functioning as endoribonucleases that cleave mRNAs, have been reported to be activated upon exposure to various abiotic stress conditions such as amino acid starvation, treatment with antibiotics, thymine starvation, oxidative stress, DNA damage and heat (Christensen-Dalsgaard *et al*, 2010; Hazan *et al*, 2004; Sat *et al*, 2003). Apart from these, another toxin endoribonuclease, *yafNO* identified in *E.coli*, has been studied to be function during mitomycin C treatment, thereby suggesting that TA systems are activated in different ways upon different stress exposures (Christensen-Dalsgaard *et al*, 2010). To cope with these conditions, the microorganisms have evolved with various acclimative and adaptive mechanisms at the cellular level. The short term acclimative mechanisms make them tolerant to the stress, letting them survive until the return of favorable conditions. One such acclimative response is the ability of microorganisms to alternate from unicellular to multicellular organization, like microbial colonies, aggregates and biofilms when required (Claessen *et al*, 2014; Johnson, 2008).

1.4.2 TA systems in biofilm formation

It has been studied that most bacteria have the capacity of 'multicellular-like' behavior instead of existing as individual organisms when necessary, adhering to either biotic or abiotic surfaces upon formation of an extracellular matrix surrounding them, thereby forming a biofilm (Stewart & Franklin, 2008). We know that bacteria can communicate with each other though quorum sensing (QS), and utilizing this process, bacteria can modulate and

synchronize their gene expression as a response to change in their cell density; thereby giving bacteria the ability to behave as multicellular organisms (Figure 1.4i) (Ng & Bassler, 2009). This capacity has been demonstrated to be a strategy adapted by the bacterial population as a whole, to evade stress conditions such as host defense responses in pathogenic bacteria such as *Pseudomonas* (Rybtke *et al*, 2011). TA systems have been reported to be involved in these stress-responsive biofilm formations. The *mqsRA* TA system was the first to be reported to have a role in inducing biofilm formation in *E. coli* (Ren *et al*, 2004). Apart from this, the involvement of five other TA systems (*mazEF*, *yoeB/yoeM*, *relBE*, *chpB* and *yafQ/dinJ*) in biofilm formation was also reported. The deletion of these five TA systems was shown to decrease biofilm formation up to 8 h, followed by a gradual increase after 24 h. These TA loci were also found to work in correlation with YjgK protein, as a deletion in these loci showed a significant upregulation in expression of a single gene, *yjgK* (Kim *et al*, 2009). Within these biofilms, as a survival strategy, a part of the bacterial population is programmed to die and the remaining cells (persisters) can strive till the return of favorable conditions.

1.4.3 TA systems in PCD

The importance of mechanisms of PCD such as autophagy and apoptosis in multicellular eukaryotes have been well understood but the need for PCD in single-celled prokaryotes has still been a debate for quite some time. Recently, several studies have proved the benefits of PCD under stress conditions in several bacterial species such as *E. coli*, *Staphylococcus*, *Bacillus*, *Mycobacterium* and *Pseudomonas* (Engelberg-Kulka *et al*, 2006). PCD in bacteria is a population phenomenon, where a sub-population of cells are programmed to die, mediated by the TA systems (Figure 1.4ii). Within the multicellular-like organization of bacteria such as biofilms, PCD might be involved in mediating several functions such as: i) formation of channels for ease of transportation of nutrients and waste to and from the cells that are deeply located within the biofilm; ii) release of material that can

be utilized in the formation of the extracellular matrix for structuring the biofilm; and iii) allowing the surviving cells to disperse from the biofilm containment when required (West *et al*, 2007; Kim *et al*, 2009). A type II TA system, *mazEF* has been well characterized and observed to be involved in mediating PCD in correlation with the levels of guanosine 3' 5'-bispyrophosphate (ppGpp) under several stress conditions, especially during nutrient starvation (Aizenman *et al*, 1996; Sat *et al*, 2003; Hazan *et al*, 2004). The PCD which is reported to be induced upon treatment with rifampicin only in dense cultures but not in cultures at low cell densities was observed to be eliminated on deletion of this TA locus (Kolodkin-Gal *et al*, 2007).

Though the solid evidences supporting the benefits of PCD in bacteria could not yet be ascertained, the Engelberg-Kulka group proposed 3 possible functions of bacterial PCD. The first function being that the cells programmed to die might be a food source for the surviving cells (persisters) till the return of favorable conditions, thereby sustaining the bacterial population (Engelberg-Kulka & Glaser 1999). Secondly, PCD might function as a defense mechanism by inhibiting the spread of phage infection (Hazan & Engelberg-Kulka, 2004). The third function of PCD could be to maintain the stability of the genome by removing mutations or deficient cells from the bacterial population (Engelberg-Kulka *et al*, 2004).

1.4.4 TA systems in persistence

Within a bacterial population, that behaves as a multicellular organism under stress conditions, as we have studied that a sub-population of cells are programmed to die by induction of PCD mediated by TA systems, the remaining cells called persisters are supported to survive till the return of favorable conditions (Figure 1.4iv). The persisters are generally defined as a sub-population of cells reported to survive antibiotic treatments by entering a state of dormancy that is transient (Balaban *et al*, 2004; Lewis, 2010; Balaban,

2011; Brauner *et al*, 2016). The first TA system reported to be involved in inducing persister formation, was the *hipBA* TA system in *E. coli*. A mutant version of the toxin, HipA7 was observed to have increased the persister count by 1000-10,000 fold upon treatment with ampicillin (Moyed & Bertrand, 1983). Deletion of another toxin, MqsR in *E. coli* was also demonstrated to have lowered the level of persister formation upon ampicillin treatment (Kim & Wood, 2010). Apart from these observations, consecutive deletions of 10 endoribonucleolytic TA systems were demonstrated to lower the level of persisters gradually (Maisonneuve *et al*, 2011). Persister formation in *E. coli* was recently proposed to be caused by TA systems whose activity is controlled by (p)ppGpp (Maisonneuve *et al*, 2013). Under this study, upon treatment with antibiotics, RelA and SpoT, the (p)ppGpp synthetases were observed to be functional, leading to the accumulation of (p)ppGpp, which thereby inhibited the exopolyphosphatase that degrades inorganic phosphate. Therefore, the increased level of inorganic polyphosphate activates the Lon proteases that degrades the antitoxins, causing the respective toxin to become free to function and lead to a reversible growth inhibition, thereby inducing persistence (Maisonneuve *et al*, 2013).

1.4.5 TA systems and Extracellular death factors (EDF)

Upon exposure to stress, within the multicellular organization of bacteria, we have so far studied how a sub-population undergoes PCD and aid the survival of the persister cells that are metabolically slow or inhibited until the return of favorable conditions. But, it is interesting to study how the bacterial cells within a population decide which of the cells are supposed to die and which of them should enter the transient growth inhibition phase. This led to the discovery of the production of a quorum-sensing linear pentapeptide, Asn-Asn-Tro-Asn-Asn, named as EDF (Kolodkin-Gal *et al*, 2008). Upon sensing high cell density, the bacterial cells within a multicellular aggregate, secrete the EDF pentapeptides into their surroundings (Figure 1.4ii). EDF then bind to a sub-population of cells, tagging them for

death, while the remaining cells become the persisters (Figure 1.4iii). EDF was reported to compete with the MazE antitoxin from the MazE-MazF complex in *E. coli*, leading to enhancing the endoribonuclease activity of the MazF toxin (Belitsky *et al*, 2011). Upon activation, the MazEF TA system has been reported to cause selective synthesis of two groups of small proteins: i) 'dead proteins' that lead to the death of the cells, and ii) 'survival proteins' that lead to the survival of the cells by inducing a state of growth arrest in them. The EDF probably works in correlation with the *mazEF* TA system to decide the synthesis of either the dead or survival proteins, differentiating which sub-population should undergo death and which of the cells in the population become the persisters. Apart from *E. coli*, EDF were also isolated from other bacterial species such as *Pseudomonas aeruginosa* and *Bacillus subtillis* (Kumar *et al*, 2013).

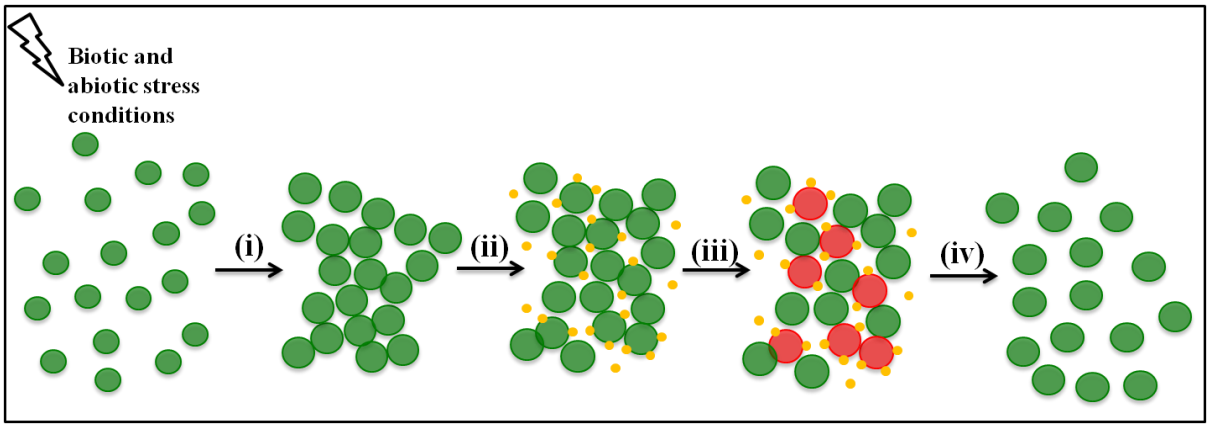

Figure 1.4: Survival strategy of bacterial population during stress conditions. **(i)** Upon exposure to stress (biotic and abiotic), bacteria with the ability to alternate from unicellular to multicellular organization, from microbial colonies, multicellular aggregates or biofilms. **(ii)** Within the multicellular organization, at high cell densities, bacterial cells secrete EDF (●) into their surroundings. **(iii)** EDF in correlation with activated TA systems induce death in only a subpopulation of cells that are tagged by the EDF (●) whereas the subpopulation of cells with only active TA system and no EDF tagged enter a state of growth arrest, becoming the persisters (●), **(iv)** Upon return of favourable conditions, the persister cells resume growth and replenish the population.

1.5 Multi-stress responsive TA system, MazEF

The most well characterized chromosomal located *mazEF* TA system of *E. coli* was the first to be identified, that is regulated and involved in mediating bacterial PCD under different stress conditions (Figure 1.5) (Aizenman *et al*, 1996). Under normal conditions, the MazE antitoxin and the MazF toxin proteins form a non-toxic hetero-hexameric complex that is safe for the cell (Kamada *et al*, 2003). The MazF toxin is a very stable protein in comparison to the labile antitoxin MazE, which is easily degraded by the ATP dependent serine proteases *in vivo*. Upon degradation of the MazE antitoxin, the free MazF toxin functions as an inhibitor of cellular translation by sequence-specific mRNA cleavage (single stranded mRNA) at ACA sequences (Zhang *et al*, 2003b). Therefore, because of its low stability, the MazE antitoxin has to be continuously replenished to be maintained in the cell, in order to suppress the function of the MazF toxin. Several stress responses have been studied to target this TA system at the transcription or translation level, disturbing the MazE-MazF protein balance, thereby inducing death of growth arrest of the cell.

The first condition reported to show the involvement of *mazEF* TA system in cell death was the over production of ppGpp, the signalling molecule of amino acid starvation. The accumulation of ppGpp was observed to inhibit the *mazEF* operon transcription, thereby leading to cell death (Aizenman *et al*, 1996; Engelberg-Kulka *et al*, 1998). Later, the inhibition of this TA system at the level of transcription and/or translation was also reported on exposure to antibiotics such as chloramphenicol, rifampicin and spectinomycin, leading to the activation of death or growth arrest in the cells by the MazF toxin (Sat *et al*, 2001). The MazEF mediated cell death was also reported under thymine starvation, where the *mazEF* promoter P2 activity was observed to be significantly reduced (Sat *et al*, 2003). Apart from these, cell death by this TA locus was also examined under various other stress conditions such as high temperature of 50ºC, oxidative stress by treatment with H_2O_2, and upon DNA

damage caused due to UV irradiation, nalidixic acid and mitomycin C treatment. Under these conditions, the Δ*mazEF* strains were reported to be more stable and viable than the wild type *E. coli* strains, showing the involvement of the MazEF TA in inducing death under all these stress conditions; but the exact mechanism of activation of this TA system under these conditions are yet to be characterized (Hazan *et al*, 2004).

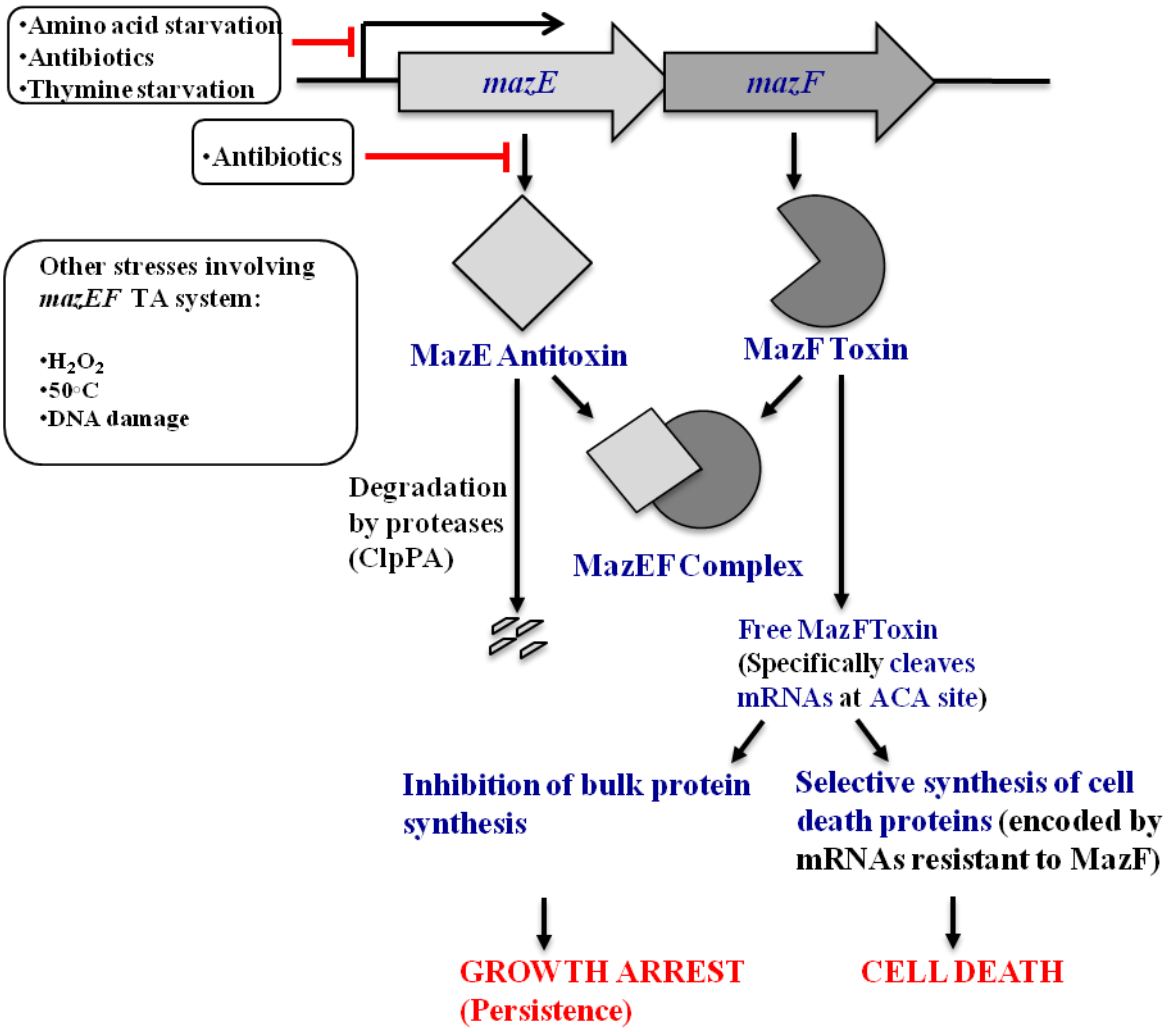

Figure 1.5. Activation of MazEF TA systems under different stress conditions. Under normal conditions, MazE masks the function of MazF by forming a complex, and the cells grow normally. Under stress conditions, the transcription of the operon or translation of mazE is regulated, leading to degradation of labile antitoxin MazE, thereby freeing the MazF toxin. The MazF toxin cleaves mRNAs leading to cell growth arrest or cell death. (Figure adapted from Engelberg-Kulka, 2005)

1.6 Cyanobacteria and multicellular-like behaviour

Some of the cyanobacterial species were also observed to behave as multicellular organizations under stress conditions. One of the recent studies showed that the cyanobacterial species growing on cultural monuments like the Buddha statue, Gandhi statue and the Elephant sculpture in the cultural heritage site at Santiniketan in India were observed to form biofilms (Figure 1.6A, B and C) (Keshari & Adhikary, 2013). The cyanobacteria within these biofilms were reported to be able to survive the hot Indian summers (March-June) where the temperatures go upto 60ºC, and were able to resume their growth upon the return of moisture during the monsoon rains (July-October). Three main cyanobacterial species identified in these biofilms were *Scytonema millei*, *Scytonema sp.* and *Tolpothrix campylonemoides*; along with several other associated cyanobacteria (Keshari & Adhikary, 2013). Viability staining of the organisms within the biofilms showed a part of the population to be dead, and the remaining cells able to survive the high temperatures (Figure 1.6D, E and F) (Keshari & Adhikary, 2013). These results probably indicate a PCD that could have been mediated by TA systems in a sub-population of cells in the biofilm due to high temperatures, aiding the survival of the remaining cells until the return of favourable conditions such as the monsoon rains in this study. However, the link between this survival strategy of cyanobacteria and the TA systems has not yet been explored.

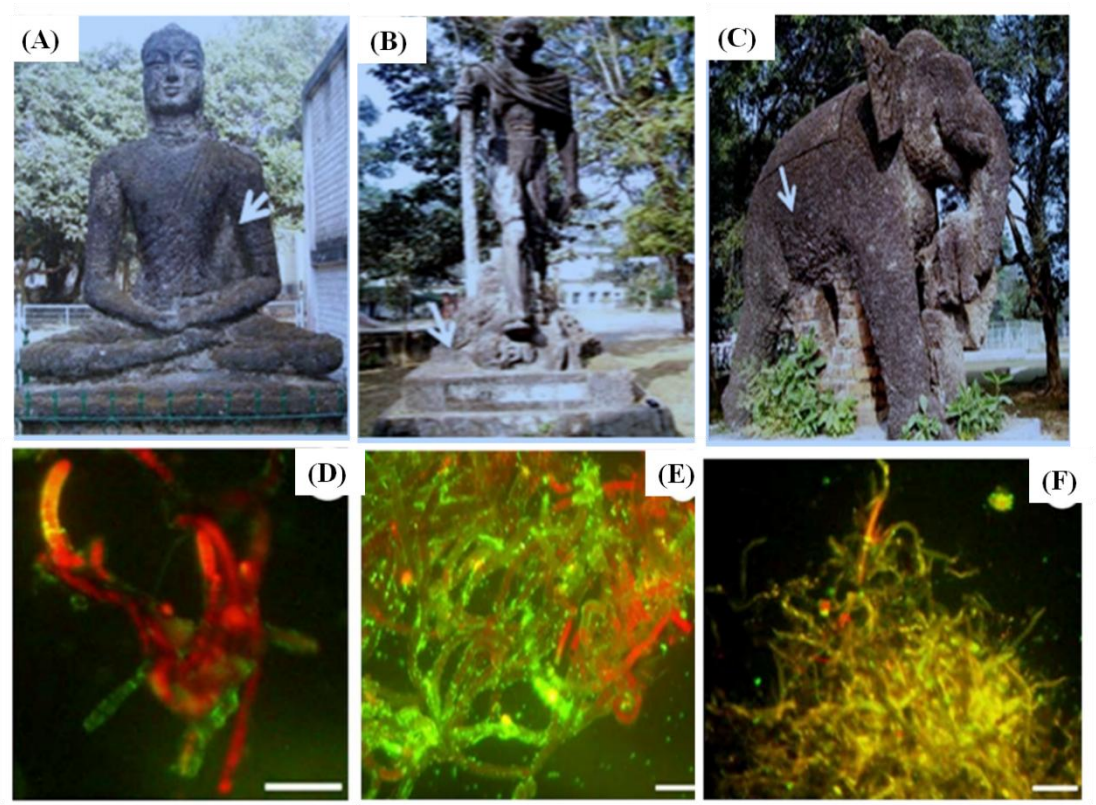

Figure 1.6. Possible survival strategy of Cyanobacterial species growing on statues and sculptures at Santiniketan in West Bengal, India, by forming biofilms during summers. Cyanobacterial species were identified to form thick biofilms on Buddha statue **(A)**, Gandhi statue **(B)** and elephant sculpture **(C)** during hot Indian summers (March-June). The biofilm samples collected from the Buddha statue **(D)**, Gandhi statue **(E)** and elephant sculpture **(F)** were stained with a BacLight viability kit and viewed using epifluorescence microscopy. Within these biofilms, few of the cells remained viable and were able to revive upon the return of moisture during monsoon (July-October) Scale bars = 30 μm. (Keshari & Adhikary, 2013)

1.7 Cyanobacterium *Synechocystis* sp. PCC6803 as a model organism

A freshwater cyanobacterium, *Synechocystis* sp. PCC6803 (here after *Synechocystis*) is one of the highly studied organism due to its ability to grow both phototrophically and heterotrophically. Because of the high similarity of its photosynthetic apparatus to that of plants, it is mostly used as a model to study photosynthesis. Apart from this, it is also used to study Carbon and Nitrogen assimilation, abiotic stress responses and the evolution of plant plastids. The genome of *Synechocystis* was the first among photosynthetic organisms to be completely sequenced and made available in an easily accessible website named Cyanobase

(http://www.kazusa.or.jp/cyano/cyano.html) (Kaneko *et al*, 1996). Ability of being naturally transformable, ease of maintenance and growth makes *Synechocystis* an attractive cyanobacterium for many research groups.

1.7.1 *Synechocystis* genome

The genome of Synechocystis consists of around 12 copies of a single circular chromosome of around 3.755Mb size, along with 4 large and 3 small naturally occurring plasmids. The 4 large plasmids include pSYSM (120Kb), pSYSX (106Kb), pSYSA (103Kb) and pSYSG (44Kb); and the 3 small plasmids include pCC5.2 (5.2Kb), pCA2.4 (2.4Kb) and pCB2.4 (2.4Kb). The sequences of all these plasmids have also been deposited in the Cyanobase. Overall, the genome of *Synechocystis* consists of around 3,725 genes, the functions of most of which are yet to be characterized.

1.7.2 TA systems in *Synechocystis*

Initially, 29 pairs of Type II TA systems were identified in *Synechocystis* (Makarova *et al*, 2009). But, recently the number of predicted putative Type II TA systems increased to 69, consisting of 47 TA pairs located on the chromosome and 22 TA pairs located on the 4 large plasmids; pSYSM, pSYSX, pSYSA and pSYSG (Figure 1.7) (Kopfmann *et al*, 2016). Among these 4 of the predicted TA systems, 3 of which are chromosomally located (*sll0525-ssl1004*, *all1092-ssl2138* and *ssl2923-ssl2922*) and 1 TA systems located on the plasmid pSYSG, slr8014-slr8013 were functionally verified, where the predicted toxins were observed to cause growth inhibition which was reported to be prevented upon co-expression of the respective predicted antitoxin (Kopfmann *et al*, 2016). Apart from these, 3 other chromosomal TA systems, 5 TA systems on the pSYSA plasmid and 1 TA system on the pSYSX plasmid were also studied experimentally (Čelešnik et al., 2016; Ning et al., 2013; Ning et al., 2013; Ning et al., 2011). But, the exact or detailed mechanism of activation and action of none of these identified TA systems has been characterized so far.

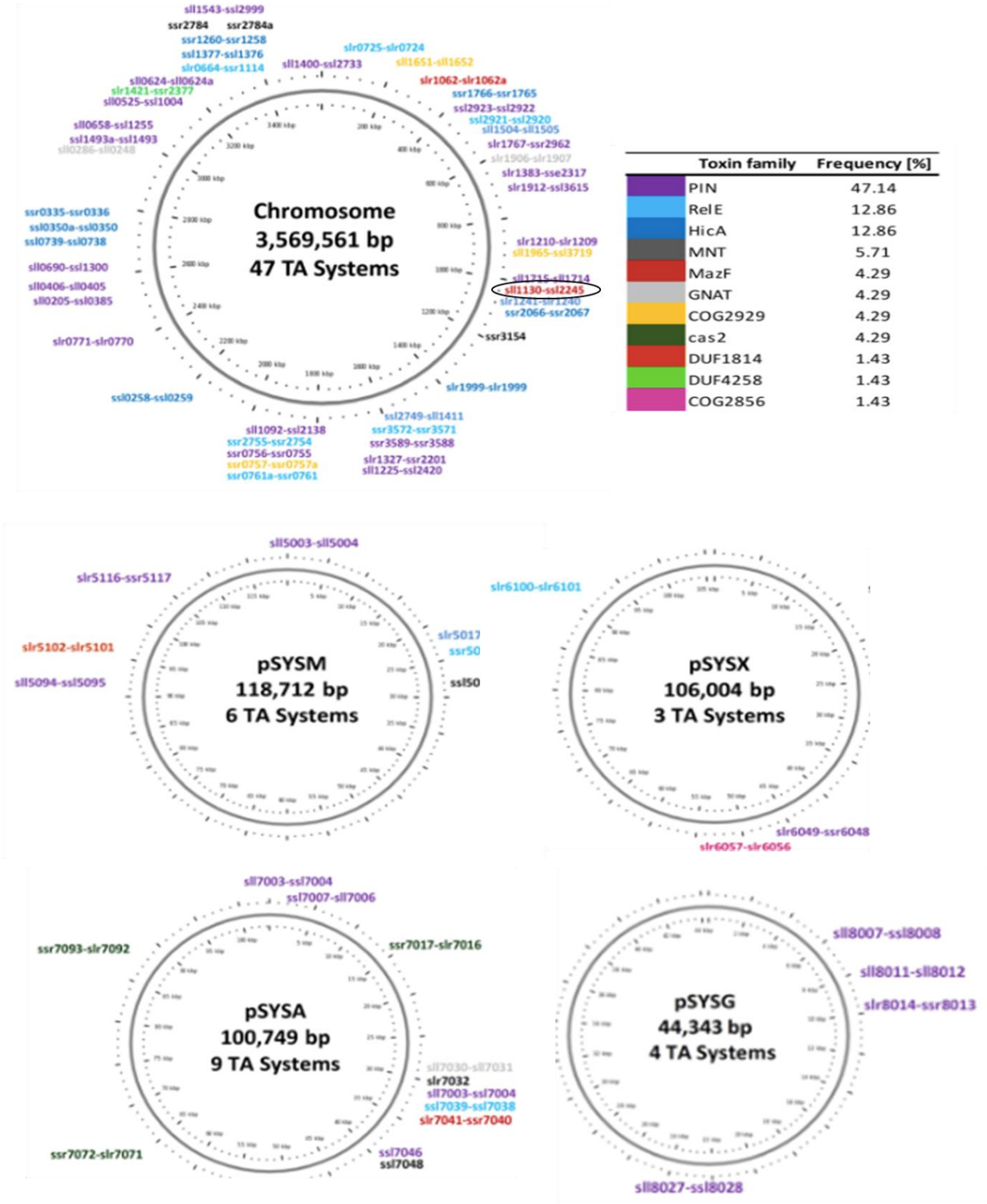

Figure 1.7. TA systems predicted in the genome of *Synechocystis*. Several TA systems have been predicted on the chromosome and the 4 large plasmids pSYSM, pSYSX, pSYSA and pSYSG of *Synechocystis*. The predictions were based on similarity of the genes to different toxin families, depicted by different colors. The TA system of this study, *ssl245-sll1130* is circled in black. Figure from Kopfmann *et al*, 2016.

The TA system characterized in this study is the Sll1130-Ssl2245 TA locus located on the chromosome of *Synechocystis*, which is predicted to be similar to the type II MazEF TA family. The genes in this TA system are organized in a manner similar to most of the well characterized type II TA systems, with the predicted antitoxin gene (*ssl2245)* preceding the predicted toxin gene (*sll1130*) with these two genes having a 4 base pair overlap (Figure 1.8). The genes of this TA system have been reported to be down-regulated upon heat shock, indicating a probable involvement of this TA system in heat stress acclimation, giving us a base to design our objectives for this study (Suzuki, 2005).

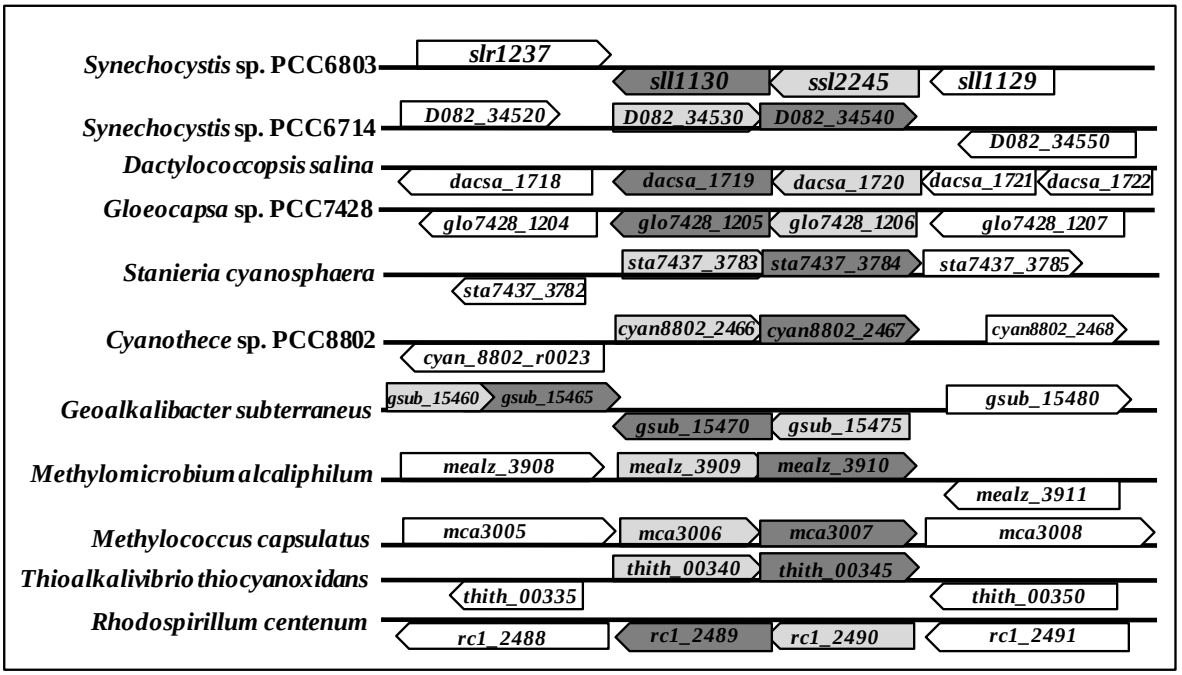

Figure 1.8. *ssl2245* and *sll1130* genes are structurally organized in a dicistronic operon. The orientation of the *ssl2245-sll1130* operon is graphically represented along with its closely related orthologs that were obtained from gene clusters of the KEGG database. The putative antitoxin and toxin genes are represented with grey and dark grey arrows, respectively.

2. OBJECTIVES

Present work was designed to characterize the predicted Ssl2245-Sll1130 TA system in *Synechocystis* by mutations, phenotype characterization, microarray analysis and by studying functions of the purified proteins *in vitro* at optimum conditions as well as upon heat stress.

Proposed objectives

I. **To characterize the Toxin-Antitoxin properties of the predicted Ssl2245-Sll1130 TA system.**

1. Phylogenetic relation of Ssl2245-Sll1130 with its orthologs.
2. Over-expression of Sll1130 in ΔΔ*ssl2245-sll1130* double mutant and comparison of growth with WT.
3. RNase activity of Sll1130 and antagonistic property of Ssl2245.
4. DNA microarray analysis to check gene expression changes due to mutations in *ssl2245* and *sll1130* genes.

II. **To study the effect of Heat stress on the Ssl2245-Sll1130 TA system.**

1. Viability of WT and Δ*sll1130* mutant cells on exposure to heat stress.
2. DNA microarray analysis to check gene expression changes due to heat stress in WT *Synechocystis* cells.
3. RNA integrity of WT and Δ*sll1130* mutant cells under heat stress.
4. Analysis of Ssl2245 and Sll1130 protein levels under heat stress.

III. **To probe the physical interaction between Ssl2245 and Sll1130.**

1. Interaction between Ssl2245 and Sll1130 proteins using Bacterial two hybrid system.
2. Over-expression of His-Ssl2245-Sll1130 to check co-purification of Sll1130 along with His –tagged Ssl2245.

3. Gel exclusion chromatography to check the hetero-oligomerization state of the complex formed between Ssl2245 and Sll1130 proteins.

IV. **To demonstrate the effect of Heat on the interaction between Ssl2245-Sll1130 proteins.**

1. Isothermal Titration Calorimetry (ITC) to determine the stoichiometry of interaction between Ssl2245 and Sll1130 proteins and effect of heat on their interaction.
2. Differential scanning Calorimetry (DSC) to check the unfolding temperatures of the proteins Ssl2245 and Sll1130.
3. Circular Dichroism (CD) spectroscopy to determine the conformational changes in the proteins at high temperatures.
4. Ribonuclease assay of Sll1130 at high temperature.

3. MATERIALS AND METHODS

3.1 *Escherichia coli*

Escherichia coli (DH5α) was used for the maintenance of plasmid clones, cloning and DNA modification experiments, *E. coli* BL-21 (DE3) pLysS was used for the expression of His-tagged recombinant proteins and the *E. coli cya*$^{-}$ (DHP1) strain was used for bacterial two hybrid screening experiments. Bacterial cultures were grown/maintained in Luria and Bertani (LB) broth or LB plates, respectively, with appropriate antibiotic(s) at 37°C.

3.1.1 L.B. MEDIUM

The ingredients for the preparation of 1 liter of LB medium consisted of 10 g of Tryptone, 5 g of Yeast extract and 10 g of NaCl. All these ingredients were first dissolved in 950ml of double distilled water (DDW) after which the solution was made up to 1 liter with DDW. For the preparation of LB Agar, 1.5% of agar (w/v) (Cat. No. GRM026, Himedia) was added to the LB solution. The media was then sterilized by autoclaving at 15 psi pressure for 15-20 minutes. In case of LB Agar, the media was allowed to cool to 50°C before addition of the appropriate antibiotics. About 25ml of LB agar media was poured into 90mm Petri plate each, and allowed to solidify. These solidified LB agar plates were stored at 4°C until used.

3.1.2 Preparation of LB-Antibiotic medium

For selection pressure, appropriate antibiotic stocks were added to the LB medium prior to inoculation. The stocks of the antibiotics, Kanamycin, Ampicillin and Chloramphenicol were filter sterilized and added to a final concentration of 25µg/ml, 100µg/ml and 20µg/ml respectively.

3.2 *Synechocystis* sp. PCC 6803 GT-1

Wild type *Synechocystis* was a glucose-tolerant strain that was originally obtained from Dr J.G.K. Williams (Dupont de Nemours, Wilmington, DE, U.S.A.). Wild type cells were grown photoautotrophically at 34°C in a specialized cyanobacterial BG-11 medium buffered with 20 mM Hepes / NaOH (pH 7.5) under continuous illumination at 70 µmol of photons/m^2 per s as described previously (Wada and Murata, 1989). The Δ*ssl2245*, Δ*sll1130 and ΔΔssl2245-sll1130* cultures, in which the *ssl2245* and *sll1130* genes both individually and together were disrupted by inserting a Sp^R (Ω-spectinomycin gene cassette), a Kan^R (kanamycin-resistance gene) cassette and both Sp^R (Ω-spectinomycin gene cassette)-Kan^R (kanamycin-resistance gene) respectively were grown under the same conditions as described above with the exception that the culture medium contained spectinomycin at 20 µg/ml and kanamycin at 25 µg/ml respectively in the pre-cultures. Density of the cells in the culture was measured by optical density at 730 nm using a spectrophotometer (Thermo Scientific Nanodrop 2000c). For heat treatment, wild type culture was grown to mid-exponential phase (an absorbance of ~0.6 at 730 nm) at 34°C and then shifted to a water bath maintained at 44°C for DNA microarray analysis of wild type cells, and at 50°C for western blotting and RNA stability analysis with continuous illumination (70 µmol of photons/m^2 per s). For viability test, wild type and Δ*sll1130* mutant cultures were grown at 34°C to mid-exponential phase (~ 0.6 OD at 730nm) and then incubated at 50°C over a course of time in a water bath. Cells were harvested before and during heat treatment for viability test.

3.2.1 Preparation of BG-11 for *Synechocystis* culture

BG-11 (supplemented with 20mM HEPES –NaOH, pH 7.5)

Stock 1: The ingredients for preparation included 0.3 g of Citric acid, 0.3 g of Ferric ammonium citrate and 0.05 g of Ethylenediaminetetraacetic acid (EDTA) that were dissolved and made up to 100 ml with milliQ water, filter sterilized and stored in dark at 4ºC.

Stock 2: The ingredients for preparation included 30 g of $NaNO_3$, 0.7 g of K_2HPO_4 and 1.5 g of $MgSO_4.7H_2O$ that were dissolved and made up to 1 liter with milliQ water.

Stock 3: The ingredient for preparation included 1.9 g of $CaCl_2.2H_2O$, dissolved and made up to 100 ml with milliQ water.

Stock 4: The ingredient for preparation includes 2 g of Na_2CO_3, dissolved and made up to 100 ml with milliQ water.

Stock 5: The ingredients for preparation included 2.86 g of H_3BO_3, 1.81 g of $MnCl_2.4H_2O$, 0.222 g of $ZnSO_4.7H_2O$, 0.391 g of $Na_2Mo_4.2H_2O$, 0.079 g of $CuSO_4.5H_2O$ and 0.049 g of $Co(NO_3)_2.6H_2O$ dissolved and made up to 1 liter with milliQ water.

Stock 6: The ingredient for preparation included 119.15 g of HEPES. weighed and dissolved in 750 ml of milliQ water, the pH was then adjusted to 7.5 with 2M NaOH and volume made up to 1 litre with milliQ water.

All the stocks were stored at 4ºC.

Table 3.1. BG-11 media preparation from stocks

Stock solution	1X - 1000ml	2X - 500ml
Stock 2	50ml	50ml
Stock 3	2ml	2ml
Stock 4	1ml	1ml
Stock 5	1ml	1ml
Stock 6	40ml	40ml
Milli Q water	Up to 1000ml	Up to 500ml

Table 3.1. Volume of stocks required for BG-11 nutrient medium preparation.

Two ml of Stock 1 was added prior to inoculation in 1000 ml of 1X BG-11 medium after autoclaving.

3.2.2 Preparation of BG-11 Agar plates

For preparation of BG-11 agar plates, 2X BG-11 with $Na_2S_2O_3.5H_20$ (3 g for 500ml) and 2X agar (3% agar, Cat. No. RM301, Himedia) were autoclaved separately, and then mixed in 1:1 ratio. To this mixture, filter sterilized stock 1 was added and poured in sterile Petri plates.

3.2.3 Preparation of BG-11 Antibiotic medium

To give a selection pressure, appropriate antibiotics were added prior to inoculation to the above mentioned BG-11 medium. Filter sterilized Kanamycin, Spectinomycin and Chloramphenicol were added to a final concentration of 25µg/ml, 20µg/ml and 20µg/ml respectively.

3.2.4 Preparation of BG-11 nutrient limited medium

For protein over expression by induction on addition of cobalt, cobalt-free BG-11 medium was prepared. For this, $Co(NO_3)_2.6H_20$ in stock 5 was eliminated.

3.3 Kits, enzymes, chemicals and reagents

Molecular biology kits and enzymes were procured from Sigma-Aldrich (USA), Qiagen (Germany), MBI Fermentas (Germany) and Takara bio (Japan). Precautions were taken as per manufacturers' instructions. The chemicals and reagents were of analytical grade and obtained from Sigma-Aldrich (USA), GE health care (USA), Fermentas (Germany), Agilent technologies (USA) Himedia (India), SRL (India) and Qualigens fine chemicals (India).

3.4 Molecular biology protocols

Plasmid and genomic DNA isolation, agarose gel electrophoresis, restriction digestion, ligation, competent cell preparation and transformation were according to Sambrook et al, 1989 and/or as per manufacturers' protocol.

3.5 Plasmid DNA vectors

pSyn2030-31, a *Synechocystis* expression vector with a *coaT* promoter, specifically designed in our lab was used for induced expression of the *sll1130* gene upon addition of cobalt. pET28a(+) a high copy number prokaryotic expression vector was used for the cloning and expression of *sll1130, ssl2245* genes separately and together in *E. coli*. pT18 and pT25 vectors were used for bacterial two hybrid screening to test protein-protein interactions in the *E. coli cya*$^{-}$ (DHP1) strain.

3.6 Quantification of DNA and RNA

The quality and concentration of RNA and DNA was examined by agarose gel electrophoresis using ethidium bromide and spectrophotometric analysis (Nanodrop 2000c Spectrophotometer, Thermo Scientific). The concentrations of DNA and RNA were

determined using spectrophotometry by measuring their absorbance at 260 nm and 280 nm. A value of OD_{260} =1 corresponds to 50 µg/ml for DNA, while OD_{260} =1 corresponds to 40 µg/ml for RNA. A value of OD_{260}/OD_{280} between 1.8 and 2.0 and between 1.9 and 2.1 was considered as pure form of DNA and RNA, respectively.

3.7 Oligonucleotides and sequencing

All DNA oligonucleotides were synthesized by either Sigma Aldrich, GCC biotech or Eurofins. Nucleic acid sequencing was carried out by Xcelris, GCC biotech or Eurofins as per requirement. All the expression clones used for protein purifications were confirmed by sequencing prior to being purified.

3.8 Phylogenetic analysis of Ssl2245 and Sll1130

Orthologs of Ssl2245 and Sll1130 were downloaded from from the KEGG and NCBI databases (http://www.kegg.jp/dbget-bin and http://www.ncbi.nlm.nih.gov/gquery/). The amino acid sequences of Ssl2245 and Sll1130 and their respective homologs from other bacteria were concatenated and aligned using CLUSTALW (Chenna *et al*, 2003). Phylogenetic relationships were inferred by Minimum Evolution (Rzhetskyand Nei, 1992) as implemented in MEGA 7.0 (Kumar *et al*, 2016). Bootstrap values were obtained through 1,000 repetitions.

3.9 Generation of *Synechocystis* ΔΔ*ssl2245-sll1130* strain over-expressing Sll1130 (ΔΔ*sll1130*+) and growth analysis due to the over-expression

We used the ΔΔ*ssl2245-sll1130* double mutant strain previously generated in the lab to generate a ΔΔ*sll1130*+ strain where the Sll1130 protein is over-expressed upon induction with cobalt. The *sll1130* gene was PCR amplified using specific primers, *sll1130*-pSyn FP :

5’ GGTCATATGAATACAATTTACGAACAATTTG 3’ and *sll1130*-pSyn RP : 5’ GGAGGTACCACCGAGTTTAAAAACATGGGGAA 3’. The obtained 354 base pair (bp) fragment was ligated at the NdeI and KpnI restriction enzyme sites in the plasmid pSyn2030-31, a *Synechocystis* expression vector with a cobalt (Co^{2+}) inducible *coaT* promoter. The resultant plasmid, pSyn2030-31-*sll1130* was then transformed into the ΔΔ*ssl2245*-*sll1130* double mutant *Synechocystis* strain by tri-parental mating (Zinchenko *et al*, 1999). The culture was then spread onto a chloramphenicol gradient BG-11 agar plate. The transformed colonies obtained were then selected by antibiotic selection pressure of 25 µg/ml, 20 µg/ml and 20 µg/ml of Kanamycin, Spectinomycin and Chloramphenicol respectively. The strain thus generated was termed as ΔΔ*sll1130*+ due to the expression of *sll1130* gene alone, in the absence of the *ssl2245*-*sll1130* operon. For growth analysis, the ΔΔ*sll1130*+ and wild type *Synechocystis* cells were grown in BG-11 media lacking cobalt, till an $O.D_{(730nm)}$ of around 0.6 after which they were induced with the addition of 6.4 µM cobalt ($Co(No_3)_2.6H_2O$) for over-expression of the Sll130 protein. The growth of the ΔΔ*sll1130*+ and wild type cells were monitored by measuring their optical density at 730nm over a period of 96 hours.

3.10 Expression and purification of Ssl2245 and Sll1130 proteins for Isothermal titration calorimetry, Ribonuclease assays and CD spectroscopic measurements

Individual pET28a constructs carrying the His-tagged *ssl2245* and *sll1130* respectively were generated. DNA fragment covering the *ssl2245* and *sll1130* ORFs were amplified from *Synechocystis* genomic DNA by PCR using the specific primer sets, Ssl2245-Exp-FP : 5’-CGGCATATGTCTTATCAATGCTTACAAACTAGCTACG-3’, Ssl2245-Exp-RP : 5’-GGCAAGCTTTCATAGGTGTCGGTATGCCAGAATTATCAGC-3’ and Sll1130-Exp-FP : 5’-GCAGGCATATGAATACAATTTACGAAC-3’, Sll1130-Exp-RP 5’-CGTCGAATTCCTAACCGAGTTTAAAAACATGG-3’ respectively. The amplified 267 bp

fragment of *ssl2245* was digested with NdeI and HindIII and 348 bp fragment of *sll1130* was digested with NdeI and EcoRI respectively, and then ligated to pET28a(+) vector (Cat. No: 69864-3, Novagen), which had also been digested with the same enzymes, so as to generate the HisSsl2245-pET28a and HisSll1130-pET28a constructs respectively. These constructs were then transformed and expressed in the BL21(DE3) pLysS *E. coli* host strain and were purified using the Nickel affinity gel (His60 Ni Superflow resin, Cat. No. 635660, Clontech laboratories Inc.). Expression of these proteins was induced by the addition of 1 mM final concentration of IPTG. Bacterial cells were collected 3 hours after induction by centrifugation at 10,000 rpm for 10 min at 4ºC. Cell pellets were resuspended in lysis buffer (20 mM Tris-HCl, pH 7.5 / 500 mM NaCl / 1 mM PMSF), lysed by Sonication at an amplitude of 40%, each cycle consisted of a pulse run for 45 seconds with 1 min cooling on ice and this process was repeated for 19 more cycles. The sonicated cultures were then centrifuged at 10,000 rpm for 10 min at 4°C to remove the unlysed cells. The supernatant was filtered through a 0.45 µm filter to remove unlysed cells and then loaded onto the Nickel affinity column. The column was washed twice with 20 mM Tris-HCl, pH 7.5 / 500 mM NaCl / 40 mM imidazole and sequentially the His-tagged Ssl2245 and Sll1130 proteins were eluted with 20 mM Tris-HCl, pH 7.5 / 500 mM NaCl / 100 mM, 200 mM, 300 mM and 400 mM imidazole respectively. The fractions which gave a single band at the expected region on the gel were combined and dialyzed against 20 mM Tris-HCl, pH 7.5 / 150 mM NaCl. The purified and dialyzed proteins were then concentrated using Amicon ultra centrifugal filters with a 3 kDa cutoff. The purity of both the proteins was examined by SDS-gel electrophoresis and these pure proteins were further used for ITC experiments, Ribonuclease assays and CD spectroscopic measurements.

3.11 *In vitro* transcription for ribonuclease activity of Sll1130

In vitro transcriptions for all RNAs were performed with the TranscriptAid T7 High Yield Transcription Kit (Cat. No. K0441, Thermo Fisher Scientific). Fragments of *16S rDNA* and *slr1788-slr1789* genes were amplified from the *Synechocystis* genomic DNA using gene specific primer sets with a T7 RNA polymerase promoter sequence added, *16s rDNA invitro* FP : 5´-GAAATTAATACGACTCACTATAGGG ACAATGGAGAGTTTGATCCTGGCTCAGG-3´, *16s rDNA invitro* RP : 5'-AAAGGAGGTGATCCAGCCACACCTTCC-3' and *slr1788-1789 invitro* FP : 5´-GAA ATTAATACGACTCACTATAGGGATGGTTAGAGCTATACGTCCTCCC-3', *slr1788-1789 invitro* RP: 5'-CTAAGAAGGAATTGGCGCTATGG-3' respectively such that the PCR products generated had a T7 RNA polymerase promoter sequence. The PCR products thus obtained were used as templates, and transcription was carried out according to the manufacturer's instructions, including the optional DNase treatment and phenol/chloroform extraction. Purified Sll1130 and Ssl2245, 250 ng of each, were incubated with 400 ng of target *in vitro* transcripts at 30°C or 37°C for 30 - 120 min in 25 mM Tris-HCl (pH 7.5), 60 mM KCl, 100 mM NH_4Cl, 5 mM $MgCl_2$ and 0.1 mM DTT respectively. Duplex RNA formation was achieved as described previously (Stazic *et al*, 2011) with the following modification. The reaction mixture was complemented with 25 mM Tris-HCl (pH 7.5), 60 mM KCl, 5 mM $MgCl_2$, 100 mM NH_4Cl, and 0.1 mM DTT. Purified Sll1130, Ssl2245 and controls were also incubated with target transcripts at 37°C, 50°C and 60°C to test temperature dependency on the toxic activity masking property of the Ssl2245. Reactions were stopped by adding 1 volume of RNA Loading buffer (Thermo Fisher Scientific). Samples were heated at 95ºC for 5 min prior to electrophoretic separation on 6-10% of 7M urea polyacrylamide gels run at 6 mA for 1.5 to 2.5 h.

3.12 Total RNA extraction

Isolation of total RNA from *Synechocystis* cells was performed essentially by following the method of Los et al., 1997. Fifty ml of actively growing wild type, Δ*ssl2245* and Δ*sll1130 Synechocystis* cultures (treated and/or untreated) till an optical density at 730nm of around 0.6 were collected and killed immediately by addition of equal volume of chilled 5% (w/v) phenol-ethanol solution. The cells were then harvested by centrifugation at 3500 rpm for 5 min at 4^{o}C and the cell pellets thus obtained were flash-frozen in liquid nitrogen and stored at -80^{o}C until used. Cell lysis was performed using hot phenol method by treating the cells with acid phenol (Cat. No. P4682, Sigma-Aldrich) in the presence of a solution containing 50mM Tris-HCl (pH 8.0) , 5mM EDTA and 0.5 % SDS at 70ºC. The obtained nucleic acids were then treated with DNaseI and ProteinaseK to remove any contaminating DNA and proteins in the solution and purified using phenol/chloroform/isoamylalcohol. The purified RNA was then precipitated with 3M NaOAc (pH 5.2) and chilled absolute ethanol and the obtained pellet was dissolved in 20 µl of DEPC.

3.13 DNA microarray analysis

Genome-wide analysis of transcript levels was performed with custom made DNA microarray chips (*Synechocystis* microarray chip with 8 x 15 K format, Agilent, La Jolla, CA) that covered 3611 genes including the genes of all native plasmids of *Synechocystis*. The chips used in these studies were custom made using Agilent's noncontact inkjet technology. The arrays were printed with probes of 60-mer oligomers selected from the 3' end of the genes. On an average, 3 to 5 probes per transcript were present on each array. cDNA was prepared using the fair playIII microarray labeling kit (Cat.No. 252009, Agilent, La Jolla, CA). Cy3 and Cy5 dyes (Cat.No. PA23001 and PA25001, GE healthcare) were coupled to the prepared cDNA as per the manufacturer's instructions. Dye coupled cDNA was purified

using microspin columns and hybridized to the DNA microarray chip as per the manufacturer's recommendations (Gene expression hybridization kit, Cat. No. 5188-5281). Total 45 µl of the hybridization mix with Cy3 and Cy5 labeled DNA, was allowed to hybridize for 16 h at 65^{o}C in a hybridization chamber. After hybridization, the microarrays were rinsed with 2 X SSC (1X SSC is 150 mM NaCl and 15 mM Sodium citrate) at room temperature. They were then washed with 2X SSC for 10 min at 60^{o}C and 0.2 X SSC, 0.1 % SDS at 60^{o}C for 10 min, followed by being rinsed with distilled water at room temperature for 2 min. Prior to being scanned, air spray was used to remove moisture. The chip was scanned using Agilent microarray chip scanner (G2505B, Microarray scanner, Agilent technologies). Scanning was performed using green and red PMT at 100% (XDR Hi 100%) as well as at 70%. Feature extraction was done using Agilent feature extraction (FE) software version 9.5.1 as per protocol mentioned in the web site (www.agilent.com/chem/feprotocols). The signal from each gene on the microarray was normalized by reference to the total intensity of signals from all genes. Then the change in the level of the transcript of each gene relative to the total amount of mRNA was calculated.

3.14 Quantitative real-time PCR analysis

RNA isolated from wild type, Δ*ssl2245* and Δ*sll1130* cells was used for cDNA synthesis with the Affinity Script cDNA synthesis kit, following the manufacturer's protocol (Cat. No: 600559, Agilent Technologies Inc.). qRT-PCR was carried out using the Power SYBR Green Master Mix kit (Cat. No: 4368708, Applied Biosystems). Each reaction was carried out in a 25 µl volume containing 12.5 µl of SYBR green master mix, 0.2 µM of each of the forward and reverse primers and 5 µl of diluted cDNA (21 ng). All reactions were run in duplicates, using a qRT-PCR instrument (Mx3005P, Agilent Technologies Inc.,). The instrument was programmed for 95°C for 10 min, 40 cycles of 30 s at 95°C, 60 s at 60°C and 60 s at 72°C. For each reaction, the melting curve was analyzed to check the specific

amplification of the target gene by corresponding primers. Expression levels were normalized using the *gap1* gene as an internal reference. Primers used for qRT-PCR are listed in a table 6.4.

3.15 Atomic Force Microscopy (AFM) to check pili formation

Synechocystis wild type and Δ*sll1130* cells were cultivated in liquid BG-11 media till an optical density at 730 nm of around 1.0 was reached. Twenty µl of this bacterial suspension was placed onto freshly cleaved surface of mica sheets and dried in a laminar airflow chamber for 30 minutes for adsorption. The samples were then imaged with a scanning probe microscope (SPA400, Seiko, Japan) using the tapping mode at the scan rate of 1 – 2 Hz and a resonance frequency of 110 – 150 kHz.

3.16 Viability test

To test the effect of high temperature on the viability of wild type and Δ*sll1130* *Synechocystis* cells, actively growing cultures of these cells were first grown at optimal conditions with temperature of 34ºC till an optical density at 730nm of 1.0 was reached and then shifted to high temperature of 50ºC. Samples were collected at 0, 4, 8 and 24 h time points. These cells were stained with ViaGram^{TM} Red^{+} Bacterial Gram Stain and Viability Kit according to the manufacturer's instructions (V-7023, Molecular probes, Invitrogen, Carlsbad, CA). Sixty µL of water was added to dilute 3 µL of the SYTOX Green stain. To 50 µL of each cell suspension, 2.5 µL of the diluted SYTOX Green stain was added and incubated for 15 min at room temperature (28ºC). Thereafter, 10 µL of the stained cell suspension was examined with an inverted fluorescence microscope (Olympus, model 1X71, Tokyo, Japan).

3.17 RNA integrity of wild type and Δ*sll1130 Synechocystis* cells

To test the effect of high temperature on the integrity of RNA in wild type and Δ*sll1130 Synechocystis* cells, actively growing cultures of these cells were first grown at optimal conditions with temperature of 34ºC till an optical density at 730nm of around 0.6 was reached and then shifted to high temperature of 50ºC. Fifty ml of samples were collected at 0, 1, 3, 6, 8 and 20 h time points and killed instantly by the of equal volume of chilled 5% (w/v) phenol-ethanol solution. The cells were then harvested by centrifugation at 3500 rpm for 5 min at 4^{o}C and the cell pellets thus obtained were flash-frozen in liquid nitrogen and stored at -80^{o}C until used. RNA was isolated from all the samples as described previously (Total RNA extraction). Hundred ng of RNA from each sample at different time points was loaded onto an RNA pico chip and run using a micro-capillary based electrophoretic cell that determines RNA integrity (Agilent 2100 Bioanalyzer).

3.18 Western blotting analysis

Soluble proteins from wild type and Δ*sll1130 Synechocystis* cells were extracted by disruption mechanically using glass beads (106-µm diameter, Sigma). *Synechocystis* cell pellets dissolved in 500 µL of buffer consisting of 50 mM Tris-HCl (pH 8.0), 500 mM NaCl and 1 mM PMSF were mixed with around 500 mg of glass beads in a thick walled glass tube and disrupted by mixing vigorously at maximum speed on a vortex mixer for 30 seconds, followed by 1 min cooling on ice. Vortex mixing and cooling on ice was repeated for 17 cycles to ensure the maximum disruption of cells. The cells thus disrupted were centrifuged at 20,000 *g* for 20 min to separate the soluble proteins from insoluble material and unbroken cells. The concentrations of the proteins in the supernatant were measured using a the slope obtained from graph generated using different known concentrations of BSA (slope, y=0.052x+0.003). Ten µg of soluble proteins from each sample (control and heat treated)

were loaded on to SDS-PAGE gel. After electrophoresis, the gels were washed thoroughly with DDW and the separated proteins on the gel were transferred onto polyvinylidene fluoride membrane (Immobilon-P; Millipore) in a semidry transfer apparatus (TE77-PWR semi dry transfer unit, GE health care). The levels of Ssl2245 and Sll1130 proteins were determined using ECL chemiluminescence detection system according to the manufacturer's instructions (Pierce ECL western blotting substrate, Cat. No. 32106, Thermo Fisher Scientific). Polyclonal antibodies raised in rabbits against His-Ssl2245 and His-Sll1130 protein were used as primary antibodies and Horse radish peroxidase-conjugated antibody raised in goat against rabbit IgG was used as the secondary antibody (Cat. No. NA934V, Amersham Biosciences).

3.19 Bacterial two hybrid system for protein-protein interactions

Constructs carrying *sll1130* and *slr1139* were cloned into plasmid pT25, by PCR amplification of *sll1130* and *slr1139* genes from the *Synechocystis* genomic DNA using gene specific primer pairs *sll1130*-T25-FP: 5' GGGCTGCAGGGATGAATACAATTTACGAACAATTTGACGTC 3', *sll1130*-T25-RP: 5' GGACCCGGGCCTAACCGAGTTTAAAAACATGGGGAAAAG 3' and *slr1139*-T25-FP: 5' GGGCTGCAGGGATGAGTTTACTGGAAATCACCGACGC 3', *slr1139*-T25-RP: 5' GGACCCGGGCTTAAATAAAATCCAATTCCTCTTTCAGTAACTC 3' respectively. The PCR fragments thus obtained were ligated into the pT25 plasmid using the PstI and BamHI restriction enzyme sites. Constructs carrying *ssl2245* and *sll1130* were cloned into plasmid pT18 by PCR amplification of *ssl2245* and *sll1130* genes from *Synechocystis* genomic DNA using gene specific primer pairs *ssl2245*-T18-FP: 5' GGGCTCGAGGATGTCTATCAATGCTTACAAACTAGCTACG 3', *ssl2245*-T18-RP: 5' GGAAAGCTTATTAGGTGTCGGTATGCAGAATTATCAGC 3' and *sll1130*-T18-FP: 5'

GGCTCGAGGATGAATACAATTTACGAACAATTTGACGTC 3', *sll1130*-T18-RP: 5' CGGAAGCTTATACCGAGTTTAAAAACATGGGGAAAAGCAC 3' respectively. The PCR fragments thus obtained were ligated into the pT18 plasmid using the XhoI and HindIII restriction enzyme sites. The plasmid combinations pT25-Sll1130 & pSsl2245-T18, pT25-Slr1139 & pSsl2245-T18, pT25-Slr1139 & pSll1130-T18 and positive control pT25-RhlB & pPNP-T18 respectively, were co-transformed into DHP1 to screen for protein-protein interaction as described and plated onto MacConkey agar plates (Karimova *et al*, 1998). Color changes on the MacConkey agar due to the interactions between the proteins were monitored.

3.20 Over expression and co-elution of Ssl2245 and Sll1130

A DNA fragment covering the *ssl2245* and *sll1130* ORFs was amplified from *Synechocystis* genomic DNA by PCR using the primer set, His2245-1130-F: 5' GGACATATGTCTATCAATGCTTACAAACTAGC 3' and His2245-1130-R: 5' CTCAAGCTTCTAACCGAGTTTAAAAACATGGG 3'. The amplified fragment was digested with NdeI and HindIII, and then ligated to pET28a(+) vector (Cat. No: 69864-3, Novagen), which had also been digested with the same enzymes, so as to generate the HisSsl2245-Sll1130-pET28a construct. The N-terminal 6x-histidine tagged Ssl2245 and untagged Sll1130 proteins were transformed and expressed in the BL21(DE3) pLysS *E. coli* host strain and were purified using the Nickel affinity gel (His60 Ni superflow resin, Cat. No. 635660, Clontech laboratories Inc.). Expression of these proteins was induced by addition of 1 mM final concentration of IPTG. Bacterial cells were collected 3 hours after induction by centrifugation at 10,000 rpm for 10 min at 4ºC. Cell pellets were resuspended in lysis buffer (20 mM Tris-HCl, pH 7.5 / 500 mM NaCl / 1 mM PMSF), lysed by French press thrice at a pressure of 1000 psi and centrifuged at 10,000 rpm for 10 min at 4°C. The supernatant was

filtered through a 0.45 µm filter to remove unlysed cells and then loaded onto the Nickel affinity column. The column was washed twice with 20 mM Tris-HCl, pH 7.5 / 500 mM NaCl / 40 mM imidazole and sequentially the His-tagged Ssl2245-Sll1130 were eluted with 20 mM Tris-HCl, pH 7.5 / 500 mM NaCl / 100 mM, 200 mM, 300 mM and 400 mM imidazole respectively. The purity of each fraction was examined by SDS-gel electrophoresis. The fractions, which gave a single band at the expected region on the gel were combined and dialyzed against 20 mM Tris-HCl, pH 7.5 / 150 mM NaCl.

3.21 Gel permeation chromatography of Ssl2245-Sll1130 proteins

Gel permeation chromatography of purified and co-eluted Ssl2245-Sll1130 proteins (100µg) was performed on a Sephacryl S-100 column (dimensions: 50 x 0.5 cm) in 20 mM Tris buffer (pH 7.5). The molecular weight markers for gel filtration, Thyroglobulin, Apoferritin, β-Amylase, Bovine γ-globulin, Transferrin and Ovalbumin were dissolved at a concentration of 0.1 mg/ml in 100 µl of purified Ssl2245-Sll1130 protein solution and loaded onto the chromatography column (100 µl sample on a Sephacryl S-100, GE Healthcare). Fractions 38 to 46 (each equivalent to 0.25 ml) were collected for analysis. The elutes were first estimated for the presence of proteins by UV absorption at 280 nm and equal volumes of collected fractions were then resolved on SDS-PAGE (15%).

3.22 Isothermal titration calorimetric studies

Thermodynamics governing the interaction between Ssl2245 and Sll1130 proteins was investigated by ITC measurements using a MicroCal VP-ITC equipment (MicroCal LLC, Northampton, MA, USA) (Narahari *et al*, 2011). The purified protein solutions were first degassed under vacuum before use in the ITC experiments. Typically, 15-25 consecutive injections of 5 µL aliquots of Ssl2245 at a concentration of 500-900 µM were added with the

help of a rotator stirrer-syringe into the calorimeter cell of 1.445 ml volume, filled with Sll1130 protein at a final concentration of 70-100 µM. In order to minimize the contribution of heat of dilution to the measured heat change, the protein solutions were prepared in the same buffer. Injections were made at intervals of 5 minutes for all titrations. In order to ensure proper mixing after each injection, a constant stirring speed of 300 rpm was maintained throughout the experiment. Control experiments were performed by injecting Ssl2245 into the buffer solution in an identical manner and the resulting heat changes were subtracted from the measured heats of binding. Since the first injection is often inaccurate, the first data point was deleted before the remaining data were analyzed. The data obtained from these calorimetric titrations were analyzed using the *one set of sites* binding model available in the Origin ITC data analysis software (Narahari *et al*, 2011; Wiseman *et al*, 1989), supplied by the instrument manufacturer.

3.23 Differential scanning calorimetric studies

The thermal stability of Ssl2245 and Sll1130 proteins was investigated by DSC studies using a MicroCal VP-DSC microcalorimeter (MicroCal LLC, Northampton, MA, USA), equipped with fixed reference and sample cells (0.545 ml each) (Kavitha *et al*, 2010). Protein solutions were dialyzed extensively against large volumes of 20 mM Tris buffer, pH 6.5, containing 150 mM NaCl and thoroughly degassed under vacuum for 5 min at room temperature and then carefully loaded in the calorimeter cells. DSC thermograms were recorded at a scan rate of 60 degrees / h (Celsius scale). A background scan collected with buffer in both cells was subtracted from each scan. The temperature dependence of the molar heat capacity of the protein was further analyzed using the Origin DSC analysis software supplied by the manufacturer.

3.24 Circular dichroism spectroscopy

Ssl2245 and Sll1130 protein structural changes at different temperatures from 25ºC to 60ºC were determined using circular dichroism measurements, carried out in a Jasco-J1500 CD spectrometer at a scan rate of 50 nm/min with a 1 nm data pitch and 2 seconds response using a 2 mm band width. Temperature was varied by means of a Peltier thermostat supplied by the manufacturer. Spectra in the far-UV region (260 – 190 nm) were recorded with samples taken in a 1.0 mm quartz cell whereas for measurements in the near UV region (320 – 250 nm) a 10 mm path length cell was used. For measurements in the far UV region the concentrations of Sll1130 and Ssl2245 used were 10 µM and 8.5 µM, respectively, whereas the corresponding concentrations used for measurements in the near UV region were 66 µM and 285 µM, respectively.

4. RESULTS

4.1 Phylogenetic relation of Ssl2245-Sll1130 with its orthologs

The Ssl2245 and Sll1130 proteins are encoded by two genes of a dicistronic operon having a 4 nuclotide overlap at the stop codon of the first gene, *ssl2245* and the start codon of the second gene, *slll1130* respectively. Ssl2245 is a protein with an unknown function, having similarity to AbrB like transcriptional regulators, and Sll1130 has a conserved PemK-like domain that is found in MazF transcriptional regulators. This observation was found to be consistent with a previous study that reported a regulatory function of Sll1130 (Krishna *et al*, 2012). Upon BlastP analysis of these two proteins, the best hits were observed to be mostly from bacteria that could survive under high-temperature and high-salt conditions. Among these were also few thermophilic cyanobacteria that were reported to be thermo-epilithic biofilm forming species (Foster *et al*, 2009; Pandey, 2013). Orthologs of these proteins with high sequence similarity were retrieved from the KEGG database. Apart from these, the MazE antitoxin and MazF toxin protein sequences from *E. coli* and other closely related species were also retrieved simultaneously. The phylogenetic relation of Ssl2245 and Sll1130 with their orthologs is shown in figure 4.1. The phylogenetic tree generated shows that both the proteins are more closely related to the putative toxin-antitoxin proteins of bacteria belonging to high temperature and high salt environments than with the MazE and MazF proteins of *E. coli* or other related species, which were therefore observed to form a separate clade. The Ssl2245 and Sll1130 proteins showed only 21.2 and 35.3% sequence identity with the MazE and MazF proteins of *E. coli* whereas a higher sequence identity of 59 and 74.1% with the antitoxin and toxin protein homologs from *Dactylococcopsis salina* sp. PCC 8305 isolated from a heliothermal saline pool (Walsby *et al*, 1983) and 50 and 70% similarity with those of *Microcystis aeruginosa* sp. PCC 9432 respectively (Sabart *et al*, 2013). The higher

sequence similarity of the putative Ssl2245-Sll1130 TA system with that of homologs from thermophilic bacteria led to an understanding of a probably involvement of this TA system in heat stress response.

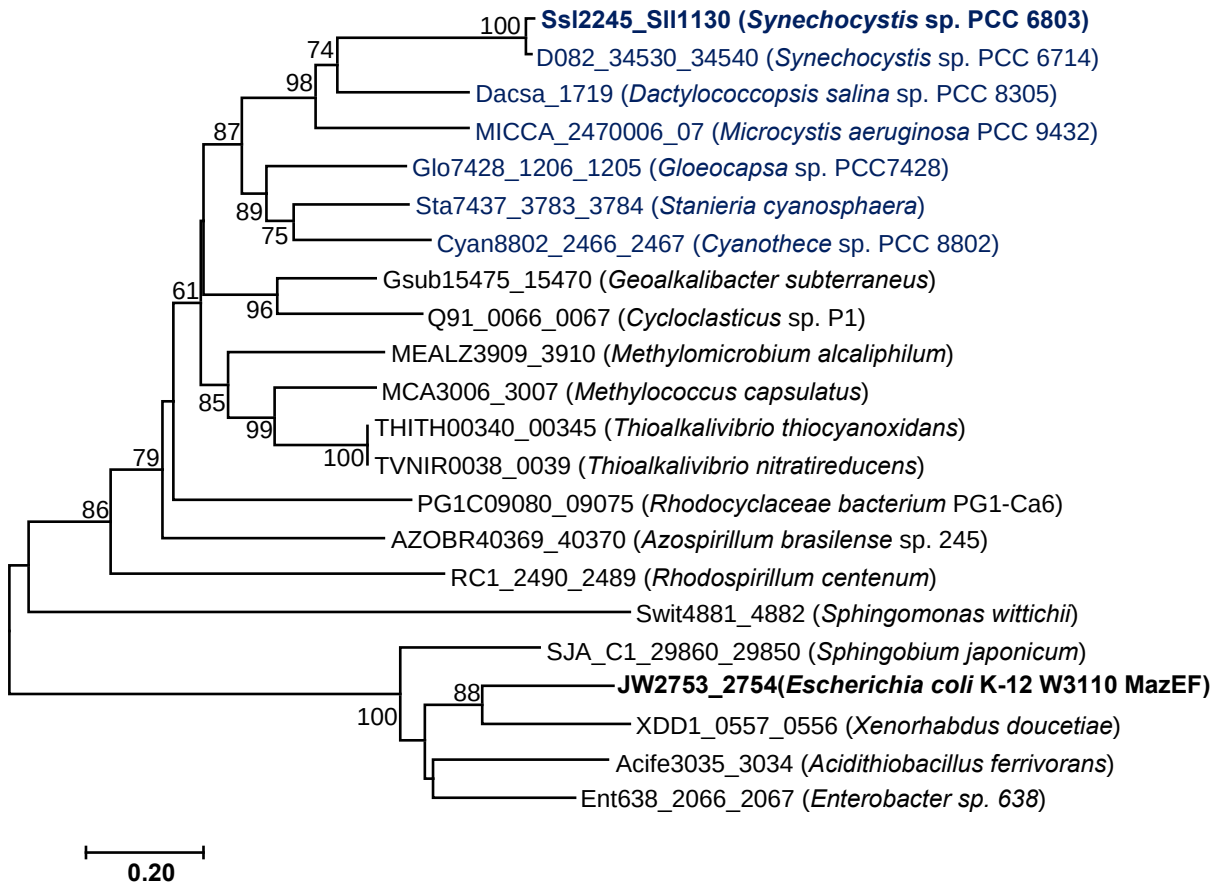

Figure 4.1. Phylogenetic relationship of Ssl2245 and Sll1130 with their closely related orthologs. The complete amino acids sequences of Ssl2245 and Sll1130 were concatenated and aligned with their putative orthologs using CLUSTALW (Chenna *et al*, 2003) yielding a multiple sequence alignment of 208 positions. All cyanobacterial proteins are highlighted in blue and the here investigated *Synechocystis* proteins, Ssl2245 and Sll1130, are in bold font. The archetypical *Escherichia coli* K-12 MazEF (black-boldface) and four proteins more closely related to it were also included. Phylogenetic relationships were inferred by Minimum Evolution (Rzhetsky and Nei, 1992) as implemented in MEGA 7.0 (Kumar *et al*, 2016) using the pairwise deletion option. The optimal tree with the sum of branch length = 7.90605607 is shown. The percentage of replicate trees in which the associated taxa clustered together in the bootstrap test (1000 replicates) is shown next to the branches when ≥60. The tree is drawn to scale, with branch lengths in the same units as those of the evolutionary distances used to infer the phylogenetic tree. The evolutionary distances are given in the number of amino acid substitutions per site as indicated by the scale bar representing 0.2 substitutions per amino acid. The compared protein sequences were retrieved from the KEGG and NCBI databases (http://www.kegg.jp/dbget-bin and http://www.ncbi.nlm.nih.gov/gquery/).

4.2 Sll1130 is a toxic protein

The Sll1130 protein is well conserved in several bacterial species and was observed to have similarity to the PemK superfamily proteins. Since the proteins containing the PemK domain have been reported to be toxins, involved in stress mediated growth regulation such as antibiotic treatment or other abiotic stresses and in plasmid maintenance, we assumed a similar function for Sll1130 (Masuda *et al*, 1993; Gerdes *et al*, 2005). To check whether Sll1130 is a toxic protein, it was expressed in ΔΔ*ssl2245-sll1130* mutant strain, lacking both the genes of the operon. The *Synechocystis* expression vector pSyn2030-31, which contains a pCoT promoter that is inducible upon addition of cobalt was used for the expression of Sll1130. Growth profiles of the ΔΔ*ssl2245-sll1130 Synechocystis* strain expressing Sll1130 (ΔΔSll1130^{+}) and wild type *Synechocystis* cells were measured and compared as cell density at 730nm. The expression of Sll1130 was induced by addition of 6.4 μM of cobalt nitrate ($Co(No_3)_2.6H_2O$) once the cells reached an $O.D_{(730nm)}$ of around 0.6. It can be clearly observed from figure 4.2 that upon expression of Sll1130 in cells containing mutations in both *ssl2245* and *sll1130* genes, the ΔΔSll1130^{+} strain demonstrated a significantly slower growth compared to wild type cells. These results indicated that Sll1130 is toxic to the cells when expressed alone, in the absence of its putative antitoxin protein, Ssl2245.

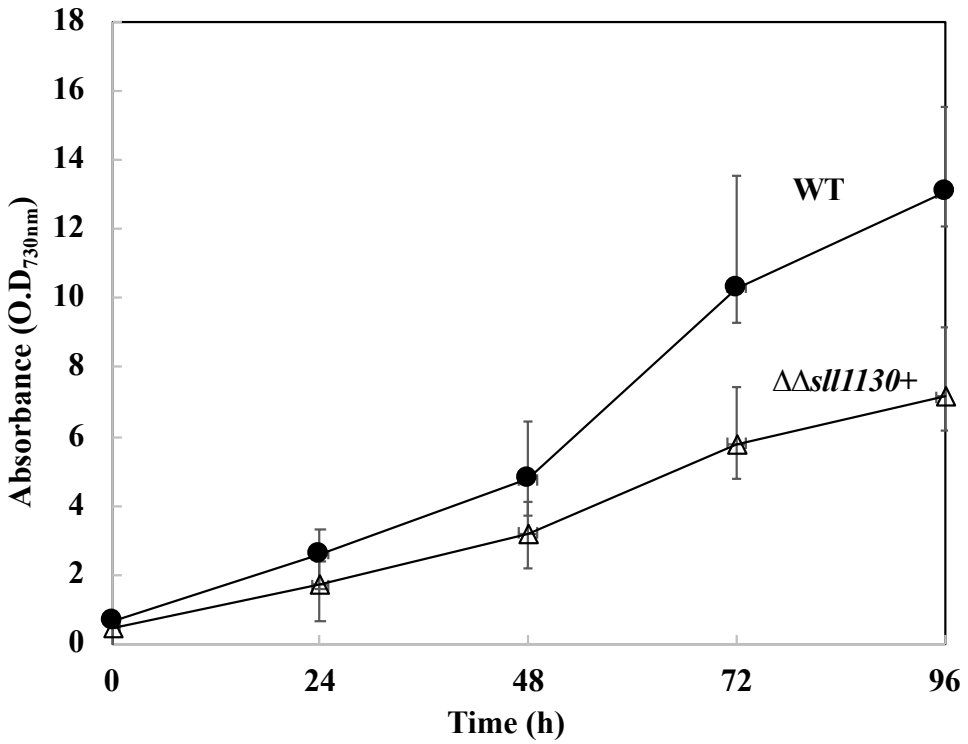

Figure 4.2. Growth profiles to check whether Sll1130 is a toxic protein. Sll1130 was expressed in ΔΔ*ssl2245-sll1130 Synechocystis* cells using pSyn2030-31 *Synechocystis* expression vector (ΔΔSll1130^{+}). Wild type (WT) *Synechocystis* cells were used as control. Growth profiles of ΔΔ*ssl2245-sll1130* cells (Δ) and wild type cells (•) induced upon addition of cobalt were monitored and measured as cell density in terms of O.D at 730nm.

4.3 Over-expression and purification of Ssl2245 and Sll1130 by affinity chromatography

To study the biochemical properties of purified proteins, Ssl2245 and Sll1130 that were tagged with 6X-His tag at their N-terminal were over-expressed using pET28a(+) in *E. coli* BL-21 (DE3) pLysS as mentioned in materials and methods. Protein expression was induced upon addition of 1 mM final concentration of IPTG and the expressed proteins were purified using Ni-NTA column by His-affinity chromatography. Purified 6X-His tagged Ssl2245 and Sll1130 proteins resolved at their expected sizes of around 12 and 15 kDa respectively (Figure 4.3). The pure protein elutes were pooled and dialyzed against buffer containing 20mM Tris-HCl and 150mM NaCl to remove imidazole present in the elution buffers. The dialyzed samples were then used for further experiments.

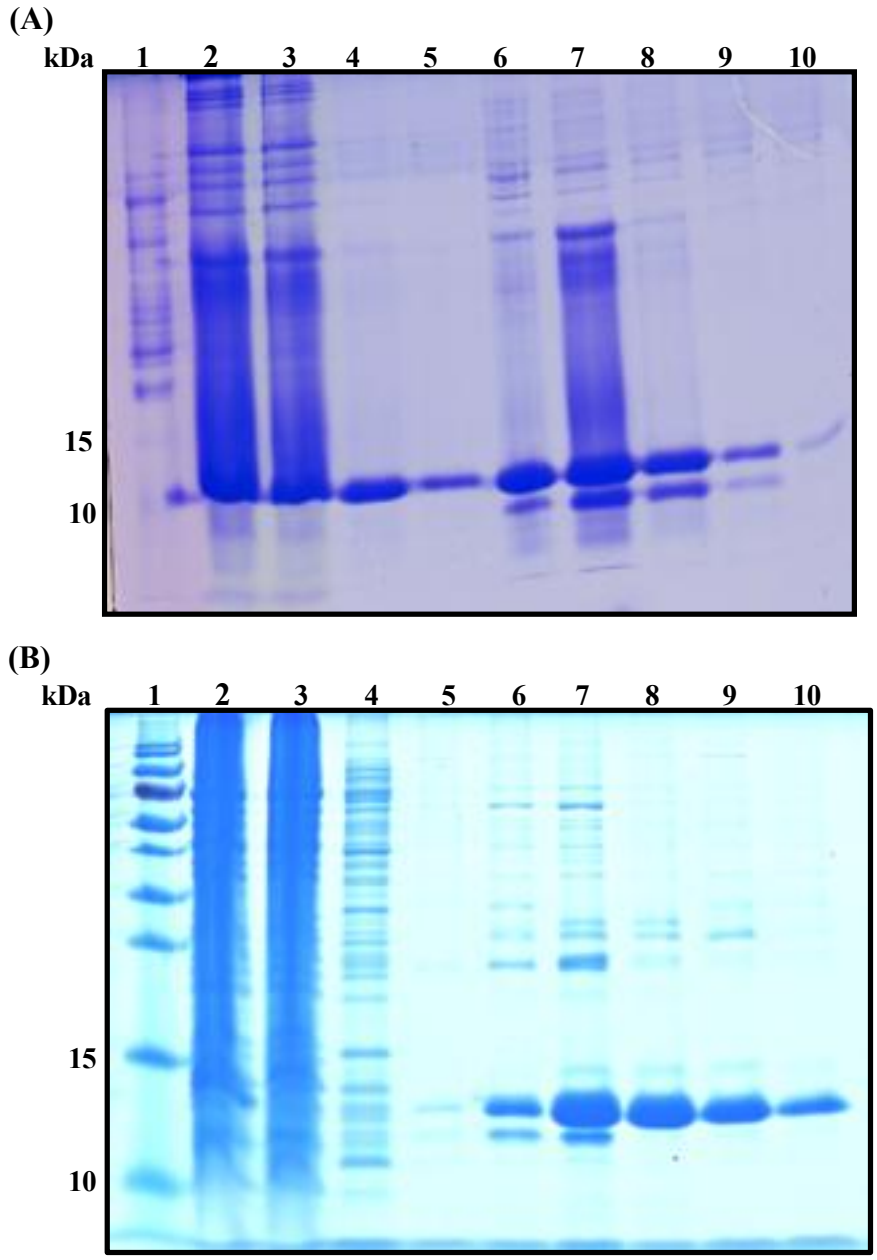

Figure 4.3. SDS–PAGE analysis of expressed and purified His-tagged Ssl2245 (A) and Sll1130 (B) recombinant proteins in *E. coli* BL21 (DE3). Lane 1, protein molecular weight standards (Cat No. 26616, Thermo Scientific); lane 2, whole cell lysate of induced *E. coli* harboring plasmid pET-*ssl2245* and pET-*sll1130* in (A) and (B) respectively; lane 3, Flow through collected from Ni-NTA column; lane 4 & 5, Protein washes of Ni-NTA column with 40mM imidazole used for eluting non-specifically bound proteins; lane 6-10, protein elutes with increasing concentrations of 100, 100, 200, 300 and 400 mM imidazole. The molecular masses of standards are shown in the left margin.

4.4 Sll1130 toxin is a Ribonuclease, whose function is antagonized by the antitoxin Ssl2245

The toxins of most of the well characterized TA systems are reported to function in inhibiting protein translation by digestion of RNAs (rRNA, mRNA, tRNA, sRNA and tmRNA) (Yamaguchi & Inouye, 2011; Cook *et al*, 2013). Few of the toxin ribonucleases reported to cleave RNA are MazF, RelE, YoeB and Yaf (Christensen et al., 2003; Kamada and Hanaoka, 2005; Pedersen et al., 2003; Zhang et al., 2003; Zhang and Inouye, 2009). Therefore, to check if the toxin Sll1130 is also a ribonuclease, *in vitro* synthesized partial 16S rRNA and *slr1788-slr1789* mRNA transcripts were chosen as substrates. These substrates were incubated with purified Sll1130 or purified Ssl2245 or both the proteins together. Upon incubation with only Sll1130, cleavage of the RNA was observed (Figure 4.4). Whereas, incubation with Ssl2245 alone had no effect on the RNA (Figure 4.4). Apart from these, the incubation of the substrates with both Sll1130 and Ssl2245 proteins together also had no effect on the RNA as the substrates were observed to be intact (Figure 4.4). This demonstration of a significant degradation of both the RNA substrates by Sll1130 indicates its function as a endoribonuclease. Whereas, the loss of this degradation upon incubation with Sll1130 and Sssl2245 together indicated a function of Ssl2245 as an antitoxin that inhibited the endoribonuclease function of Sll1130, thereby leaving the substrates intact.

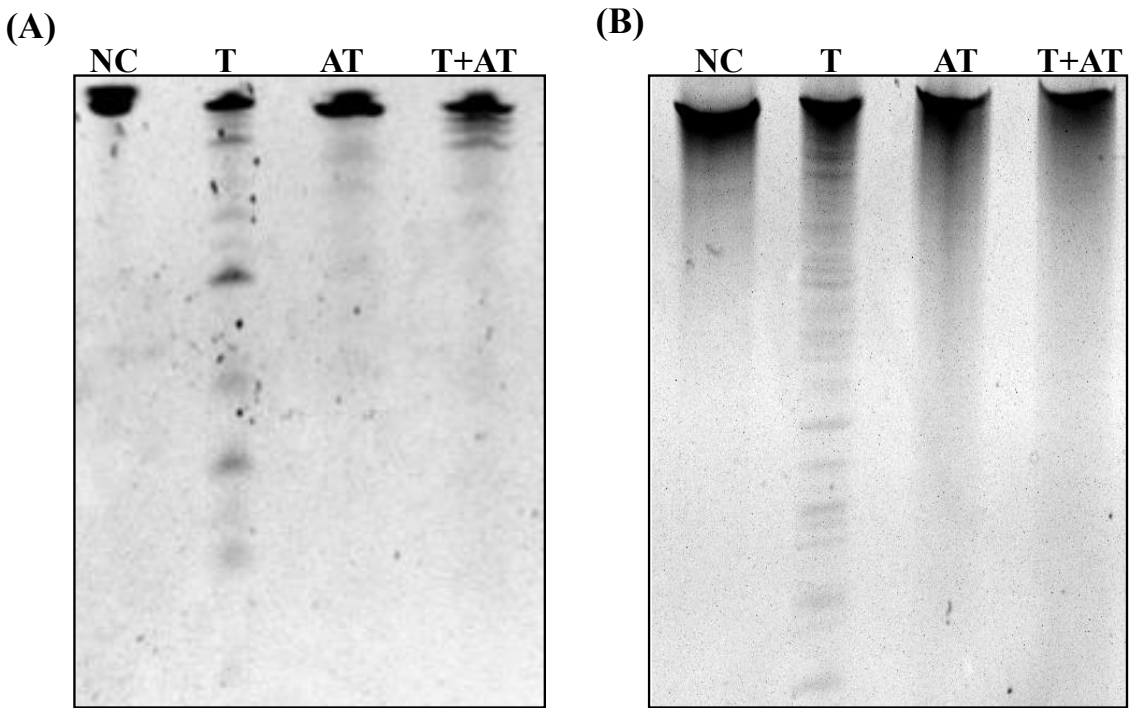

Figure 4.4. Sll1130 possesses endoribonuclease activity which is counteracted by Ssl2245. *In vitro*-synthesized partial *Synechocystis* 16S rRNA fragment **(A)** and *slr1788-slr1789* mRNA **(B)** was incubated for 30 min with Sll1130 (T), with Ssl2245(AT), or both Sll1130 and Ssl2245 (T+AT) respectively. The addition of Sll1130 resulted in degradation of the RNA, which was prevented by concurrent addition of Sll1130 and Ssl2245 together.

4.5 Gene expression changes due to mutations in *ssl2245* and *sll1130* genes

Wild type, Δ*ssl2245* and Δ*sll1130* cells were grown photoautotrophically at 34ºC in BG-11 medium buffered with 20 mM Hepes/NaOH (pH 7.5) under continuous illumination at 70 μmol of photons/m^2/s till an $O.D_{(730nm)}$ of around 0.6. Total RNA was isolated and differentially expressed genes in Δ*ssl2245* and Δ*sll1130* when compared to wild type were identified using a new custom made DNA microarray chip (15K Agilent), which was designed to included probes that covered genes present on the genome as well as on the 7 plasmids of *Synechocystis*. The gene expression changes due to both *ssl2245* and *sll1130* gene mutations were analysed individually. Table 4.1 shows the list of genes that were significantly either up or down-regulated in both the mutants, compared to the wild type cells. The genes with mean induction ratio greater than 2.0 in at least either of the two mutants,

were listed as up- regulated, and those with an induction ratio below 0.3 in both the mutants, were listed as down-regulated. Among the up-regulated genes, were several genes located on the large plasmids, pSYSA, pSYSX and pSYSM in both Δ*ssl2245* as well as Δ*sll1130*. It was interesting to observe the genes up-regulated specifically on the pSYSA plasmid, with most of the genes encoding parts of the CRISPR (Clustered Regularly Interspaced Short Palindromic Repeats) system. CRISPR systems have been reported to be involved in providing adaptive immunity against phage invasion. Three different classes of CRISPR-Cas systems have been identified on the plasmid pSYSA, called CRISPR1, CRISPR2 and CRISPR3 (Scholz *et al*, 2013). These systems have been classified as subtype I-D, subtype III-D and subtype III-B respectively, according to (Makarova *et al*, 2015). The genes up-regulated in Δ*ssl2245* and Δ*sll1130* have been observed to belong to CRISPR2 (genes *sll7062-sll7067*) and CRISPR3 (*genes sll7085-sll7090*) systems, whereas expression of the genes belonging to the CRISPR1 cassette remained unchanged. Apart from these CRISPR systems, the pSYSA plasmid also harbours several other TA systems (Kopfmann & Hess, 2013). However, expression of the genes of these TA systems was also not affected, similar to the unchanged expression of CRISPR1 genes. These results clearly indicate that the higher expression of the pSYSA-located CRISPR2 and CRISPR3 genes in the two mutants is not a consequence of a higher pSYSA plasmid copy number, but points to a specific regulatory effect. The up-regulation of CRISPR-associated genes in the Δ*ssl2245* and Δ*sll1130* suggests a possible role of the Ssl2245-Sll1130 TA system as master regulators that might be involved in viral defense. There have been reports on the repression of CRISPR arrays by the heat-stable nucleoid structuring (H-NS) protein, a global transcriptional repressor, in some strains of *E. coli* (Westra *et al*, 2010). On the contrary, these results suggest that Ssl2245 and Sll1130 could be involved in controlling a process that leads indirectly to the activation of the genes of the CRISPR system, e.g. as part of a lifestyle change. Supporting this possible role

of the Ssl2245-Sll1130 TA system, there have been several other TA systems that were previously reported to be involved in virus defense (Hazan & Engelberg-Kulka, 2004). Thus, the Ssl2245- Sll1130 system could act in a multifunctional way, like *E. coli's* MazEF exhibiting multiple stress responses (Hazan *et al*, 2004). Apart from the CRISPR genes and genes located on the pSYSX and pSYSM plasmids of *Synechocystis*, several heat-shock genes, pilin genes as well as other hypothetical genes were also observed to be up-regulated, indicating a possible function of the genes of this TA system directly or indirectly in regulation of pili formation and also in heat-stress response. The genes of the *slr1788-slr1789* dicistronic operon, and heat responsive *frpC*, pilin genes which were previously confirmed to be up- regulated in the Δ*sll1130* mutant were also commonly up-regulated in this study (Krishna *et al*, 2012). All transcriptome data have been deposited in the KEGG database from where they can be downloaded under http://www.genome.jp/kegg-bin/get_htext?htext=Exp_DB&hier=1.

Table 4.1. Gene expression changes due to mutation in Δ*ssl2245* and*Δsll1130*

ORF No.	Gene	Location	Function	Δssl2245/WT	Δsll1130/WT
Genes whose expression was commonly upregulated in both Δ*ssl2245* and Δ*sll1130*					
sll7090	*cmr2, cas10*	pSYSA	unknown protein	18.91 ± 2.16	22.08 ± 0.54
sll7065	*csm3, cas7*	pSYSA	unknown protein	17.81 ± 0.22	27.59 ± 2.75
sll7089	*cmr3*	pSYSA	unknown protein	17.64 ± 3.85	17.8 ± 1.18
sll7064	*csx19*	pSYSA	unknown protein	17.25 ± 3.64	31.55 ± 5.25
slr7023		pSYSA	hypothetical protein	17.2 ± 3.53	9.41 ± 0.26
sll7087	*cmr4*	pSYSA	unknown protein	17.12 ± 2.6	12.84 ± 1.13
sll7086		pSYSA	unknown protein	16.75 ± 2.42	13.9 ± 1.23
slr0179			hypothetical protein	14.59 ± 1.91	21.99 ± 2.56
ssr6024		pSYSX	unknown protein	13 ± 6.03	14.31 ± 1.91
ssr6027		pSYSX	unknown protein	12.74 ± 3.49	11.69 ± 0.99
slr1788			unknown protein	11.75 ± 1.39	11.14 ± 0.42
slr1789			unknown protein	10.68 ± 1.14	6.2 ± 0.5
slr7091	*csx18*	pSYSA	hypothetical protein	10.22 ± 0.86	8.08 ± 1.93
slr1764	*capA*		similar to tellurium resistance TerE	9.85 ± 0.55	4.2 ± 0.37
ssr6026		pSYSX	unknown protein	8.78 ± 0.61	5.86 ± 1.7
sll7067	*cmr2, cas10*	pSYSA	unknown protein	8.52 ± 0.75	13.16 ± 1.67
sll7085	*cmr6*	pSYSA	unknown protein	8.1 ± 1.87	8.2 ± 4.35

sll7066	*cas7*	pSYSA	unknown protein	7.91 ± 0.71	12.63 ± 0.56
sll7062	*csm6*	pSYSA	unknown protein	7.03 ± 0.5	11.69 ± 1.29
sll1009	*frpC*		unknown protein	7.02 ± 0.77	3.47 ± 0.28
sll7063	*cas7*	pSYSA	unknown protein	6.24 ± 2.65	19.24 ± 1.21
slr0105			hypothetical protein	6.21 ± 0.75	8.44 ± 2.3
ssr6030		pSYSX	unknown protein	5.6 ± 0.01	11.57 ± 0.01
sll7075		pSYSA	unknown protein	5.52 ± 1.85	7.32 ± 3.22
slr0869			hypothetical protein	5.5 ± 0.46	4.4 ± 3
sll5097		pSYSM	hypothetical protein	5.42 ± 2.01	10.04 ± 0.59
slr6025		pSYSA	probable antirestriction protein	4.92 ± 2.94	8.15 ± 5.64
ssr6089		pSYSX	unknown protein	4.81 ± 0.01	14.28 ± 0.01
sll0041	*pixJ1, pisJ1*		phytochrome-like photoreceptor	4.65 ± 1.18	3.06 ± 2.37
sll0444			unknown protein	4.63 ± 0.17	4.25 ± 0.18
sll0445			unknown protein	4.03 ± 0.28	4.8 ± 0.22
slr0106			unknown protein	3.72 ± 0.33	7.99 ± 0.36
slr1920			unknown protein	3.59 ± 0.32	3.39 ± 1.13
sll7070		pSYSA	unknown protein	3.54 ± 0.27	20.44 ± 1.8
sll7069		pSYSA	hypothetical protein	3.24 ± 0.15	10.39 ± 0.94
sll1660			hypothetical protein	3.21 ± 0.56	5.15 ± 0.77
slr0820	*gumD*		probable glycosyltransferase	3.19 ± 1.89	4.53 ± 1.44
sll0327			unknown protein	4.55 ± 0.21	2.03 ± 0.1
slr7097		pSYSA	hypothetical protein	3.73 ± 1.91	2.35 ± 1.46
slr6028		pSYSX	unknown protein	3.27 ± 1.68	2.05 ± 0.52
slr2016	*pilA10*		type 4 pilin-like protein, essential	3.06 ± 0.22	2.74 ± 0.21
sll0033	*crtH*		carotene isomerase	2.82 ± 4.58	6.77 ± 6.83
ssl8024		pSYSG	unknown protein	2.67 ± 1.06	3.47 ± 1.3
slr1594	*rre5, patA*		two-component response regulator	2.55 ± 0.12	4.97 ± 0.37
slr5111		pSYSM	unknown protein	2.53 ± 0.19	4.67 ± 0.57
ssr6046		pSYSX	hypothetical protein	2.48 ± 0.12	3.56 ± 0.19
ssr1473			hypothetical protein	2.36 ± 1.33	3.57 ± 2.54
ssl5098		pSYSM	unknown protein	2.26 ± 0.49	3.19 ± 0.23
sll1240			unknown protein	2.16 ± 0.19	9.18 ± 0.62
sll1239			unknown protein	2.07 ± 0.15	17.6 ± 2.52

Genes whose expression was up-regulated only in Δ*ssl2245*

slr7092	*cas1*	pSYSA	Cas1	3.58 ± 1.31	1.29 ± 0.6
slr2017	*pilA11*		type 4 pilin-like protein, essential	3.45 ± 1.33	1.69 ± 0.15
sll1578	*cpcA*		phycocyanin alpha subunit	3.42 ± 0.54	1.05 ± 0.12
sll0034	*vanY*		putative carboxypeptidase	3.31 ± 0.35	0.59 ± 0.04

Genes whose expression was up-regulated only in Δ*sll1130*

sll0909	*dnaJ*		unknown protein	1.82 ± 0.18	4.2 ± 3.16
sll1241			unknown protein	1.8 ± 0.23	3.56 ± 0.95
ssl2384			unknown protein	1.77 ± 0.23	3.57 ± 0.48
sll0016	*mltA*		probable transglycosylase A	1.75 ± 2.04	3.33 ± 2.88

slr1512	*sbtA*		sodium-bicarbonate transporter	1.73 ± 1.58	3.15 ± 1.09
sll1708	*rre17, narL*		two-component response regulator	1.7 ± 0.75	4.33 ± 0.38
ssr1256			hypothetical protein	1.67 ± 1.05	3.93 ± 0.78
slr1232			unknown protein	1.59 ± 0.73	3.47 ± 0.86
sll1515	*gifB*		glutamine synthetase inactivating factor IF17	1.5 ± 0.92	23.83 ± 10.8
slr0888			hypothetical protein	1.49 ± 0.02	3.37 ± 0.4
slr1963	*Ocp*		water-soluble carotenoid protein	1.46 ± 0.47	3.51 ± 0.92
ssr0692			hypothetical protein	1.35 ± 0.66	3.85 ± 0.62
slr0875	*mscL*		large-conductance mechanosensitive	1.35 ± 0.15	3.72 ± 0.48
slr1957			hypothetical protein	1.32 ± 0.44	7.47 ± 2.11
sll1608			hypothetical protein	1.27 ± 0.14	5.57 ± 3.12
slr2076	*groEL1*		60kD chaperonin	1.27 ± 0.55	3.47 ± 1.62
slr0967	*rfrP*		hypothetical protein	1.25 ± 0.08	3.39 ± 1.08
slr0006			unknown protein	1.24 ± 0.05	3.44 ± 0.33
sll1384	*dnaJ*		similar to DnaJ protein	1.21 ± 0.06	3.23 ± 0.11
ssl1911	*gifA*		glutamine synthetase inactivating factor IF7	1.19 ± 0.08	12.76 ± 1.6
sll0022			unknown protein	1.17 ± 0.05	4.53 ± 0.41
slr0007			probable nucleotidyltransferase	1.15 ± 0.06	3.71 ± 0.13
ssr0693			unknown protein	1.14 ± 0.51	3.37 ± 1.11
slr0772	*chlB*		light-independent protochlorophyllide	1.09 ± 0.24	5.45 ± 0.44
sll0283			hypothetical protein	1.09 ± 0.08	4.02 ± 0.4
slr6043	*copA*	pSYSX	probable cation efflux system protein	1.06 ± 0.87	7.51 ± 1.97
slr1851	*rfrH*		hypothetical protein	1.04 ± 0.31	4.22 ± 0.06
slr0518	*abfB*		similar to alpha-L-arabinofuranosidase	1.04 ± 0.1	4.03 ± 0.21
ssl1923			hypothetical protein	1.03 ± 0.23	3.02 ± 0.85
sll0430	htpG		HtpG, heat shock protein 90,	1.02 ± 0.01	8.12 ± 1.32
slr0701	*merR*		transcriptional regulator	1.02 ± 0.08	6.62 ± 0.31
slr1152	*rfrK*		hypothetical protein	0.99 ± 0.39	17.62 ± 4.89
sll0416	*groEL-2*		60 kDa chaperonin 2	0.96 ± 0.15	9.43 ± 0.66
sll0170	*dnaK2*		DnaK protein 2, heat shock protein 70,	0.94 ± 0.05	6.59 ± 1.46
sll1074	*leuS*		leucyl-tRNA synthetase	0.94 ± 0.14	3.05 ± 2.9
sll1030	*ccmL*		carboxysome assembly protein	0.91 ± 0.19	6.04 ± 2.57
sll0528			hypothetical protein	0.9 ± 0.08	3.38 ± 1.32
sll1198	*trmD*		tRNA (guanine-N1)-methyltransferase	0.88 ± 0.37	3.1 ± 1.39
sll0846			hypothetical protein	0.85 ± 0.22	8.53 ± 0.89
sll0005	*spkH*		hypothetical protein	0.8 ± 0.09	6.1 ± 0.66
slr1185	*petC2*		Rieske iron sulfur protein	0.8 ± 0.07	3.79 ± 0.76
slr0798	*ziaA*		zinc-transporting P-type ATPase	0.77 ± 0.09	4.61 ± 1.49
slr1641	*clpB1*		ClpB protein	0.76 ± 0.05	5.07 ± 1.35
slr0013			hypothetical protein	0.76 ± 0.06	4.08 ± 2.96
sll1514	*hspA*		16.6 kDa small heat shock protein	0.74 ± 0.47	9.4 ± 4.19

slr1501			probable acetyltransferase	0.74 ± 0.05	7.47 ± 0.98
ssr3129			unknown protein	0.73 ± 0.05	3.59 ± 0.5
slr6016		pSYSX	unknown protein	0.73 ± 0.03	3.54 ± 0.46
sll0253			hypothetical protein	0.66 ± 0.03	3.8 ± 0.26
sll0065	*ilvN*		acetolactate synthase small subunit	0.66 ± 0.03	3.21 ± 1.8
slr0852			hypothetical protein	0.64 ± 0.02	3.41 ± 0.29
slr0667			unknown protein	0.62 ± 0.06	3.62 ± 0.31
slr6044	*copC*	pSYSX	hypothetical protein	0.62 ± 0.04	3.58 ± 0.51
sll1613			unknown protein	0.61 ± 0.07	3.5 ± 1.24
slr1670			unknown protein	0.61 ± 0.04	3.03 ± 1.39
ssr1038			unknown protein	0.59 ± 0.01	5.65 ± 1.8
slr1675	*hypA1*		putative hydrogenase protein	0.53 ± 0.37	4.09 ± 2.16
slr1915			hypothetical protein	0.44 ± 0.08	4.5 ± 1.11
slr6040	*pcopR,rreP*		two-component response regulator	0.38 ± 0.01	3.38 ± 0.42
slr0895	*prqR*		transcriptional regulator	0.33 ± 0.13	3.88 ± 1.35
Genes whose expression was commonly down regulated in both Δ*ssl2245* and Δ*sll1130*					
sll1724			probable glycosyltransferase	0.27 ± 0.04	0.19 ± 0.03
sll1723			probable glycosyltransferase	0.26 ± 0.05	0.12 ± 0.03
slr1704			hypothetical protein	0.24 ± 0.01	0.07 ± 0.01
sll0858			hypothetical protein	0.21 ± 0.06	0.18 ± 0.03
sll0857			unknown protein	0.21 ± 0.01	0.14 ± 0.01
sll5014		pSYSM	similar to maturase	0.19 ± 0.05	0.22 ± 0.08
ssl5015		pSYSM	unknown protein	0.16 ± 0.02	0.29 ± 0.06
sll0856	*sigH, rpoE*		RNA polymerase ECF-type	0.16 ± 0.01	0.12 ± 0.01
sll1722			hypothetical protein	0.16 ± 0.01	0.11 ± 0.01
ssl6023		pSYSX	unknown protein	0.15 ± 0.01	0.26 ± 0.03
sll1396			unknown protein	0.11 ± 0.08	0.27 ± 0.17
slr0909			unknown protein	0.11 ± 0.06	0.14 ± 0.08
ssl2245			unknown protein	0.1 ± 0.01	0.3 ± 0.04
sll6010		pSYSX	unknown protein	0.06 ± 0.01	0.16 ± 0.05
sll1130			unknown protein	0.01 ± 0.001	0.07 ± 0.01

Table 4.1. Gene expression changes due to mutation in Δ*ssl2245* and*Δsll1130*. Wild type, Δ*ssl2245* and Δ*sll1130* cells were grown at 34^{o}C and fold changes in gene expression were analysed using Agilent custom-made DNA microarray chips. The numbering of ORFs corresponds to that of (Kaneko *et al*, 1996). Plasmid-located genes are indicated with the name of the plasmid against its ORF number. Expression changes of the ORF numbers depicted in bold letters were confirmed by qRT-PCR analysis. All transcriptome data have been deposited in the KEGG database from where they can be downloaded under http://www.genome.jp/kegg-bin/get_htext?htext=Exp_DB&hier=1.

4.6 qRT-PCR analysis confirms DNA microarray expression changes

The first gene of plasmid-localized operons which were differentially expressed due to mutation in both *ssl2245* and *sll1130*, were selected for qRT-PCR validation of their expression changes, as observed in the DNA microarray analysis (Table 4.1, ORF numbers in bold letters). The genes selected were *sll7064, sll7067, sll7085, sll7090, slr7091, sll5097* and *sll6010*. Apart from these, two chromosome-located genes, *slr0909* and *sll1396* were also selected. qRT-PCR was performed with specific primers designed for each gene (Table 6.4). The qRT-PCR data generated demonstrated that the genes *sll7064, sll7067, sll7085, sll7090, slr7091, sll5097* were up-regulated and the genes *sll6010, slr0909* and *sll1396* were down-regulation in both the mutants in comparison to the wild type *Synechocystis* cells. These results confirmed that the gene expression changes observed by both DNA microarray and qRT-PCR analysis were consistent (Figure 4.5) and indeed suggested a direct or indirect involvement of Ssl2245 and Sll1130 in the regulation of expression of CRISPR2 and CRISPR3, as well as of certain chromosomal genes.

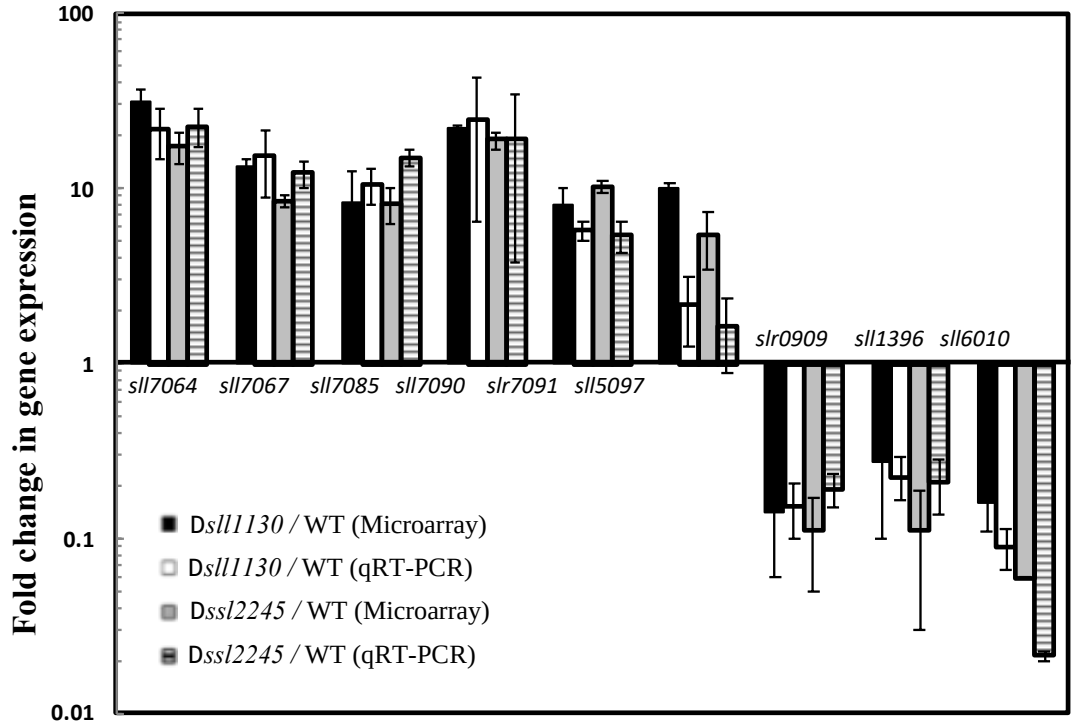

Figure 4.5. Confirmation of DNA microarray gene expression changes by qRT-PCR. Genes whose expression was up-regulated (*slr7064*, *sll7067*, *sll7085*, *sll7090*, *slr7091*, and *sll5097*) and the genes whose expression was down-regulated (*slr0909*, *sll1396*, and *sll6010*) due to mutation in Δ*sll1130* as well as in Δ*ssl2245* cells were selected for qRT-PCR analysis. *Black* and *grey bars* represent -fold changes observed by DNA microarray analysis; *white* and *striped bars* represent -fold changes observed by qRT-PCR analysis due to the mutation in *sll1130* and *ssl2245*, respectively. Similar results were obtained in two independent experiments; data are presented as mean ratios ± S.D. (*error bars*).

4.7 Enhanced pili formation in Δ*sll1130*

Synechocystis has been reported to consist of 4 individual pilin genes (*slr0079, slr1120, slr1456* and *sll135*) and also 3 operons consisting of pilin genes that are arranged in consecutive order (*sll1693–1696, slr1928–1931* and *slr2015–2017*). Though the pilin protein pilA1, encoded by the gene *sll1694* of the *sll1693–1696* operon has been reported to be the main protein involved in the extracellular pili formation, pilins encoded by the genes of the operon *slr2015 / slr2016 / slr2017* have also been reported to be critical for the locomotion of *Synechocystis* cells (Bhaya *et al*, 1999, 2000, 2001; Yoshihara *et al*, 2001). Since we observed up-regulation of the pilin genes *slr2016* and *slr2017* due to mutation in Δ*ssl2245 and* Δ*sll1130* (Table 4.1), we compared the pilus formation in wild type and Δ*sll1130* cells

using Atomic Force Microscopy (AFM). Wild type and *Δsll1130* cells growing in BG-11 liquid media were deposited onto mica sheets and were observed to be around 1 to 1.5 microns in diameter. The surface of the wild type cells appeared to have very few appendages or pili (Figure 4.6A). In contrast, the Δ*sll1130* cells were distinctly surrounded with multiple thread-like appendages (Figure 4.6B), suggesting a possible role of Sll1130 in regulating pilin expression and pilus formation in *Synechocystis*.

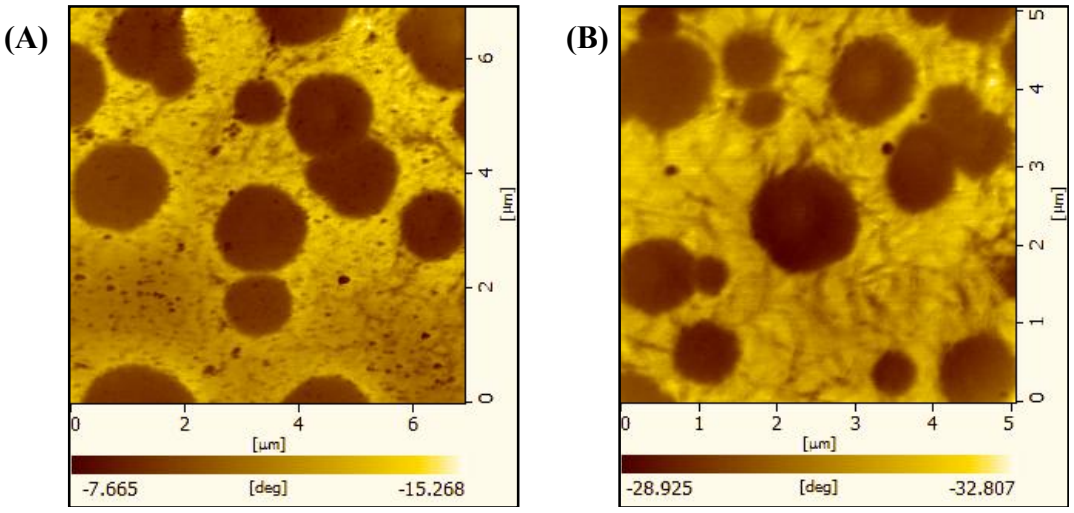

Figure 4.6. Atomic Force Microscopic images of air-dried wild type and Δ*sll1130* *Synechocystis* cells. **(A)** Wild type cells grown in liquid BG11 medium observed with very few appendages with relatively smooth surfaces and **(B)** Δ*sll1130* mutant cells grown in liquid BG11 medium observed with numerous hair-like appendages. Cells scanned and imaged with a scanning probe microscope (SPA400, Seiko, Japan) using the tapping mode at the scan rate of 1–2 Hz and a resonance frequency of 110–150 kHz.

4.8 Δ*sll1130* mutant cells are more heat tolerant than wild type *Synechocystis* cells

Since we obtained clues of a probable involvement of the putative Ssl2245-Sll1130 TA system in heat response from the phylogenic studies (Figure 4.1) and also due to the up-regulation of several heat-shock genes due to mutation is *ssl2245* and *sll1130* (Table 4.1), the effect of heat on the viability of Δ*sll1130* mutant cells was studied in comparison to wild type *Synechocystis* cells. Wild type and Δ*sll1130* cells were grown photoautotrophically at 34ºC in BG-11 medium buffered with 20 mM Hepes/NaOH (pH 7.5) under continuous illumination

at 70 μmol of photons / m^2 / s till an $O.D_{(730nm)}$ of around 0.6 and then shifted to 50°C. Wild type and Δ*sll1130* mutant cells were collected before and after heat treatment and stained with SYTOX green dye to check viability. Sytox stains viable cells as red fluorescence and dead cells as green fluorescence. We observed that in comparison to the wild type cells, the Δ*sll1130* mutant cells recovered faster upon heat shock, with a relatively greater number of mutant cells remaining viable, during prolonged incubation at 50°C. Figure 4.7 shows the heat tolerance of Δ*sll1130* mutant in comparison with wild type cells. Before incubation of cells at high temperature, both wild type and Δ*sll1130* cells appeared as bright red fluorescent cells, indicating that the cells were equally viable at the optimal growth temperature of 34°C (Figure 4.7A and E). When the exponentially growing cells were shifted to 50°C for 8 hours, while only 25-30% of the total wild type cells were viable (Figure 4.7C and I), almost 70-80% of the Δ*sll1130* cells remained viable (Figure 4.7G and I). Microorganisms have developed several strategies to survive unfavourable conditions. Among them, one such response of bacteria that has been reported is their ability to evade unfavourable conditions (biotic and abiotic) until the return of favourable conditions by alternating from unicellular to multicellular organization, like microbial colonies, aggregates and biofilms (Claessen *et al*, 2014; Johnson, 2008). Interestingly, a similar type of response was observed by the wild type cells, showing a tendency to form clumps during prolonged incubation at 50°C, although some of the cells continued to exist individually (Figure 4.7D). In contrast, mutant cells always existed as individual entities throughout the period of incubation at 50°C (Figure 4.7H). These results indicate that disruption of *sll1130* leads to a higher thermo-tolerance in *Synechocystis* and also pointed towards a possible involvement of the Ssl2245-Sll1130 TA system in the death of the wild type cells at high temperature of 50°C.

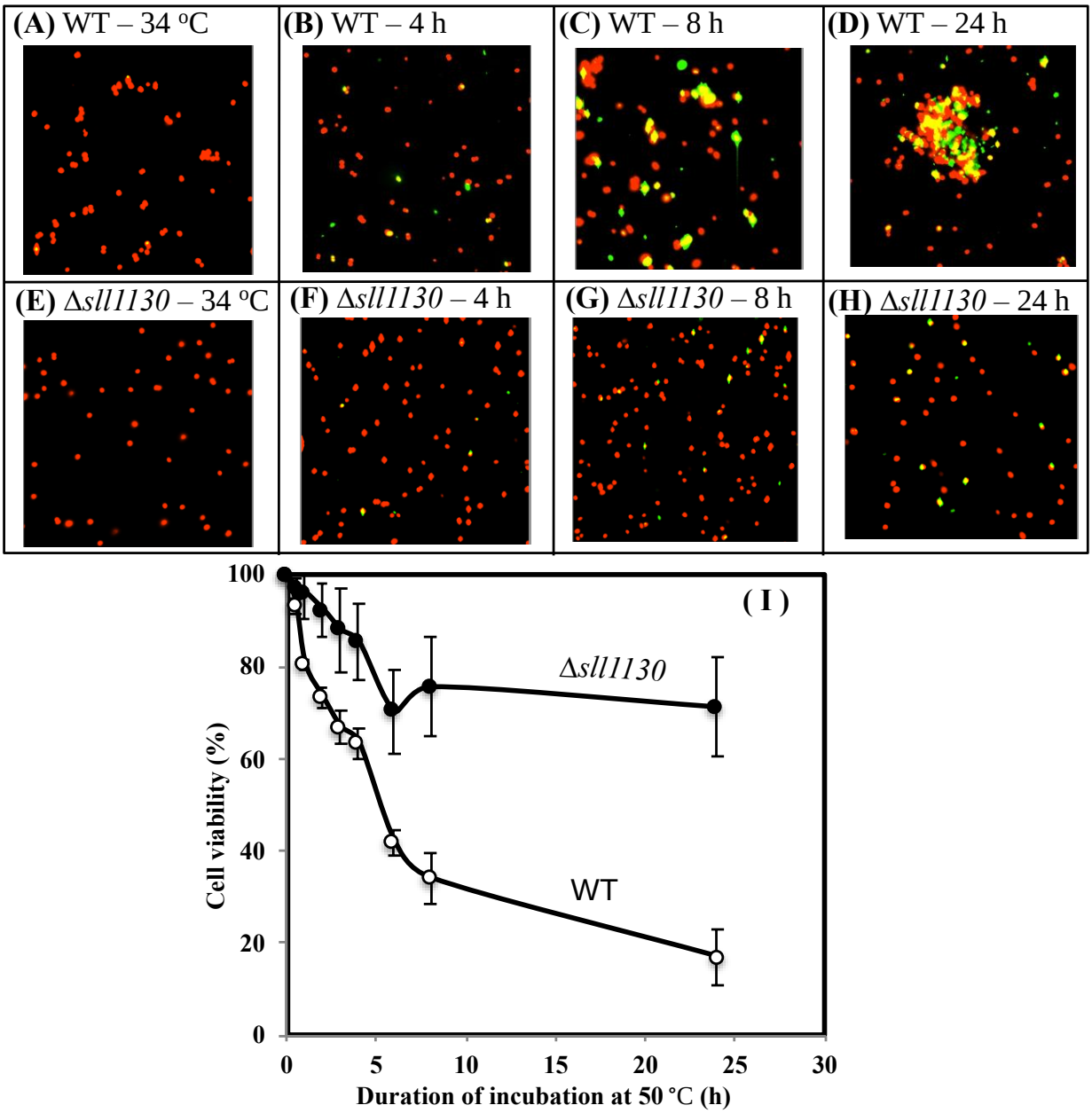

Figure 4.7. Survival rate of *Synechocystis* wild type and Δ*sll1130* cells during incubation at high temperature. Wild type and *Δsll1130* cells were grown at 34°C for 16 h (**A**, WT-34°C cells; **E**, Δ*sll1130*-34°C). Wild-type and Δ*sll1130* cells that were grown at 34°C for 16 h, subjected to heat treatment at 50°C for 4 h, 8 h and 24 h (**B**, WT-4 h; **C**, WT-8 h; **D**, WT-24 h; **F**, Δ*sll1130*-4 h; **G**, Δ*sll1130*-8 h; **H**, Δ*sll1130*-24 h). Scale bar = 10 μm. Cells were stained with SYTOX Green dye and the percentage of viable cells (red) and dead cells (green) in the wild type and Δ*sll1130* mutant before and during the course of incubation at 50°C were determined **(I)** by counting under 40x magnification using a confocal microscope. Open circles, wild-type cells; closed circles, Δ*sll1130* mutant cells. Data represents the mean ± SD for three independent experiments.

4.9 Gene expression changes due to heat stress in wild type *Synechocystis* cells

Wild type *Synechocystis* cells were grown photoautotrophically at 34°C in BG-11 medium buffered with 20 mM Hepes/NaOH (pH 7.5) under continuous illumination at 70 μmol of photons/m^2/s till an $O.D_{(730nm)}$ of around 0.6 and then shifted to 44°C for 3 hours. Total RNA was isolated from samples collected before and during heat treatment, and differentially expressed genes in heat treated wild type cells compared to untreated were identified using a new custom made DNA microarray chip (15K Agilent), which was designed to included probes that covered genes present on the genome as well as on the 7 plasmids of *Synechocystis*. As expected, due to the heat treatment, several heat-shock genes were observed to be up-regulated and among these were also few proteases (Table 4.2) . This data is consistent with the previous data on gene expression profiling during heat shock in *Synechocystis* (Suzuki *et al*, 2006). Proteases have been reported to function in degrading the comparatively labile antitoxin proteins during various stress conditions, thereby freeing the toxin from the TA complex, letting the toxin exert its function. The MazE antitoxin protein of the MazE-MazF TA system in *E. coli* has been reported to be degraded by the Serine protease ClpPA, under amino acid starvation (Aizenman *et al*, 1996). Similarly, a function of Lon proteases in its degradation during nutritional starvation has also been reported (Christensen *et al*, 2003). Several other antitoxin proteins like CcdA and RelB have been studied to be degraded by Lon proteases (Christensen *et al*, 2001; Van Melderen *et al*, 1996). Therefore, in correlation to these studies and the lower viability of wild type *Synechocystis* cells in comparison to *Δsll1130* cells during heat treatment, the up-regulation of proteases at high temperature in wild type cells indicated their possible involvement in degradation of the antitoxin protein Ssl2245. Among the genes down-regulated were the *ssl2245-sll1130* gene pair and several genes related to RNA polymerases and ribosomal proteins (Table 4.2). These results indicate a regulation of the *ssl2245-sll1130* TA system and translational

inhibition or rRNA degradation due to the heat stress in wild type cells.

Table 4.2. Gene expression changes due to heat stress in wild type *Synechocystis* cells

ORF No.	Function	WT-44°C (20min)	WT-44°C (60min)	WT-44°C (120min)	WT-44°C (180min)
Genes whose expression was up-regulated due to heat stress					
sll1514	16.6 kDa small heat shock protein	168.34±11.4	81.14± 8.31	49.46± 5.1	23.63± 1.91
sll0430	HtpG, heat shock protein 90	15.55±64.25	11.31± 5.64	16.7± 7.45	5.88± 0.45
sll0846	hypothetical protein	14.78± 5.07	5.69± 2.16	3.93± 1.37	2.56± 1.51
slr2075	10kD chaperonin	14.41± 1.77	34.51± 0.9	40.96± 2.27	28.37± 2.04
sll0170	DnaK protein 2, heat shock protein 70	14.35± 0.26	8.11± 0.76	8.47± 0.71	4.57± 0.35
slr1641	ClpB protein	14.06±14.75	4.3± 0.35	3.29± 0.43	2.1± 0.13
slr2076	60kD chaperonin	12.25± 1.21	33.29± 1.16	34± 1.28	27.55± 1.39
slr1674	hypothetical protein	10.22± 0.95	8.4± 0.84	7.4± 0.61	4.88± 0.19
sll0416	60 kDa chaperonin 2, GroEL2	8.45± 2.63	12.8± 0.64	14.73± 6.11	11.33± 0.47
sll0811	unknown protein	8.04 ± 0.54	2.62 ± 0.42	4.01 ± 0.34	3.84 ± 0.65
sll0306	RNA polymerase group 2 sigma factor	7.93± 8.81	3.48± 0.55	4.59± 0.23	2.4± 0.54
slr0093	DnaJ protein, heat shock protein 40, molecular chaperone	7.62± 0.69	3.92± 2.02	3.03± 0.75	2.2± 0.87
slr0967	hypothetical protein	5.16± 0.12	3.96± 0.18	3.38± 0.12	2.06± 0.11
slr1603	hypothetical protein	4.45± 0.13	2.09± 0.72	1.75± 2.46	1.38± 0.69
slr0095	O-methyltransferase	4.43± 0.22	1.95± 0.81	1.62± 0.08	1.3± 0.34
sll0021	probable exonuclease	4.42± 2.63	3.75± 0.55	1± 2.38	4.79± 0.31
sll0008	unknown protein	4.29± 0.45	0.58± 0.1	2.95± 3.17	0.79± 0.13
slr1915	hypothetical protein	3.87± 0.42	2.58± 2.84	2.37± 0.19	1.54± 0.76
slr0008	carboxyl-terminal processing protease	3.87± 0.17	2.57± 0.32	2.6± 0.87	1.89± 0.12
slr1963	water-soluble carotenoid protein	3.18± 0.16	1.95± 0.83	1.63± 0.53	1.07± 0.04
slr1516	superoxide dismutase	3.14± 0.08	2.16± 0.23	1.8± 0.16	1.45± 0.42
sll1106	hypothetical protein	3.03± 0.17	1.56± 0.11	1.23± 1.93	1.02± 0.08
sll0020	ATP-dependent Clp protease ATPase	3.03± 0.11	5.41± 0.86	4.06± 0.26	4.2± 0.82
sll0031	hypothetical protein	2.94± 0.26	1.19± 1.08	1.7± 0.49	2.54± 1.62
sll0939	hypothetical protein	2.88± 1.61	1.72± 0.03	2.23± 2.32	1.59± 0.08
sll0578	carboxylase ATPase subunit	2.84± 1.32	1.17± 0.05	1.13± 0.19	1.1± 0.04
sll0385	ATP-binding protein of ABC transporter	2.83± 1.45	0.98± 0.66	1.52± 1.8	1.68± 0.81
sll0608	hypothetical protein YCF49	2.8± 0.93	1.41± 0.72	1.87± 0.26	1.59± 0.39
ssl2971	hypothetical protein	2.79± 1.65	1.64± 0.17	1.39± 0.1	1.19± 0.08
slr1675	hydrogenase expression protein HypA1	2.75± 0.21	2.04± 0.07	2.34± 1.48	2.14± 0.1
slr7076	hypothetical protein	2.75± 0.22	1.49± 0.82	1.91± 0.06	1.86± 0.13
sll0310	hypothetical protein	2.7± 1.03	1.07± 0.05	1.08± 0.1	0.98± 0.07
sll8031	NADH dehydrogenase subunit NdhK	2.69± 0.18	1.17± 0.14	1.41± 0.08	1.08± 0.13
sll0060	hypothetical protein	2.62± 0.3	0.7± 0.04	5.1± 0.1	5.79± 0.35
sll0055	processing protease	2.62± 0.12	0.75± 0.06	4.6± 3.11	1.88± 2.28
sll0688	unknown protein	2.61± 0.18	1.89± 0.81	1.74± 0.27	1.66± 0.39

slr0364	hypothetical protein	2.6± 0.4	1.08± 0.64	1.25± 1.41	1.07± 0.75
sll0085	unknown protein	2.59± 0.82	0.92± 0.09	1.12± 0.04	0.92± 0.03
sll7027	unknown protein	2.59± 0.08	1.07± 0.06	1.53± 0.06	1.32± 0.05
sll0044	unknown protein	2.58± 10.29	3.97± 0.61	0.76± 1.75	4.94± 0.37
sll0723	unknown protein	2.55± 0.66	1.06± 0.1	1.43± 0.09	0.95± 0.09
sll0047	hypothetical protein YCF12	2.54± 1.52	1.5± 1.19	2.44± 0.19	3.37± 0.07
slr8022	hypothetical protein	2.52± 0.16	1.2± 0.13	1.49± 1.49	1.28± 0.1

Genes whose expression was down-regulated due to heat stress

slr0041	bicarbonate transport system permease	0.08±0.04	0.03±0	0.06± 2.16	0.04± 0
slr0012	ribulose bisphosphate carboxylase	0.09±0	0.14±0.12	0.15± 0.02	0.13± 0.2
slr1513	periplasmic protein, function unknown	0.11±0	0.06±0.01	0.1± 0.05	0.06± 0.02
slr1512	sodium-dependent bicarbonate transporter	0.13±0.01	0.08±0.04	0.14± 0	0.06± 0
slr0011	possible Rubisco chaperonin	0.14±0.12	0.17±0.02	0.18± 0.18	0.14± 0.02
slr1065	plobable glycosyltransferase	0.14±0.02	0.3±0.03	0.18± 0.05	0.29± 0.01
sll1696	hypothetical protein	0.15±0.1	0.25±0.05	0.28± 0.18	0.45± 0.03
slr1241	hypothetical protein	0.15±0.01	0.26±0.02	0.2± 0.05	0.23± 0
slr0737	photosystem I subunit II	0.16±0.01	0.43±0.02	0.21± 0	0.22± 0.08
ssr1375	hypothetical protein	0.16±0.01	0.3±0.11	0.19± 0.01	0.22± 0.01
sll1695	pilin polypeptide PilA2	0.17±0.01	0.24±0.02	0.29± 0.02	0.32± 0.02
slr0144	hypothetical protein	0.17±0.11	0.14±0.01	0.11± 0.01	0.09± 0.03
slr0040	bicarbonate transport substrate-binding	0.18±0.02	0.07±0.04	0.13± 0.25	0.08± 0.02
sll1694	pilin polypeptide PilA1	0.18±0.01	0.4±0.02	0.39± 0.25	0.33± 0.24
slr0009	ribulose bisphosphate carboxylase	0.18±0.02	0.24±0.02	0.3± 0.02	0.2± 0
slr0623	thioredoxin	0.18±0.12	0.3±0.02	0.22± 0.01	0.24± 0.23
sll1184	heme oxygenase	0.19±0.15	0.3±0.02	0.19± 0.01	0.18± 0.12
slr0906	photosystem II core light harvesting	0.19±0	0.85±0.18	0.64± 0.32	0.72± 0.2
slr0343	cytochrome b6-f complex subunit 4	0.19±0.15	0.73±0.04	0.64± 0.29	0.89± 0.03
slr1152	hypothetical protein	0.2±0.01	0.26±0.02	0.14± 0.07	0.15± 0.01
slr1957	hypothetical protein	0.2±0.01	0.16±0.01	0.1± 0.03	0.11± 0.01
sll1099	elongation factor Tu	0.2±0.06	0.81±0.71	1.07± 0.08	1.88± 0.16
ssr0536	unknown protein	0.21±0.15	0.33±0.11	0.21± 0.02	0.32± 0.26
slr1852	unknown protein	0.21±0.01	0.3±0.02	0.27± 0.02	0.32± 0.01
sll1130	unknown protein	0.23±0.02	0.47±0.05	0.51± 0.03	0.59± 0.02
ssl2245	unknown protein	0.27±0.04	0.38±0.04	0.36± 0.01	0.36± 0.01
sll1789	RNA polymerase beta prime subunit	0.23±0.13	0.26±0.16	0.32± 0.09	0.9± 0.05
ssl3445	50S ribosomal protein L31	0.24±0.05	0.71±0.01	1.13± 0.09	2.75± 0.27
slr1545	RNA polymerase ECF sigma-E factor	0.25±0.02	0.25±0.02	0.13± 0.15	0.14± 0.13
sll1712	DNA binding protein HU	0.27±0.98	0.29±0.02	0.18± 0.08	0.17± 0.06
ssl1426	50S ribosomal protein L35	0.28±0	0.56±0.03	0.68± 0.04	0.99± 0.59
sll0767	50S ribosomal protein L20	0.29±0.02	0.56±0.04	0.9± 0.32	1.26± 0.22
sll1322	ATP synthase A chain of CF(0)	0.29±0.01	0.26±0.01	0.26± 0.01	0.33± 0.02
sll1732	NADH dehydrogenase subunit 5	0.29±0.03	0.15±0.02	0.24± 0.01	0.17± 0.08
sll0541	acyl-lipid desaturase (delta 9)	0.3±0.02	0.31±0.1	0.39± 0.04	0.45± 0.05
slr1329	ATP synthase beta subunit	0.3±0.01	0.63±0.01	0.67± 0.03	0.94± 0.06

sll1745	50S ribosomal protein L10	0.32±0.02	0.5±0.03	0.68± 0.74	0.79± 0.07
ssl2615	ATP synthase C chain of CF(0)	0.33±0.02	0.28±0.08	0.29± 0.18	0.4± 0.07
sll1323	ATP synthase subunit b' of CF(0)	0.34±0.02	0.36±0.02	0.38± 0.01	0.56± 0.04
sll1746	50S ribosomal protein L12	0.34±0.01	0.64±0.06	0.72± 0.09	0.84± 0.08
ssl1784	30S ribosomal protein S15	0.35±0.02	0.7±0.02	0.82± 0.05	1.22± 0.11
sml0006	50S ribosomal protein L36	0.38±0.02	1.08±0.11	1.37± 0.11	2.46± 0.07
sll1824	50S ribosomal protein L25	0.39±0.19	1.3±0.03	1.25± 0.68	2.12± 60.2
ssl3437	30S ribosomal protein S17	0.4±0.01	0.92±0.04	1.09± 0.05	1.69± 0.03
sll1807	50S ribosomal protein L24	0.41±0.02	0.84±0.03	1.02± 0.06	1.7± 0.11
ssl2233	30S ribosomal protein S20	0.42±0.04	1.13±0.03	1.25± 0.13	1.46± 0.04

Table 4.2. **Gene expression changes due to heat treatment at 44ºC in wild type cells**. Wild type cells were grown at 34^{o}C and then shifted to 44^{o}C and fold changes in gene expression at 20, 60, 120 and 180 min were analysed using Agilent custom-made DNA microarray chips. The numbering of ORFs corresponds to that of (Kaneko *et al*, 1996).

4.10 Antitoxin Ssl2245 is less stable compared to toxin Sll1130

Toxin and antitoxin proteins of well characterized TA systems have been studied to have differential stability, with the antitoxin being less stable compared to the toxin and prone to degradation by cellular proteases upon exposure to stress. Therefore, the stablility of the Ssl2245 antitoxin and Sll1130 toxin proteins was tested during heat treatment. Western blotting analysis of the wild type *Synechocystis* cells shifted to 50°C for 12 h was carried out using anti-Sll1130 and anti-Ssl2245 antibodies. These results indicated that though there was a down-regulation of the genes of this operon upon heat treatment (Table 4.2), the Ssl2245 and Sll1130 protein levels increased upon heat treatment, with maximum levels observed at 3 h (Figure 4.8). Following this, the levels of Ssl2245 protein appeared to have significantly decreased in comparison with Sll1130 protein, indicated a lower stability of Ssl2245 (Figure 4.8).

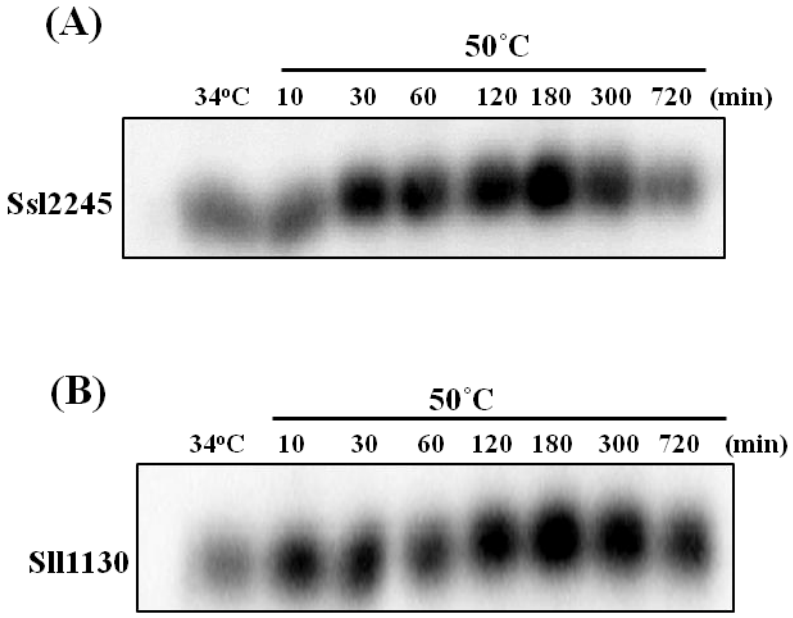

Figure 4.8. Stability analysis of Ssl2245 and Sll1130 proteins using Western blotting. Soluble proteins were extracted from wild type cells that were grown at 34°C for 16 h and then incubated at 50°C for 10, 30, 60, 120, 180, 300 and 720 min. Samples equivalent to 10 µg proteins were loaded in each well of a polyacrylamide gel (15%). Anti-Ssl2245 **(A)** and anti-Sll1130 **(B)** antibodies generated in rabbit were used to detect the respective proteins on the blot.

4.11 RNA integrity in wild type and Δ*sll1130* mutant cells at high temperature

Due to observation of the down-regulation of several genes related to ribosomal proteins and RNA polymerases, indicating a possible rRNA degradation upon exposure to high temperature in wild type cells (Table 4.1), the RNA integrity of wild type and Δ*sll1130* cells on treatment at high temperature was compared. We observed that at optimum temperature of 34°C, the RNA of both wild type and Δ*sll1130* cells remained intact (Figure4.9 A and B). However, upon shift to high temperature of 50°C, the RNA in wild type cells was observed to have degraded within 1 h (Figure 4.9A), whereas, the RNA of Δ*sll1130* cells was stable up to almost 8 h of heat treatment (Figure 4.9B). These results confirm the involvement of the endoribonuclease Sll1130 in the degradation of RNA in wild type cells due to heat treatment.

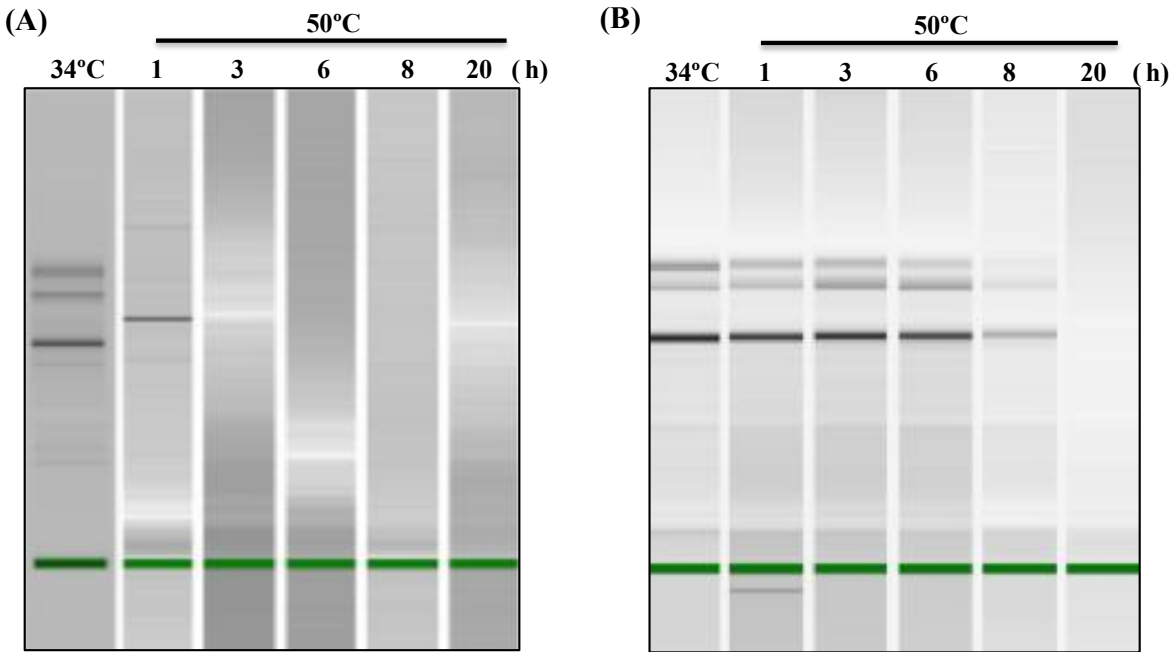

Figure 4.9. RNA Stability analysis in wild type and Δ*sll1130* cells at high temperature. RNA was isolated from wild type and Δ*sll1130* cells grown at 34°C till an $O.D_{(730nm)}$ of 0.6 was reached and then shifted to 50°C for 1, 3, 6, 8 and 20 h, respectively. Hundred ng of RNA from each sample at different time points was loaded onto an RNA pico chip. RNA from wild type cells degraded within 1 h of heat treatment **(A)** whereas, RNA from Δ*sll1130* cells were more stable, being intact till almost 8 h of heat treatment **(B)**.

4.12 Ssl2245 and Sll1130 physically interact with each other

Since Ssl2245 and Sll1130 showed similarity mostly to type II TA systems of other bacteria, where the toxin and antitoxin proteins are known to interact with each other, we tested the possibility of interaction between Ssl2245 and Sll1130. To test this interaction, a bacterial two hybrid system involving two plasmids, pT25 and pT18, harboring the ORFs *sll1130* and *ssl2245* respectively, was utilized. These plasmids were co-transformed into *E. coli* DHP1 strain that lacks adenylate cyclase (Δ*cya*) (Karimova *et al*, 1998). Simultaneously, the interaction of thioredoxin B (Slr1139) with Ssl2245 as well as Sll1130 was tested, because

Ssl2245 was reported to be a possible target of this thioredoxin (Hosoya-Matsuda *et al*, 2005). As expected, the DHP1 cells harboring empty plasmids, pT25 and pT18 (as a negative control) without any DNA inserts, did not change their color upon incubation of cells at 30^{o}C even after 48 h (Figure 4.10a). The DHP1 cells harboring pT25-RhlB and pPNP-T18 (as a positive control), turned to dark pink color upon plating onto MacConkey agar (Tseng *et al*, 2015) (Figure 4.10b). We observed a dark pink color formation on plating the DHP1 cells co-transformed with pT25-Sll1130 & pSsl2245-T18, demonstrating the strong interaction between Ssl2245 and Sll1130 (Figure 4.10c). Color change was not observed with the cells harboring pT25-Slr1139 & pSsl2245-T18 or pT25-Slr1139 & pSll1130-T18, suggesting that Slr1139 neither interacts with Ssl2245 nor Sll1130 (Figure 4.10d and e).

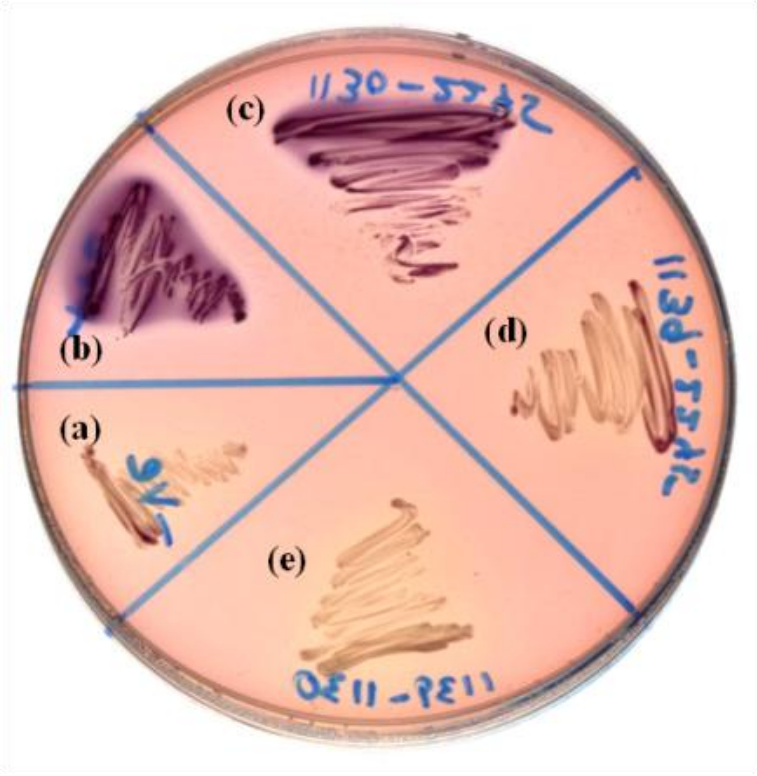

Figure 4.10. Ssl2245 and Sll1130 proteins are physically associated. (A) Demonstration of interaction between Ssl2245 and Sll1130 using a bacterial two hybrid system. The *E. coli* strain DHP1 carrying the plasmids encoding different proteins were plated on a MacConkey/maltose plate as indicated to visualize protein-protein interactions. The cells carrying pT25 and pT18 were negative controls **(a)**. The cells carrying pT25-RhlB and pPNP-T18 were positive controls **(b)**. The cells harboring, pT25-Sll1130 along with pSsl2245-T18 **(c)**; pT25-Slr1139 with pSsl2245-T18 **(d)**; pT25-Slr1139 with pSll1130-T18 **(e)**.

4.13 Ssl2245 and Sll1130 are co-eluted and form a stable multimeric complex

To verify the physical association demonstrated between Ssl2245 and Sll1130 using bacterial two hybrid system, the *ssl2245* and *sll1130* genes were cloned together in the pET28a *E. coli* expression vector in such a way that both proteins were expressed from the same plasmid upon induction, and only one protein contained the 6X His-tag. Thus, only Ssl2245 was expressed with an N-terminal 6X His-tag (His-Ssl2245). SDS-PAGE analysis of the purified protein elutes revealed that, along with the His-tagged Ssl2245, the Sll1130 protein was co-eluted despite lacking the purification tag (Figure 4.11A, lane 5 to 10). The calculated masses of His-Ssl2245 and Sll1130 were 11.29 and 12.92 KDa respectively. These results indicated a stable and strong physical interaction between Ssl2245 and Sll1130. The physical association between these two proteins could probably be due to electrostatic interactions, with Ssl2245 being an acidic protein with a pI of 4.2 and Sll1130 being a basic protein with a pI of 8.8. In addition, we observed a protein band at ~38 kDa, suggesting the association of these proteins possibly in a molecular ratio of 1:2 (Ssl2245:Sll1130) (Figure 4.11A, lane 6 to 9).

We determined the oligomeric state of the Ssl2245-Sll1130 protein complex by fractionating the purified and dialysed elute containing both the proteins along with known appropriate markers, such as thyroglobulin (669 kDa), apoferritin (440 kDa), β-amylase (232 kDa), bovine γ-globulin (160 kDa), transferrin (76 kDa) and ovalbumin (43 kDa) on a gel exclusion column. We observed that the Ssl2245-Sll1130 protein complex eluted with maximum intensity along with transferrin (Figure 4.11B). The molecular mass of the complex was around 76 kDa, indicating that the complex might consist of one Ssl2245 dimer, predicted to be around 22.58 kDa because the molecular mas of His-Ssl2245 was calculated to be 22.29 kDa and two Sll1130 dimers, predicted to be around 55.68 kDa because the

molecular mass of Sll1130 was calculated to be 12.92 kDa based on amino acid sequence, thereby forming a hetero-hexamer. This result is in correlation with the formation of a complex of Ssl224 and Sll1130 proteins in a 1:2 molecular mass ratio based on SDS-PAGE analysis. This prediction is similar to the identification of the formation of a hetero-hexamer ($MazF_2$-$MazE_2$-$MazF_2$) by the well characterized MazEF TA system of *E. coli* (Zhang et al., 2003).

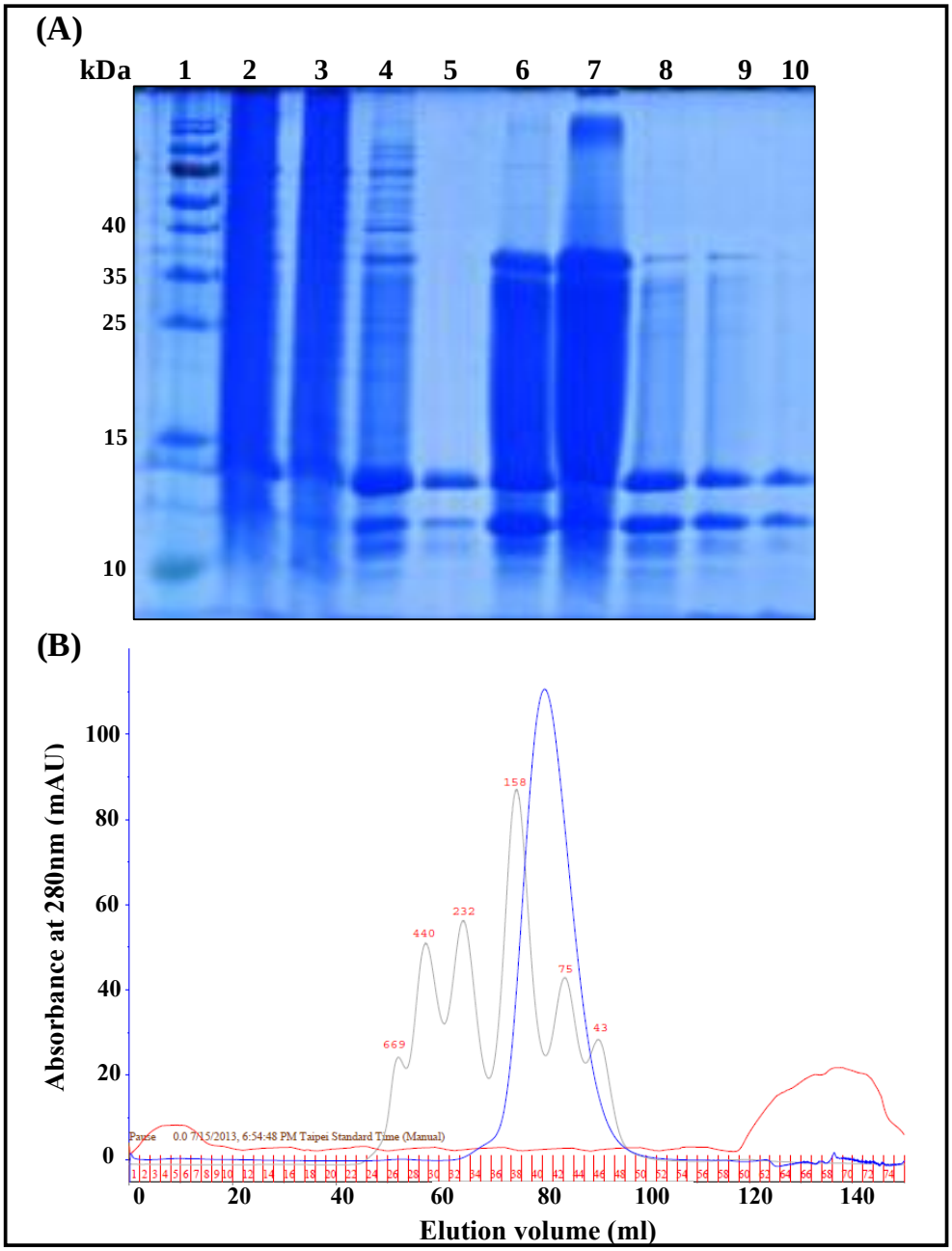

Figure 4.11. (A) SDS–PAGE analysis of co-expressed and purified His-tagged Ssl2245 and Sll1130 recombinant proteins in *E. coli* BL21 (DE3). Lane 1, protein molecular weight standards (Cat No. 26616, Thermo Scientific); lane 2, whole cell lysate of induced *E. coli* harboring plasmid pET-*ssl2245-sll1130*; lane 3, Flow through collected from Ni-NTA column; lane 4 & 5, Protein washes of Ni-NTA column with 40mM imidazole used for eluting non-specifically bound proteins; lane 6-10, protein elutes with increasing concentrations of imidazole of 100mM, 100Mm, 200mM, 300mM and 400mM. The molecular masses of protein standards are shown in the left margin. **(B) Gel exclusion chromatographic analysis of His-Ssl2245-Sll1130 protein complex on Sephacryl S-100 column.** His-Ssl2245-Sll1130 proteins mixed with gel filtration markers was loaded on to the column. Thyroglobulin (669 kDa), apoferritin (440 kDa), β-amylase (232 kDa), bovine γ-globulin (160 kDa), transferrin (76 kDa), ovalbumin (43 kDa) indicated with grey lines and His-Ssl2245-Sll1130 indicated with blue line.

4.14 Stoichiometry and effect of high temperature on interaction between Ssl2245 and Sll1130

Isothermal titration calorimetry was utilised to characterize the interaction between Ssl2245 and Sll1130 at different temperatures, based on their thermodynamic parameters. Figure 4.12A and B show typical ITC profiles generated during the binding of Ssl2245 to Sll1130 at normal temperature of 25^{o}C and high temperature of 50^{o}C respectively. These titration profiles indicated that upon injection of small aliquots of Ssl2245 into Sll1130, large exothermic heat of binding was generated and this heat of binding was observed to have decreased in magnitude gradually with subsequent injections, demonstrating saturation behaviour. The data obtained at both the temperatures could be best fitted by a non-linear least squares approach to the '*one set of sites*' binding model, which yielded the association constant (K_a), stoichiometry of binding (*n*), and the thermodynamic parameters, enthalpy of binding (ΔH) and entropy of binding (ΔS). These values are listed in Table 4.3. At 25^{o}C the stoichiometry, *n* was found to be 0.46, indicating that each molecule of Ssl2245 binds to two molecules of Sll1130, i.e., the two proteins form a complex with a 1:2 (Ssl2245:Sll1130) stoichiometry. Therefore, confirming our prediction from the results in figure 4.11 that these two proteins indeed exist as a complex in a 1:2 stiochiometric ratio. Since we predicted the involvement of the Ssl2245-Sll1130 TA system in death of cells at high temperature of 50^{o}C , in order to exhibit its function as a endoribonuclease, the Sll1130 protein has to first be freed from the Ssl2245-Sll1130 complex, where its function is being masked by the antitoxin Ssl2245. To test this hypothesis, the association between these two proteins was also studied at 50^{o}C. Table 4.3 clearly indicates that though binding constant K_a did not change significantly between 25^{o}C and 50^{o}C, the stoichiometry of interaction was observed to have decreased quite drastically from 0.46 at 25^{o}C to 0.16 at 50^{o}C. This decrease in stoichiometry of interaction indicates a probably loss of association between Ssl2245 and Sll1130 proteins

at high temperature of 50°C, strengthening the hypothesis of involvement of free Sll1130 toxin in death of the wild type cells that was observed at high temperature (Figure 4.7).

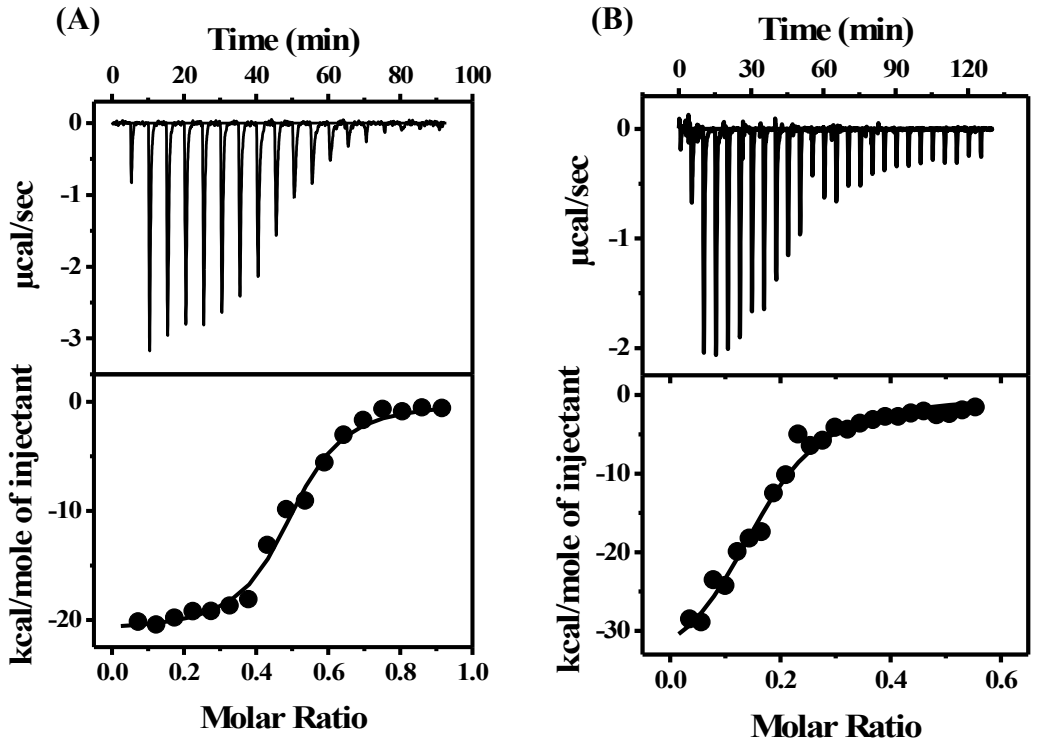

Figure 4.12. Temperature dependent analysis of interactions between Ssl2245 and Sll1130 proteins. ITC profiles corresponding to the binding of Ssl2245 to Sll1130 at 25ºC **(A)** and at 50ºC **(B)** are shown. Upper panels show the raw data for the titration of the two proteins and lower panels show the integrated heats of binding obtained from the raw data, after subtracting the heat of dilution. The solid lines in the bottom panels represent the best fits of the experimental data to the *one set of sites* binding model in the MicroCal Origin ITC data analysis software.

Table 4.3. Thermodynamic parameters obtained from ITC studies

T (^{0}C)	Stoichiometry (*n*)	$K_a \times 10^5$ (M^{-1})	ΔH (kcal.mol^{-1})	ΔS (cal.mol^{-1}.K^{-1})
25	0.46 (±0.03)	8.7 (±4.8)	-19.9 (±1.8)	-39.5 (±4.8)
50	0.16 (±0.01)	7.45 (±2.54)	-37.6 (±6.8)	-89.7 (±21.0)

Table 4.3. Thermodynamic parameters obtained from isothermal titration calorimetric studies on the interaction between Ssl2245 and Sll1130 at different temperatures. Average values obtained from 2 independent titrations are shown together with standard deviations (in parentheses).

4.15 Thermal stability of Ssl2245 and Sll1130

Most of the proteins tend to be quite unstable at high temperatures and since we observed a loss of association between Ssl2245 and Sll1130 proteins at high temperature of 50^{o}C. We tested if the loss of association could be due to denaturation of the proteins at such high temperature. Therefore, to characterize the thermal stability of Ssl2245 and Sll1130, we performed high sensitivity differential scanning calorimetry. Typical DSC thermograms of Ssl2245 and Sll1130 generated are depicted in Figure. 4.13A and B. From these thermograms, the temperatures corresponding to the unfolding transition of Ssl2245 and Sll1130 proteins were obtained as 60.6^{o}C and 62.8^{o}C respectively. This result indicates that the unfolding temperatures of both the proteins were observed to be much higher than 50^{o}C, confirming that the loss of association between Ssl2245 and Sll1130 proteins at 50^{o}C is temperature dependent and not due to denaturation or thermal inactivation of either of the proteins.

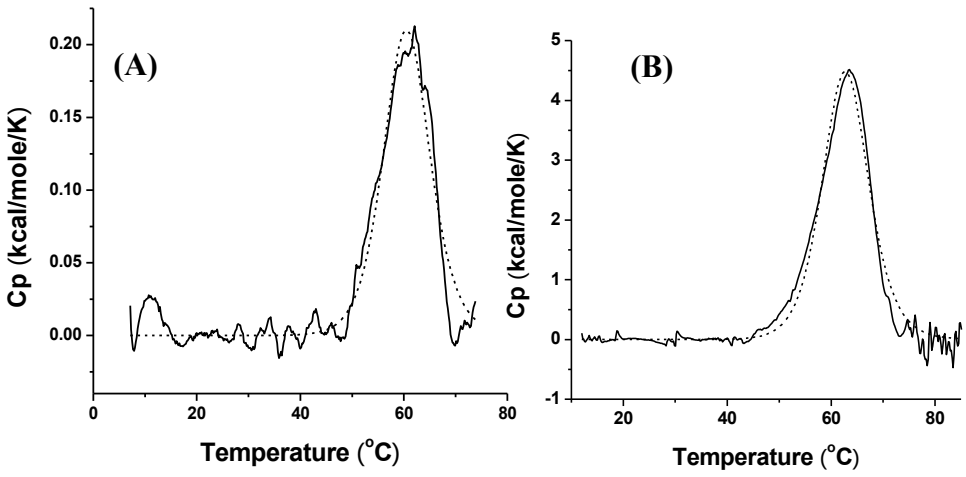

Figure 4.13. Thermal stability analysis of Ssl2245 and Sll1130 proteins. Panels **(A)** and **(B)** show DSC thermograms of Ssl2245 and Sll1130, respectively. The data points are shown as black lines, and the dotted lines are the best fits of the DSC data to a non-two-state transition model. Concentrations of Ssl2245 and Sll1130 used were 149μM and 81μM, respectively.

4.16 Ssl2245 and Sll1130 protein structural changes at high temperatures

Since the possibility of denaturation of proteins being the reason for loss of association observed between Ssl2245 and Sll1130 has been eliminated, we wanted to test the possible protein structural changes that might have happened to either of the proteins due to the high temperature. To study the protein conformational changes in detail, Circular Dichroism spectroscopic studies were carried out. CD spectra of Ssl2245 and Sll1130 proteins were recorded at various temperatures between 25 and 60^{o}C. Figure 4.14A and C depict the far UV CD spectra of Sll1130 and Ssl2245, respectively, indicating that the secondary structures of both the proteins remained unaltered between 25 and 60^{o}C, and these results are consistent with the results of DSC studies presented above (Figure 4.13). Whereas, though the near UV CD spectra of Ssl2245 was observed to remain mostly unaltered at temperatures between 25 and 60^{o}C, it was interesting to observe that the molar ellipticity in the corresponding spectra of Sll1130 exhibited significant decrease at and above 40^{o}C. These results indicate the formation of a molten-globule like structure by Sll1130 at temperatures above 40^{o}C (Arai & Kuwajima, 2000; De Laureto *et al*, 2002). The formation of this molten globule like structure by Sll1130 protein might be the reason for its loss of association from Ssl2245 at high temperatures.

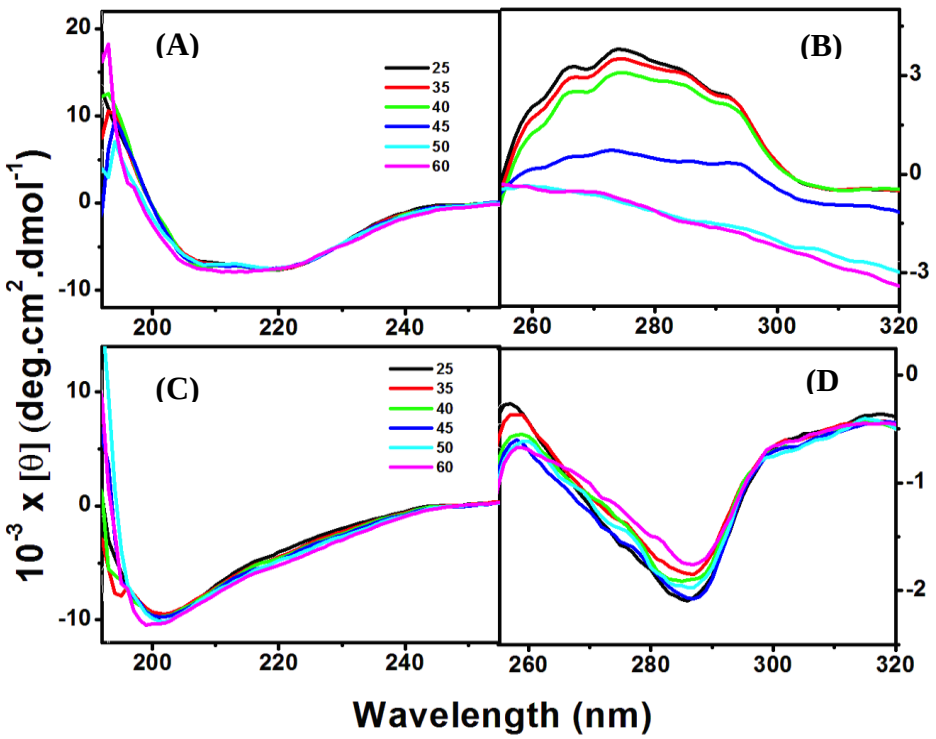

Figure 4.14: Circular dichroism spectra of Sll1130 and Ssl2245 recorded at various temperatures. Far and near UV CD spectra, respectively, of Sll1130 **(A, B)**. Far and near UV CD spectra, respectively, of Ssl2245 **(C, D)**. Spectra recorded at various temperatures have been identified by different colors as indicated in the figure.

4.17 Endoribonuclease activity of Sll1130 at high temperature

Upon observation of a conformational change and formation of a molten globule like structure of Sll1130 at and above 40^{o}C, we checked if the endoribonuclease activity of Sll1130 was retained at these temperatures. To test this, *in vitro* synthesized *slr1788-slr1789* mRNA transcripts were incubated with Ssl2245 alone, Sll1130 alone and also with both SSl2245-Sll1130 together at 37, 50 and 60^{o}C respectively. At 37^{o}C, as previously observed (Figure 4.4), Sll1130 degraded the mRNA transcript and the RNase activity of Sll1130 was masked by the antitoxin Ssl2245 (Figure 4.15A). However, at 50 and 60^{o}C, the antitoxin Ssl2245 lost its ability to mask the function of Sll1130 as the mRNA transcripts were still degraded by Sll1130 at these temperatures (Figure 4.15B and C). These results indicated that the molten globule form of Sll1130 at high temperatures is also functionally active, acting as

an RNase and the loss of ability of Ssl2245 to mask the function of Sll1130 confirmed the loss of association between these two proteins, freeing the toxin Sll1130.

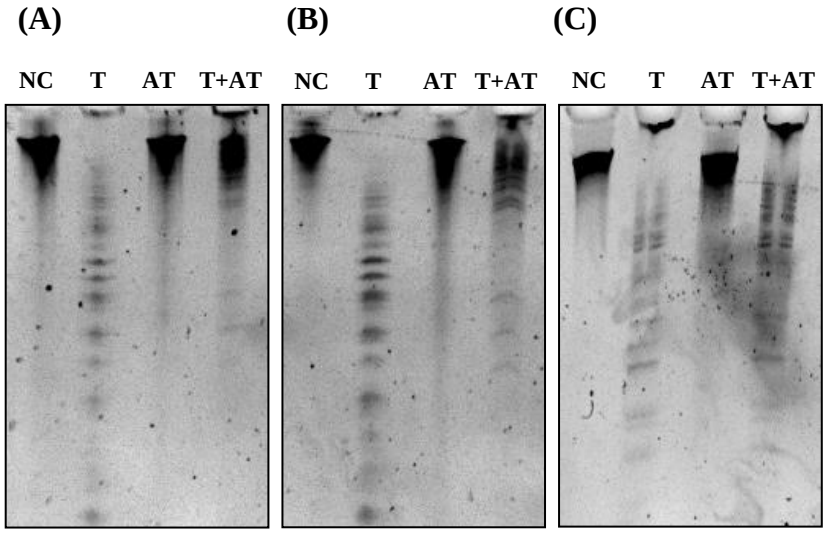

Figure 4.15: Effect of temperature on endoribonuclease activity of Sll1130 in the presence or absence of Ssl2245. *In vitro* synthesized *slr1798-slr1799* mRNA with Sll1130, with Ssl2245, or with both Sll1130 and Ssl2245 at 37ºC **(A)**, 50ºC **(B)** and 60ºC **(C)** respectively. Sll1130 degrades RNA at high temperature, even in the presence of Ssl2245. NC, negative control in which RNA was incubated for 30 min in the elution buffer without any protein.

5. DISCUSSION AND CONCLUSION

As many as 69 putative TA systems have been identified in *Synechocystis*, among which 47 TA pairs are located on the chromosome and 22 TA pairs are located on the 4 large plasmids, pSYSM, pSYSX, pSYSA and pSYSG (Kopfmann *et al*, 2016). Three of these TA systems which are chromosomally located, *sll0525-ssl1004*, *all1092-ssl2138* and *ssl2923-ssl2922*; and 1 TA system located on the plasmid pSYSG, *slr8014-slr8013* were experimentally studied. In these TA systems, the function of the putative toxins in causing growth inhibition and the function of the putative antitoxins in masking the function of their respective toxins have been verified (Kopfmann *et al*, 2016). Among the 7 TA systems located on plasmid pSYSA, only *sll7003-ssl7004* was experimentally tested, where the Sll7003 toxin has been reported to act as Mg^{2+} dependent RNase whose function is antagonised by the antitoxin, Sll7004 (Kopfmann & Hess, 2013). The *relNE* (*ssr1114-slr0664*) TA pair of *Synechocystis*, located on the chromosome, has been reported to be regulated proteolytically by ATP dependent proteases (Ning *et al*, 2011). Several TA systems have been characterized in E. coli, reported to have roles in plasmid maintenance, antibiotic resistance and under stress conditions such as nutrient deprivation (Hayes, 2003; Gerdes & Molin, 1986; Lewis, 2008; Hazan & Engelberg-Kulka, 2004; Dwyer *et al*, 2012). Recently, there have been several reports on the role of TA systems in mediating PCD and persister formation in bacterial populations exposed to various kinds of stress (Rice & Bayles, 2008; Engelberg-Kulka *et al*, 2004; Maisonneuve & Gerdes, 2014; Wen *et al*, 2014; Hu *et al*, 2010). To the best of our knowledge, this is the first detailed study of a cyanobacterial TA system, demonstrating its role in survival of *Synechocystis* under high temperature conditions. The proteins Ssl2245 and Sll1130 have properties of transcriptional regulators, containing AbrB-like and PemK- like domains, respectively. The genes of the *ssl2245-sll1130* TA system have been reported to be heat repressible (Suzuki *et al*, 2006) and the

proteins were observed to have high similarity to putative MazEF proteins from thermophilic bacteria, assumed to have roles in response to heat adaptation (Figure 4.1). Therefore, it was likely that the Ssl2245-Sll1130 TA system might have evolved for high temperature adaptation in *Synechocystis*. In almost all type II TA systems reported, the antitoxin gene is located upstream of the toxin gene, with both the genes having atleast a few nucleotide overlap and organized in the same operon. Similarly, in *Synechocystis*, the putative antitoxin gene *ssl2245* is located upstream of the putative toxin gene, *sll1130* with both the genes having a four nucleotide overlap (Figure 1.8). The toxins of TA systems are known to function by causing cell growth inhibition or cell death. Therefore, the effect of expression of Sll1130 in *Synechocystis* was tested to check its toxicity. The Sll1130 protein was expressed in the ΔΔ*ssl2245-sll1130* mutant cells, lacking the putative antitoxin Ssl2245. The Sll1130 protein was observed to have led to significantly lower the growth, confirming its toxicity (Figure 4.2). One of the major mechanisms by which toxins of TA systems induces cell death is by possessing endoribonuclease activity and the function of toxins is known to be antagonised by their respective antitoxins. Similarly, the Sll1130 toxin was observed to have endoribonuclease activity, that degraded RNA transcripts *in vitro,* while its function was masked by the antitoxin Ssl224 at optimum growth temperature (Figure 4.3). Previous studies performed on Sll1130 from our laboratory indicated that it is a negative regulator of several heat shock genes and also demonstrated that the Δ*sll1130* mutant recovered faster upon heat shock in comparison with the wild type cells (Krishna *et al,* 2012). Therefore, we were curious to check the viability of the Δ*sll1130* mutant in comparison with wild type under continuous heat treatment. We noticed that the Δ*sll1130* mutant was highly tolerant to heat even under prolonged incubation at high temperature whereas, most of the wild type cells were dead (Figure 4.4). These results indicated that the death in the wild type cells is probably mediated by the Ssl2245-Sll1130 TA system. The genes in a TA system are known

to be functionally antagonistic to each other. Since we demonstrated that the Ssl2245-Sll1130 proteins were also antagonistic to each other, with the endoribonuclease function of Sll1130 toxin masked by the antitoxin Ssl2245, we expected a physical association between these proteins. Indeed, bacterial two hybrid screening and co-elution studies revealed a strong physical interaction between the two proteins (Fig 4.10 & 4.11A). Gel exclusion chromatography demonstrated that these proteins form a complex that is eluted at around 160 kDa. The size of this complex was similar to the hetero-hexamer ($MazF_2$-$MazE_2$-$MazF_2$) formed by the well characterized MazEF TA system of *E. coli* (Zhang *et al*, 2003a), giving us an idea that Ssl2245-Sll1130 proteins also could possibly form a hetero-hexamer as the sizes of these proteins are similar to MazE and MazF proteins of *E. coli* respectively (Fig. 4.11B). As mentioned earlier, the association between the two proteins could be due to electrostatic interaction owing to the acidic and basic nature of Ssl2245and Sll1130 proteins, respectively.

The DNA microarray and qRT-PCR based gene expression profiling of Δssl2245 and Δ*sll1130* mutants revealed a role of this TA system in regulation of plasmid gene expression (Table 4.1 and Figure 4.5). The gene expression changes observed in both the mutants were found to be similar. Especially, we observed inducible expression of CRISPR-associated genes, which are known to play very important roles in phage defense (Kopfmann & Hess, 2013). There are several reports demonstrating role of TA systems in viral defense in *E. coli* (Hazan & Engelberg-Kulka, 2004). Since we observed an up-regulation of several pilin related genes in these mutants, we expected a difference in the pili formation in the mutant, in comparison with the wild type cells. As expected, our results based on the AFM imaging showed a large number of distinct pili surrounding the Δ*sll1130* mutant cells whereas, the wild type cells were found to have a comparatively smoother cell membrane (Figure 4.6). Apart from the CRISPR associated genes and pilin genes, several other heat-shock genes were also up-regulated, indicating a role of this TA system in heat stress. Hence, the

Ssl2245-Sll1130 TA system could be multifunctional, similar to the well characterized MazE-MazF TA system of *E. coli*. But, in order to confirm the involvement of this TA system in regulation of plasmid genes and in formation of pili, further detailed elucidation has to be carried out.

The gene expression profiling of wild type *Synechocystis* cells exposed to high temperatures of 44ºC, revealed the up-regulation of several heat-shock genes, along with few proteases. Among the genes down-regulated was the *ssl2245-sll1130* TA gene pair, indicating the regulation of this TA system under heat stress. Several genes belonging to RNA polymerases and ribosomal proteins were also down-regulated, which in correlation with the death of most of the wild type cells but not *Δsll1130* mutant cells observed at high temperature, gave us an idea that the cell death could have been mediated by RNA degradation, leading to translational inhibition by the endoribonuclease Sll1130. To test this hypothesis, the stability of RNA in the wild type and *Δsll1130* mutant cells exposed to high temperature was studied. As expected, at high temperature of 50ºC, the RNA of wild type cells was degraded within 1 h, whereas the RNA of *Δsll1130* mutant cells was stable upto almost 8h (Figure 4.9). Therefore, it is indeed the toxin endoribonuclease Sll1130 that functions in degradation of RNA and ultimately leads to death in wild type cells at high temperature.

The antitoxins are labile proteins, with lower stability compared to the toxin proteins. Several antitoxins have been reported to be degraded by cellular proteases under stress conditions. Since we observed up-regulation of cellular proteases in the wild type cells at high temperature, we tested the stability of Ssl2245 and Sll1130 proteins at 50ºC. Similar to the other characterized antitoxin proteins, the Ssl2245 antitoxin protein levels were observed to have decreased after 3 h of heat treatment, indicating the lower stability of Ssl2245 protein compared to Sll1130 (Figure 4.8).

TA systems are known to induce PCD under various stress conditions, whereby a portion of the bacterial population is sacrificed, aiding the survival of the remaining cells (persisters) (Allocati *et al*, 2015). In some cases, upon induction of PCD, the bacterial populations were reported to form biofilms, where the persisters reduce their metabolic activities and thrive on the nutrients obtained from the surrounding dead cells until the return of favourable conditions. High temperature is one such harsh condition that is reported to induce biofilm formation in cyanobacteria (Johnson, 2008). Interestingly, the more closely related orthologs of Ssl2245-Sll1130 proteins were identified in *Dactylococcopsis salina* from a heliothermal saline pool; *Stanieria cyanosphaera*, a thermo-epilithic biofilm forming cyanobacteria; *Microcystis aeruginosa* and several other colony forming cyanobacteria (Figure 4.1). *Microcystis aeruginosa* has been reported to show colony size distribution in its population as an adaptive strategy to any disturbances in its surroundings and in which PCD related orthocaspase and TA genes are physically linked (Klemenčič & Dolinar, 2016). These examples strongly support the role of the Ssl2245-Sll1130 TA system in PCD under heat stress with a possibility of alternation between a free-living planktonic unicellular lifestyle and a colonial/biofilm sessile lifestyle (Foster *et al*, 2009; Pandey, 2013; Walsby *et al*, 1983; Sabart *et al*, 2013). Supporting this hypothesis, we observed the formation of clumps of the wild type cells upon incubation at high temperature, which seemed to be a characteristic similar to the biofilm formation or where a part of the population within the biofilm seemed to have undergone PCD, sacrificing that portion of the cells, so that the remaining cells could survive through the heat stress (Figure 4.7).

For the toxin and antitoxin proteins to induce PCD, they have to separate from each other, in order to free the toxin protein to be able to exert its function. Therefore, since we proposed an involvement of the Ssl2245-Sll1130 TA system in inducing PCD under heat stress, we expect the dissociation of these two proteins from each other, freeing the Sll1130

toxin to function. To test this, we used ITC, which demonstrated that the stoichiometry of interaction between Ssl2245 and Sll1130 proteins decreased at high temperature (Figure 4.12B). Since most of the proteins are known to be unstable at high temperatures, we tested if the decreased association could possibly be due to degradation of the proteins. To verify this, the stability of the two proteins was tested using DSC, which confirmed their thermal stability to be quite high with unfolding temperatures above 60ºC (Figure 4.13). These unfolding temperatures were well above the temperature at which the decrease of association between these proteins was observed. We then used CD spectroscopy to determine if there were any protein structural changes that might have led to the decrease of association. These studies revealed that the Sll1130 protein exists as a molten-globule like structure at temperatures at and above 40ºC, whereas the structure of Ssl2245 protein was observed to be unaltered upto temperatures as high as 60ºC.

At optimal temperatures, since we demonstrated the inhibition of endoribonuclease activity of toxin Sll1130 by the antitoxin Ssl2245, we wanted to test how these proteins function at high temperatures. Though Sll1130 toxin exhibited protein structural changes at and above temperatures of 40ºC, it still retained its endoribonuclease activity (Figure 4.14A). The Sll1130 toxin was observed to degrade the RNA transcripts *in vitro* even when it was incubated together with the antitoxin Ssl2245 at high temperature, indicating that the antitoxin Ssl2245 lost its ability to mask the function of Sll1130, owing to their loss of association at these temperatures (Fig.4.14B and C).

In conclusion, we generated a model for our study, depicting the how the Ssl2245-Sll1130 TA system functions at optimal and high temperatures respectively in *Synechocystis*. At optimum growth temperatures, the Ssl2245 and Sll1130 proteins interact with each other with a stoichiometry of 1:2 and probably form a hetero-hexameric protein complex ($Sll1130_2$-$Ssl2245_2$-$Sll1130_2$). Within this complex, the Ssl2245 masks the function of Sll1130, and the

cells grow normally. However, at high temperature, due to protein structural changes in Sll1130 leading to formation of a molten-globule like structure, there is a loss of association with its antitoxin Ssl2245. The free toxin Sll1130, still retaining its endoribonuclease activity, degrades cellular RNA leading to translational inhibition and ultimately programmed cell death. Thus, we report for the first time a putative TA system involving heat responsive antitoxin (MazE) and toxin (MazF), encoded by the ORFs *ssl2245* and *sll1130* respectively, which mediate heat induced PCD in *Synechocystis* upon exposure to high temperature. Therefore, based on these experimental evidences, we designated these genes, *ssl2245* and *sll1130* as *mazE* and *mazF* respectively.

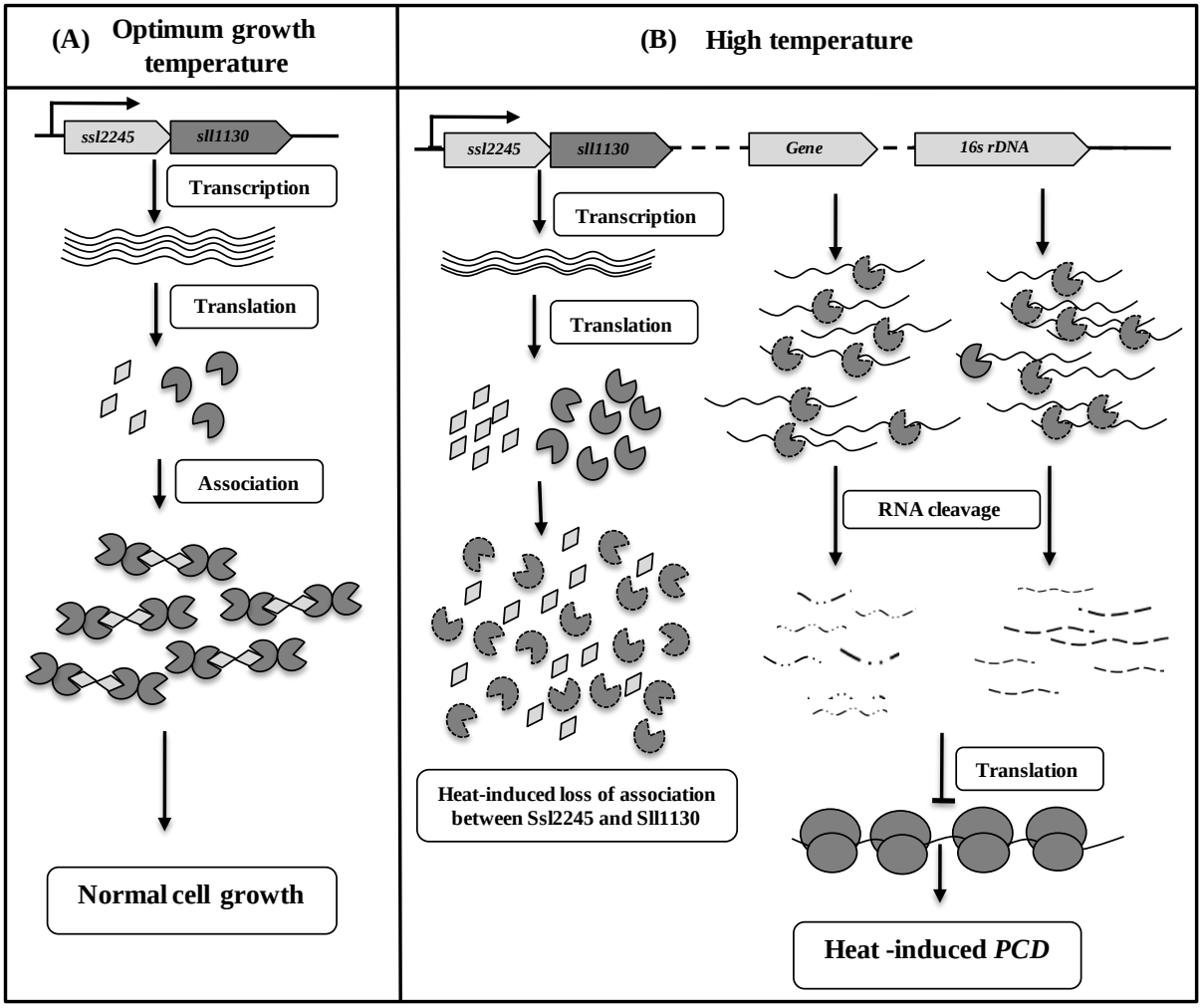

Figure 5.1. Schematic representation of heat induced programmed cell death mediated by MazE and MazF. (A) *ssl2245* and *sll1130* genes constitute a dicistronic operon and are co-transcribed. The Ssl2245 and Sll1130 form a complex under optimal growth conditions. Two molecules of Sll1130 are associated with one molecule of Ssl2245. Sll1130 is a ribonuclease whose function is masked by Ssl2245 under optimal growth conditions. **(B)** At high temperature, Sll1130 undergoes a transition to a molten globule like form and the association between Ssl2245 and Sll1130 is significantly decreased. Since Sll1130 is a stable ribonuclease, the free molecules degrade 16S rRNA and several other mRNA species. Degradation of 16S rRNA leads to inhibition of translation causing growth arrest and eventually induces PCD of the bacterial cells. ◇; Ssl2245; Sll1130; , molten-globule form of Sll1130.

6. PRIMER SEQUENCES

Table 6.1. Primers used for amplification of *sll1130* for over-expression and growth analysis

Name	Primer sequence (5'→3')	Restriction enzyme site
sll1130-pSyn FP	GGTCATATGAATACAATTTACGAACAATTTG	NdeI
sll1130-pSyn RP	GGAGGTACCACCGAGTTTAAAAACATGGGGAA	KpnI

Table 6.2. Primers used for expression of *ssl2245* and *sll1130*

Name	Primer sequence (5'→3')	Restriction enzyme site
Ssl2245-Exp-FP	CGGCATATGTCTTATCAATGCTTACAAACTAGCTACG	NdeI
Ssl2245-Exp-RP	GGCAAGCTTTCATAGGTGTCGGTATGCCAGAATTATCAGC	HindIII
Sll1130-Exp-FP	GCAGGCATATGAATACAATTTACGAAC	NdeI
Sll1130-Exp-RP	CGTCGAATTCCTAACCGAGTTTAAAAACATGG	EcoRI

Table 6.3. Primers used for amplification of *16s rDNA* and *slr1788-1789* for *in vitro* transcription

Name	Primer sequence (5'→3')	Restriction enzyme site
16s rDNA invitro FP	GAAATTAATACGACTCACTATAGGGACA ATGGAGAGTTTGATCCTGGCAGG	-
16s rDNA invitro RP	AAAGGAGGTGATCCAGCCACACCTTCC	-
slr1788-1789 invitro FP	GAAATTAATACGACTCACTATAGGGA TGGTTAGAGCTATACGTCCTCCC	-
slr1788-1789 invitro RP	CTAAGAAGGAATTGGCGCTATGG	-

Table 6.4. Primers used for qRT-PCR

Gene	Forward primer (5'→3')	Reverse primer (5'→3')
sll7064	TCCAAGCGGCGATCGGGCTG	AAGCGGGCTTCAAATACGCCTAGG
sll7067 (cmr2, cas10)	GATCGCCGCTGGGTGCAGTGTAAG	GTTAACTAGCCGACCATCAACGCTC
sll7085 (cmr6)	GCTACCAGCGTTTGATGCGTTGGG	GCCTGTGTTTTGCATCACCTCACGG
sll7090 (cmr2, cas10)	GCGATGTTTGCCCGAAGCAGTGG	CCAATGCTCCGGCTAAGGCG
slr7091	CCTTCCCGACTTCTCTTTGCCCGC	GAGCATGAAAGTCGAACAGGCCACC
sll5097	CACAGCAGGCAGAAATGAAGAATCAG	GGATGCGATACTCTCGAATACGGTC
sll6010	GGTGGGGCCAGCAACGGTGAGC	GGTATGGGAAACGTGATGTCGTACTGGG
slr0909	CAGGAGCGAATCCCAGCAAAGG	CAGCGGCAATCTGAGCTAGGG
sll1396	CCGACTGCCTCCCAGCCATG	CGGTCTGCTTTGCGGAGATAACC

Table 6.5. Primers used for amplification of ssl2245, *sll1130* and *slr1139* for bacterial two hybrid screening

Name	Primer sequence (5'→3')	Restriction enzyme site
ssl2245-T18-FP	GGGCTCGAGGATGTCTATCAATGCTTACAAACTAGCTACG	XhoI
ssl2245-T18-RP	GGAAAGCTTATTAGGTGTCGGTATGCAGAATTATCAGC	HindIII
sll1130-T18-FP	GGCTCGAGGATGAATACAATTTACGAACAATTTGACGTC	XhoI
sll1130-T18-RP	CGGAAGCTTATACCGAGTTTAAAAACATGGGGAAAAGCAC	HindIII
sll1130-T25-FP	GGGCTGCAGGGATGAATACAATTTACGAACAATTTGACGTC	PstI
sll1130-T25-RP	GGACCCGGGCCTAACCGAGTTTAAAAACATGGGGAAAAG	BamHI
slr1139-T25-FP	GGGCTGCAGGGATGAGTTTACTGGAAATCACCGACGC	PstI
slr1139-T25-RP	GGACCCGGGCTTAAATAAAATCCAATTCCTCTTTCAGTAACTC	BamHI

Table 6.6. Primers used for expression and co-elution of *ssl2245-sll1130*

Name	Primer sequence (5'→3')	Restriction enzyme site
His2245-1130-F	GGACATATGTCTATCAATGCTTACAAACTAGC	NdeI
His2245-1130-R	CTCAAGCTTCTAACCGAGTTTAAAAACATGGG	HindIII

7. REFERENCES

1. Aizenman E, Engelberg-Kulka H & Glaser G (1996) An Escherichia coli chromosomal 'addiction module' regulated by guanosine [corrected] 3',5'-bispyrophosphate: a model for programmed bacterial cell death. *Proc. Natl. Acad. Sci. U. S. A.* 93: 6059–6063
2. Allocati N, Masulli M, Di Ilio C & De Laurenzi V (2015) Die for the community: An overview of programmed cell death in bacteria. *Cell Death Dis.* 6: e1609
3. Anantharaman V & Aravind L (2003) New connections in the prokaryotic toxin-antitoxin network: relationship with the eukaryotic nonsense-mediated RNA decay system. *Genome Biol.* 4(12):R81
4. Arai M & Kuwajima K (2000) Role of the molten globule state in protein folding. *Adv. Protein Chem. 53:*209-282
5. Balaban NQ (2011) Persistence: Mechanisms for triggering and enhancing phenotypic variability. *Curr. Opin. Genet. Dev. 2(6):*768-775
6. Balaban NQ, Merrin J, Chait R, Kowalik L & Leibler S (2004) Bacterial persistence as a phenotypic switch. *Science.* 305(5690):1622-5
7. Belitsky M, Avshalom H, Erental A, Yelin I, Kumar S, London N, Sperber M, Schueler-Furman O & Engelberg-Kulka H (2011) The Escherichia coli Extracellular Death Factor EDF Induces the Endoribonucleolytic Activities of the Toxins MazF and ChpBK. *Mol. Cell.* 41(6):625-35
8. Bernard P & Couturier M (1992) Cell killing by the F plasmid CcdB protein involves poisoning of DNA-topoisomerase II complexes. *J. Mol. Biol.* 226(3):735-45
9. Bhaya D, Bianco NR, Bryant D & Grossman A (2000) Type IV pilus biogenesis and motility in the cyanobacterium Synechocystis sp. PCC6803. *Mol. Microbiol.* 37(4):941-51
10. Bhaya D, Takahashi A & Grossman AR (2001) Light regulation of type IV pilus-dependent motility by chemosensor-like elements in Synechocystis PCC6803. *Proc. Natl. Acad. Sci.* 98(13):7540-5
11. Bhaya D, Watanabe N, Ogawa T & Grossman AR (1999) The role of an alternative sigma factor in motility and pilus formation in the cyanobacterium Synechocystis sp. strain PCC6803. *Proc. Natl. Acad. Sci.* 96(6):3188–3193
12. Black DS, Irwin B & Moyed HS (1994) Autoregulation of hip, an operon that affects lethality due to inhibition of peptidoglycan or DNA synthesis. *J. Bacteriol.* 176(13): 4081–4091
13. Black DS, Kelly AJ, Mardis MJ & Moyed HS (1991) Structure and organization of hip, an operon that affects lethality due to inhibition of peptidoglycan or DNA synthesis. *J. Bacteriol.* 173(18):5732-9
14. Blower TR, Pei XY, Short FL, Fineran PC, Humphreys DP, Luisi BF & Salmond GPC (2011) A processed noncoding RNA regulates an altruistic bacterial antiviral system. *Nat. Struct. Mol. Biol.* 18(2):185-90
15. Boggild A, Sofos N, Andersen KR, Feddersen A, Easter AD, Passmore LA & Brodersen DE (2012) The crystal structure of the intact E. coli RelBE toxin-antitoxin complex provides the structural basis for conditional cooperativity. *Structure.* 20(10):1641-8
16. Brantl S & Jahn N (2015) SRNAs in bacterial type I and type III toxin-antitoxin systems. *FEMS Microbiol. Rev.* 39(3):413-27
17. Brauner A, Fridman O, Gefen O & Balaban NQ (2016) Distinguishing between resistance, tolerance and persistence to antibiotic treatment. *Nat. Rev. Microbiol.* 14(5):320-30
18. Brielle R, Pinel-Marie ML & Felden B (2016) Linking bacterial type I toxins with their actions. *Curr. Opin. Microbiol.* 30:114-121

19. Bukowski M, Rojowska A & Wladyka B (2011) Prokaryotic toxin-antitoxin systems - the role in bacterial physiology and application in molecular biology. *Acta Biochim. Pol.* 58(1):1-9
20. Castro-Roa D, Garcia-Pino A, De Gieter S, Van Nuland NAJ, Loris R & Zenkin N (2013) The Fic protein Doc uses an inverted substrate to phosphorylate and inactivate EF-Tu. *Nat. Chem. Biol.* 9(12):811-7
21. Čelešnik H, Tanšek A, Tahirović A, Vižintin A, Mustar J, Vidmar V & Dolinar M (2016) Biosafety of biotechnologically important microalgae: intrinsic suicide switch implementation in cyanobacterium Synechocystis sp . PCC 6803 . *Biol. Open. 5(4):519-28*
22. Chenna R, Sugawara H, Koike T, Lopez R, Gibson TJ, Higgins DG & Thompson JD (2003) Multiple sequence alignment with the Clustal series of programs. *Nucleic Acids Res.* 31(13):3497-500
23. Christensen-Dalsgaard M, Jørgensen MG & Gerdes K (2010) Three new RelE-homologous mRNA interferases of Escherichia coli differentially induced by environmental stresses. *Mol. Microbiol.* 75(2):333–348
24. Christensen SK, Mikkelsen M, Pedersen K & Gerdes K (2001) RelE, a global inhibitor of translation, is activated during nutritional stress. *Proc. Natl. Acad. Sci.* 98(25):14328-33
25. Christensen SK, Pedersen K, Hansen FG & Gerdes K (2003) Toxin-antitoxin loci as stress-response-elements: ChpAK/MazF and ChpBK cleave translated RNAs and are counteracted by tmRNA. *J. Mol. Biol.* 332(4):809–819
26. Claessen D, Rozen DE, Kuipers OP, Søgaard-Andersen L & Van Wezel GP (2014) Bacterial solutions to multicellularity: A tale of biofilms, filaments and fruiting bodies. *Nat. Rev. Microbiol.* 12:115–124
27. Clissold PM & Ponting CP (2000) PIN domains in nonsense-mediated mRNA decay and RNAi. *Curr. Biol.* 10(24):R888-90
28. Cook GM, Robson JR, Frampton RA, McKenzie J, Przybilski R, Fineran PC & Arcus VL (2013) Ribonucleases in bacterial toxin-antitoxin systems. *Biochim. Biophys. Acta - Gene Regul. Mech.* 1829(6-7):523-31
29. Critchlow SE, O'Dea MH, Howells AJ, Couturier M, Gellert M & Maxwell A (1997) The interaction of the F plasmid killer protein, CcdB, with DNA gyrase: Induction of DNA cleavage and blocking of transcription. *J. Mol. Biol. 273(4):*826-839
30. Cruz JW, Rothenbacher FP, Maehigashi T, Lane WS, Dunham CM & Woychik NA (2014) Doc toxin is a kinase that inactivates elongation factor Tu. *J. Biol. Chem.* 289(11):7788–7798
31. Dao-Thi MH, Van Melderen L, De Genst E, Afif H, Buts L, Wyns L & Loris R (2005) Molecular basis of gyrase poisoning by the addiction toxin CcdB. *J. Mol. Biol.* 348(5):1091-102
32. Dienemann C, Bøggild A, Winther KS, Gerdes K & Brodersen DE (2011) Crystal structure of the VapBC toxin-antitoxin complex from Shigella flexneri reveals a hetero-octameric DNA-binding assembly. *J. Mol. Biol.* 414(5):713-22
33. Dwyer DJ, Camacho DM, Kohanski MA, Callura JM & Collins JJ (2012) Antibiotic-Induced Bacterial Cell Death Exhibits Physiological and Biochemical Hallmarks of Apoptosis. *Mol. Cell* 46:561–572
34. Engelberg-Kulka H (2005) mazEF: a chromosomal toxin-antitoxin module that triggers programmed cell death in bacteria. *J. Cell Sci.* 118(Pt 19):4327-32
35. Engelberg-Kulka H, Amitai S, Kolodkin-Gal I & Hazan R (2006) Bacterial programmed cell death and multicellular behavior in bacteria. *PLoS Genet.* 2(10):e135
36. Engelberg-Kulka H GG (1999) Addiction modules and programmed cell death and antideath in bacterial cultures. *Annu. Rev. Microbiol.* 53:43–70

37. Engelberg-Kulka H, Reches M, Narasimhan S, Schoulaker-Schwarz R, Klemes Y, Aizenman E & Glaser G (1998) rexB of bacteriophage λ is an anti-cell death gene. *PNAS* 95:15481–15486
38. Engelberg-Kulka H, Sat B, Reches M, Amitai S & Hazan R (2004) Bacterial programmed cell death systems as targets for antibiotics. *Trends Microbiol.* 12:66–71
39. Falla TJ & Chopra I (1998) Joint tolerance to β-lactam and fluoroquinolone antibiotics in Escherichia coli results from overexpression of hipA. *Antimicrob. Agents Chemother.* 42(12):3282-4
40. Fineran PC, Blower TR, Foulds IJ, Humphreys DP, Lilley KS & Salmond GPC (2009) The phage abortive infection system, ToxIN, functions as a protein–RNA toxin–antitoxin pair. *Proc. Natl. Acad. Sci.* 106(3):894-9
41. Foster JS, Green SJ, Ahrendt SR, Golubic S, Reid RP, Hetherington KL & Bebout L (2009) Molecular and morphological characterization of cyanobacterial diversity in the stromatolites of highborne cay, bahamas. *ISME J.* 3(5):573-87
42. Fozo EM (2012) New type I toxin-antitoxin families from 'wild' and laboratory strains of E. coli: Ibs-Sib, ShoB-OhsC and Zor-Orz. *RNA Biol.* 9(12):1504-12
43. Galvani C, Terry J & Ishiguro EE (2001) Purification of the RelB and RelE proteins of Escherichia coli: RelE binds to RelB and to ribosomes. *J. Bacteriol.* 183(8):2700-3
44. Garcia-Pino A, Christensen-Dalsgaard M, Wyns L, Yarmolinsky M, Magnuson RD, Gerdes K & Loris R (2008) Doc of prophage P1 is inhibited by its antitoxin partner Phd through fold complementation. *J. Biol. Chem.* 283(45):30821-7
45. Gazit E & Sauer RT (1999) The Doc toxin and Phd antidote proteins of the bacteriophage P1 plasmid addiction system form a heterotrimeric complex. *J. Biol. Chem.* 274(24):16813-8
46. Gerdes K (2000) Toxin-antitoxin modules may regulate synthesis of macromolecules during nutritional stress. *J. Bacteriol.* 182(3):561-72
47. Gerdes K, Christensen SK & Løbner-Olesen A (2005) Prokaryotic toxin-antitoxin stress response loci. *Nat. Rev. Microbiol.* 3(5):371-82
48. Gerdes K & Molin S (1986) Partitioning of plasmid R1. Structural and functional analysis of the parA locus. *J. Mol. Biol.* 190(3):269-79
49. Gerdes K, Poulsen L & Thisted T (1990) The hok killer gene family in gram-negative bacteria. *New Biol.* 2(11):946-56
50. Gerdes K, Rasmussen PB & Molin S (1986) Unique type of plasmid maintenance function: postsegregational killing of plasmid-free cells. *Proc. Natl. Acad. Sci.* 83(10):3116-20
51. Germain E, Castro-Roa D, Zenkin N & Gerdes K (2013) Molecular Mechanism of Bacterial Persistence by HipA. *Mol. Cell.* 52(2):248-54
52. Gotfredsen M & Gerdes K (1998) The Escherichia coli relBE genes belong to a new toxin-antitoxin gene family. *Mol. Microbiol.* 29(4):1065-76
53. H. Wada and N. Murata (1989) Synechocystis PCC6803 Mutants Defective in Desaturation of Fatty Acids. *Plant Cell Physiol.* 30(7):971–978
54. Hayes F (2003) Toxins-antitoxins: Plasmid maintenance, programmed cell death, and cell cycle arrest. *Science (80-.).* 301:1496–1499
55. Hazan R & Engelberg-Kulka H (2004) Escherichia coli mazEF-mediated cell death as a defense mechanism that inhibits the spread of phage P1. *Mol. Genet. Genomics* 272: 227–234
56. Hazan R, Sat B & Engelberg-Kulka H (2004) Escherichia coli mazEF-mediated cell death is triggered by various stressful conditions. *J. Bacteriol.* 186(11):3663-9

57. Hosoya-Matsuda N, Motohashi K, Yoshimura H, Nozaki A, Inoue K, Ohmori M & Hisabori T (2005) Anti-oxidative stress system in cyanobacteria: Significance of type II peroxiredoxin and the role of 1-Cys peroxiredoxin in Synechocystis sp. strain PCC 6803. *J. Biol. Chem.* 280:840 – 846
58. Hu M, Zhang X, Li E & Feng Y-J (2010) Recent Advancements in Toxin and Antitoxin Systems Involved in Bacterial Programmed Cell Death. *Int. J. Microbiol.* 2010:781430
59. Hurley JM & Woychik NA (2009) Bacterial toxin HigB associates with ribosomes and mediates translation-dependent mRNA cleavage at A-rich sites. *J. Biol. Chem.* 284(28):18605-13
60. Jaffe A, Ogura T & Hiraga S (1985) Effects of the ccd function of the F plasmid on bacterial growth. *J. Bacteriol.* 163(3):841-9
61. Jiang Y, Pogliano J, Helinski DR & Konieczny I (2002) ParE toxin encoded by the broad-host-range plasmid RK2 is an inhibitor of Escherichia coli gyrase. *Mol. Microbiol.* 44(4):971-9
62. Johnson EP, Ström AR & Helinski DR (1996) Plasmid RK2 toxin protein ParE: Purification and interaction with the ParD antitoxin protein. *J. Bacteriol.* 178(5):1420-9
63. Johnson LR (2008) Microcolony and biofilm formation as a survival strategy for bacteria. *J. Theor. Biol.* 251:24–34
64. Kamada K & Hanaoka F (2005) Conformational change in the catalytic site of the ribonuclease YoeB toxin by YefM antitoxin. *Mol. Cell* 19:497–509
65. Kamada K, Hanaoka F & Burley SK (2003) Crystal structure of the MazE/MazF complex: Molecular bases of antidote-toxin recognition. *Mol. Cell.* 11(4):875-84
66. Kaneko T, Sato S, Kotani H, Tanaka A, Asamizu E, Nakamura Y, Miyajima N, Hirosawa M, Sugiura M, Sasamoto S, Kimura T, Hosouchi T, Matsuno A, Muraki A, Nakazaki N, Naruo K, Okumura S, Shimpo S, Takeuchi C, Wada T, et al (1996) Sequence analysis of the genome of the unicellular cyanobacterium synechocystis sp. strain PCC6803. II. Sequence determination of the entire genome and assignment of potential protein-coding regions. *DNA Res. 3:*109-136
67. Karimova G, Pidoux J, Ullmann A & Ladant D (1998) A bacterial two-hybrid system based on a reconstituted signal transduction pathway. *Proc. Natl. Acad. Sci. U. S. A.* 95(10):5752-6
68. Kavitha M, Bobbili KB & Swamy MJ (2010) Differential scanning calorimetric and spectroscopic studies on the unfolding of Momordica charantia lectin. Similar modes of thermal and chemical denaturation. *Biochimie.* 92(1):58-64
69. Kawano M (2012) Divergently overlapping cis-encoded antisense RNA regulating toxin-antitoxin systems from E. coli: Hok/sok, ldr/rdl, symE/symR. *RNA Biol.* 9(12):1520-7
70. Keshari N & Adhikary SP (2013) Characterization of cyanobacteria isolated from biofilms on stone monuments at Santiniketan, India. *Biofouling.* 29(5):525-36
71. Kim Y, Wang X, Ma Q, Zhang XS & Wood TK (2009) Toxin-antitoxin systems in Escherichia coli influence biofilm formation through YjgK (TabA) and fimbriae. *J. Bacteriol.* 191(4):1258-67
72. Kim Y & Wood TK (2010) Toxins Hha and CspD and small RNA regulator Hfq are involved in persister cell formation through MqsR in Escherichia coli. *Biochem. Biophys. Res. Commun.* 391(1):209-13
73. Klemenčič M & Dolinar M (2016) Orthocaspase and toxin-antitoxin loci rubbing shoulders in the genome of Microcystis aeruginosa PCC 7806. *Curr. Genet.* 62(4):669-675
74. Kolodkin-Gal I, Hazan R, Gaathon A, Carmeli S & Engelberg-Kulka H (2007) A linear pentapeptide is a quorum-sensing factor required for mazEF-mediated cell death in Escherichia coli. *Science.* 318(5850):652-5

75. Kolodkin-Gal I, Sat B, Keshet A & Engelberg-Kulka H (2008) The communication factor EDF and the toxin-antitoxin module mazEF determine the mode of action of antibiotics. *PLoS Biol.* 6(12):e319
76. Kopfmann S & Hess WR (2013) Toxin-antitoxin systems on the large defense plasmid pSYSA of synechocystis sp. pCC 6803. *J. Biol. Chem.* 288(10):7399-409
77. Kopfmann S, Roesch SK & Hess WR (2016) Type II toxin-antitoxin systems in the unicellular cyanobacterium synechocystis sp. PCC 6803. *Toxins (Basel).* 8(7)pii: E228
78. Krishna PS, Rani BR, Mohan MK, Suzuki I, Shivaji S & Prakash JSS (2012) A novel transcriptional regulator, Sll1130, negatively regulates heat-responsive genes in Synechocystis sp. PCC6803 . *Biochem. J.* 449(3):751-60
79. Kumar S, Kolodkin-Gal I & Engelberg-Kulka H (2013) Novel quorum-sensing peptides mediating interspecies bacterial cell death. *MBio*
80. Kumar S, Stecher G & Tamura K (2016) MEGA7: Molecular Evolutionary Genetics Analysis Version 7.0 for Bigger Datasets. *Mol. Biol. Evol.* 33(7):1870-4
81. de la Hoz AB, Ayora S, Sitkiewicz I, Fernandez S, Pankiewicz R, Alonso JC & Ceglowski P (2000) Plasmid copy-number control and better-than-random segregation genes of pSM19035 share a common regulator. *Proc. Natl. Acad. Sci.* 97(2):728-33
82. De Laureto PP, Frare E, Gottardo R & Fontana A (2002) Molten globule of bovine α-lactalbumin at neutral pH induced by heat, trifluoroethanol, and oleic acid: A comparative analysis by circular dichroism spectroscopy and limited proteolysis. *Proteins Struct. Funct. Genet.* 49(3):385-97
83. Lehnherr H, Maguin E, Jafri S & Yarmolinsky MB (1993) Plasmid addiction genes of bacteriophage P1: doc, which causes cell death on curing of prophage, and phd, which prevents host death when prophage is retained. *J. Mol. Biol.* 233(3):414-28
84. Lewis K (2008) Multidrug tolerance of biofilms and persister cells. *Curr. Top. Microbiol. Immunol.* 322:107–31
85. Lewis K (2010) Persister Cells. *Annu. Rev. Microbiol.* 64:357-72
86. Los DA, Ray MK & Murata N (1997) Differences in the control of the temperature-dependent expression of four genes for desaturases in Synechocystis sp. PCC 6803. *Mol. Microbiol.* 25(6):1167-75
87. Maisonneuve E, Castro-Camargo M & Gerdes K (2013) X(p)ppGpp controls bacterial persistence by stochastic induction of toxin-antitoxin activity. *Cell.* 154(5):1140-1150
88. Maisonneuve E & Gerdes K (2014) Molecular mechanisms underlying bacterial persisters. *Cell.* 157:539–48
89. Maisonneuve E, Shakespeare LJ, Jørgensen MG & Gerdes K (2011) Bacterial persistence by RNA endonucleases. *Proc. Natl. Acad. Sci.* 108(32):13206-11
90. Makarova KS, Wolf YI, Alkhnbashi OS, Costa F, Shah SA, Saunders SJ, Barrangou R, Brouns SJJ, Charpentier E, Haft DH, Horvath P, Moineau S, Mojica FJM, Terns RM, Terns MP, White MF, Yakunin AF, Garrett RA, van der Oost J, Backofen R, et al (2015) An updated evolutionary classification of CRISPR-Cas systems. *Nat. Rev. Microbiol.* 13(11):722-36
91. Makarova KS, Wolf YI & Koonin E V. (2009) Comprehensive comparative-genomic analysis of Type 2 toxin-antitoxin systems and related mobile stress response systems in prokaryotes. *Biol. Direct.* 4:19
92. Maki S, Takiguchi S, Horiuchi T, Sekimizu K & Miki T (1996) Partner switching mechanisms in inactivation and rejuvenation of Escherichia coli DNA gyrase by F plasmid proteins LetD (CcdB) and LetA (CcdA). *J. Mol. Biol.* 256(3):473-8
93. Masuda H, Tan Q, Awano N, Wu KP & Inouye M (2012) YeeU enhances the bundling of cytoskeletal polymers of MreB and FtsZ, antagonizing the CbtA (YeeV) toxicity in Escherichia coli. *Mol. Microbiol.* 84(5):979-89

94. Masuda Y, Miyakawa K, Nishimura Y & Ohtsubo E (1993) chpA and chpB, Escherichia coli chromosomal homologs of the pem locus responsible for stable maintenance of plasmid R100. *J. Bacteriol.* 175(21):6850-6
95. Meinhart A, Alonso JC, Strater N & Saenger W (2003) Crystal structure of the plasmid maintenance system epsilon/zeta: functional mechanism of toxin zeta and inactivation by epsilon 2 zeta 2 complex formation. *Proc Natl Acad Sci U S A.* 100(4):1661-6
96. Van Melderen L & De Bast MS (2009) Bacterial toxin-Antitoxin systems: More than selfish entities? *PLoS Genet.* 5(3):e1000437
97. Van Melderen L, Thi MHD, Lecchi P, Gottesman S, Couturier M & Maurizi MR (1996) ATP-dependent degradation of CcdA by Lon protease. Effects of secondary structure and heterologous subunit interactions. *J. Biol. Chem.* 271:27730–27738
98. Miallau L, Faller M, Janet C, Arbing M, Guo F, Cascio D & Eisenberg D (2009) Structure and proposed activity of a member of the VapBC family of toxin-antitoxin systems VapBC-5 from Mycobacterium tuberculosis. *J. Biol. Chem.* 284(1):276-83
99. Moyed HS & Bertrand KP (1983) hipA, a newly recognized gene of Escherichia coli K-12 that affects frequency of persistence after inhibition of murein synthesis. *J. Bacteriol.* 155(2):768-7
100. Moyed HS & Broderick SH (1986) Molecular cloning and expression of hipA, a gene of Escherichia coli K-12 that affects frequency of persistence after inhibition of murein synthesis. *J. Bacteriol.* 166(2):399-403
101. Muñoz-Gómez AJ, Santos-Sierra S, Berzal-Herranz A, Lemonnier M & Díaz-Orejas R (2004) Insights into the specificity of RNA cleavage by the Escherichia coli MazF toxin. *FEBS Lett.* 567(2-3):316-20
102. Mutschler H, Gebhardt M, Shoeman RL & Meinhart A (2011) A novel mechanism of programmed cell death in bacteria by toxin-antitoxin systems corrupts peptidoglycan synthesis. *PLoS Biol.* 9(3):e1001033
103. Narahari A, Singla H, Nareddy PK, Bulusu G, Surolia A & Swamy MJ (2011) Isothermal titration calorimetric and computational studies on the binding of chitooligosaccharides to pumpkin (Cucurbita maxima) phloem exudate lectin. *J. Phys. Chem. B.* 115(14):4110-7
104. Neubauer C, Gao YG, Andersen KR, Dunham CM, Kelley AC, Hentschel J, Gerdes K, Ramakrishnan V & Brodersen DE (2009) The Structural Basis for mRNA Recognition and Cleavage by the Ribosome-Dependent Endonuclease RelE. *Cell.* 139(6):1084-95
105. Ng W-L & Bassler BL (2009) Bacterial Quorum-Sensing Network Architectures. *Annu. Rev. Genet.* 43:197-222
106. Ning D, Liu S, Xu W, Zhuang Q, Wen C & Tang X (2013a) Transcriptional and proteolytic regulation of the toxin- Antitoxin locus vapBC10 (ssr2962/slr1767) on the chromosome of synechocystis sp. PCC 6803. *PLoS One.* 8(11):e80716
107. Ning D, Ye S, Liu B & Chang J (2011) The proteolytic activation of the relNEs (ssr1114/slr0664) toxin-antitoxin system by both proteases lons and ClpP2s/Xs of Synechocystis sp. PCC 6803. *Curr. Microbiol.* 63:496–502
108. Ning D, Zhao W & Qian Y (2013b) A hypothetical gene pair, ssl2138 and sll11092, constitutes a functional TA system on the chromosome of Synechocystis PCC 6803. *Wei Sheng Wu Xue Bao.* 53(10):1043-9
109. Ogura T & Hiraga S (1983) Partition mechanism of F plasmid: Two plasmid gene-encoded products and a cis-acting region are involved in partition. *Cell.* 32(2):351-60
110. Pandey VD (2013) Rock-dwelling cyanobacteria: survival strategies and biodeterioration of monuments. *Int. J. Curr. Microbiol. Appl. Sci.* 2:519 –524
111. Pedersen K, Zavialov A V, Pavlov MY, Elf J, Gerdes K & Ehrenberg M (2003) The bacterial toxin RelE displays codon-specific cleavage of mRNAs in the ribosomal A site. *Cell.* 112(1):131-40

112. Pullinger GD & Lax AJ (1992) A Salmonella dublin virulence plasmid locus that affects bacterial growth under nutrient-limited conditions. *Mol. Microbiol.* 6(12):1631-43
113. Ren D, Bedzyk LA, Thomas SM, Ye RW & Wood TK (2004) Gene expression in Escherichia coli biofilms. *Appl. Microbiol. Biotechnol.* 64(4):515-24
114. Rice KC & Bayles KW (2008) Molecular Control of Bacterial Death and Lysis. *Microbiol. Mol. Biol. Rev.* 72:85–109
115. Roberts RC & Helinski DR (1992) Definition of a minimal plasmid stabilization system from the broad-host- range plasmid RK2. *J. Bacteriol.* 174(24):8119-32
116. Roberts RC, Ström AR & Helinski DR (1994) The parDE operon of the broad-host-range plasmid RK2 specifies growth inhibition associated with plasmid loss. *J. Mol. Biol.* 237(1):35-51
117. Rzhetsky, A., Nei M (1992) A simple method for estimating and testing minimum evolution trees. *Mol. Biol. Evol.* 9:945–967
118. Sabart M, Misson B, Descroix A, Duffaud E, Combourieu B, Salencon MJ & Latour D (2013) The importance of small colonies in sustaining Microcystis population exposed to mixing conditions: An exploration through colony size, genotypic composition and toxic potential. *Environ. Microbiol. Rep.* 5(5):747-56
119. Sambrook J., E.F. F & Maniatis T (1989) Molecular Cloning: A Laboratory Manual, 2nd ed., Vols. 1, 2 and 3
120. Samson JE, Spinelli S, Cambillau C & Moineau S (2013) Structure and activity of AbiQ, a lactococcal endoribonuclease belonging to the type III toxin-antitoxin system. *Mol. Microbiol.* 87(4):756-68
121. Sat B, Hazan R, Fisher T, Khaner H, Glaser G & Engelberg-Kulka H (2001) Programmed cell death in Escherichia coli: Some antibiotics can trigger mazEF lethality. *J. Bacteriol.* 183(6):2041-5
122. Sat B, Reches M & Engelberg-Kulka H (2003) The Escherichia coli mazEF suicide module mediates thymineless death. *J. Bacteriol.* 185(6):1803-7
123. Scholz I, Lange SJ, Hein S, Hess WR & Backofen R (2013) CRISPR-Cas Systems in the Cyanobacterium Synechocystis sp. PCC6803 Exhibit Distinct Processing Pathways Involving at Least Two Cas6 and a Cmr2 Protein. *PLoS One.* 8(2):e56470
124. Schumacher MA, Piro KM, Xu W, Hansen S, Lewis K & Brennan RG (2009) Molecular mechanisms of HipA-mediated multidrug tolerance and its neutralization by HipB. *Science.* 323(5912):396-401
125. Schureck MA, Maehigashi T, Miles SJ, Marquez J, Cho SE, Erdman R & Dunham CM (2014) Structure of the proteus vulgaris HigB-(HigA)2-HigB toxin-antitoxin complex. *J. Biol. Chem.* 289(2):1060–1070
126. Stazic D, Lindell D & Steglich C (2011) Antisense RNA protects mRNA from RNase e degradation by RNA-RNA duplex formation during phage infection. *Nucleic Acids Res.* 39(11):4890–4899
127. Stewart PS & Franklin MJ (2008) Physiological heterogeneity in biofilms. *Nat. Rev. Microbiol.* 6(3):199-210
128. Suzuki I (2005) The Histidine Kinase Hik34 Is Involved in Thermotolerance by Regulating the Expression of Heat Shock Genes in Synechocystis. *Plant Physiol.* 138(3):1409-21
129. Suzuki I, Simon WJ & Slabas AR (2006) The heat shock response of Synechocystis sp. PCC 6803 analysed by transcriptomics and proteomics. *J. Exp. Bot.* 57:1573–1578
130. T. Rybtke M, O. Jensen P, Hoiby N, Givskov M, Tolker-Nielsen T & Bjarnsholt T (2011) The Implication of Pseudomonas aeruginosa Biofilms in Infections. *Inflamm. Allergy Drug Targets.* 10(2):141-57

131. Terawaki, Y., Kakizawa, Y., Takayasu, H., and Yoshikawa M (1968) Temperature sensitivity of cell growth in Escherichia coli associated with the temperature sensitive R(KM) factor. *Nature* 219:284–5
132. Tian QB, Ohnishi M, Tabuchi A & Terawaki Y (1996) A new plasmid-encoded proteic killer gene system: Cloning, sequencing, and analyzing hig locus of plasmid Rts1. *Biochem. Biophys. Res. Commun.* 220(2):280-4
133. Tseng YT, Chiou NT, Gogiraju R & Lin-Chao S (2015) The protein interaction of RNA helicase B (RhlB) and polynucleotide phosphorylase (PNPase) contributes to the homeostatic control of cysteine in Escherichia coli. *J. Biol. Chem.* 290:29953–29963
134. Unoson C & Wagner EGH (2008) A small SOS-induced toxin is targeted against the inner membrane in Escherichia coli. *Mol. Microbiol.* 70(1):258-70
135. Vogel J, Argaman L, Wagner EGH & Altuvia S (2004) The small RNA istR inhibits synthesis of an SOS-induced toxic peptide. *Curr. Biol.* 14(24):2271-6
136. Walsby AE, Van Rijn J & Cohen Y (1983) The biology of a new gas-vacuolate cyanobacterium, Dactylococcopsis salina sp. nov., in Solar Lake. *Proc. R. Soc. London - Biol. Sci.* 217:417–447
137. Wang X, Lord DM, Cheng HY, Osbourne DO, Hong SH, Sanchez-Torres V, Quiroga C, Zheng K, Herrmann T, Peti W, Benedik MJ, Page R & Wood TK (2012) A new type V toxin-antitoxin system where mRNA for toxin GhoT is cleaved by antitoxin GhoS. *Nat. Chem. Biol.* 8(10):855-61
138. Wang X, Lord DM, Hong SH, Peti W, Benedik MJ, Page R & Wood TK (2013) Type II toxin/antitoxin MqsR/MqsA controls type V toxin/antitoxin GhoT/GhoS. *Environ. Microbiol. 15(6):1734-1744*
139. Wen Y, Behiels E & Devreese B (2014) Toxin-Antitoxin systems: Their role in persistence, biofilm formation, and pathogenicity. *Pathog. Dis.* 70:240–249
140. West SA, Diggle SP, Buckling A, Gardner A & Griffin AS (2007) The Social Lives of Microbes. *Annu. Rev. Ecol. Evol. Syst.* 38:53–77
141. Westra ER, Pul Ü, Heidrich N, Jore MM, Lundgren M, Stratmann T, Wurm R, Raine A, Mescher M, Van Heereveld L, Mastop M, Wagner EGH, Schnetz K, Van Der Oost J, Wagner R & Brouns SJJ (2010) H-NS-mediated repression of CRISPR-based immunity in Escherichia coli K12 can be relieved by the transcription activator LeuO. *Mol. Microbiol.* 77:1380–1393
142. Winther KS & Gerdes K (2011) Enteric virulence associated protein VapC inhibits translation by cleavage of initiator tRNA. *Proc. Natl. Acad. Sci.* 108(18):7403-7
143. Wiseman T, Williston S, Brandts JF & Lin LN (1989) Rapid measurement of binding constants and heats of binding using a new titration calorimeter. *Anal. Biochem.* 179(1):131-7
144. Yamaguchi Y & Inouye M (2011) Toxin-Antitoxin Systems in Bacteria and Archaea. *Annu. Rev. Genet.* 45:61–79
145. Yoshihara S, Geng XX, Okamoto S, Yura K, Murata T, Go M, Ohmori M & Ikeuchi M (2001) Mutational analysis of genes involved in pilus structure, motility and transformation competency in the unicellular motile cyanobacterium Synechocystis sp. PCC 6803. *Plant Cell Physiol.* 42:63–73
146. Zhang J, Zhang Y & Inouye M (2003a) Characterization of the interactions within the mazEF addiction module of Escherichia coli. *J. Biol. Chem.* 278:32300–32306
147. Zhang Y & Inouye M (2009) The inhibitory mechanism of protein synthesis by YoeB, an escherichia coli toxin. *J. Biol. Chem.* 284:6627–6638
148. Zhang Y, Zhang J, Hara H, Kato I & Inouye M (2005) Insights into the mRNA cleavage mechanism by MazF, an mRNA interferase. *J. Biol. Chem.* 280(5):3143-50

149. Zhang Y, Zhang J, Hoeflich KP, Ikura M, Qing G & Inouye M (2003b) MazF cleaves cellular mRNAs specifically at ACA to block protein synthesis in Escherichia coli. *Mol. Cell.* 12(4):913-23
150. Zielenkiewicz U & Cegłowski P (2005) The toxin-antitoxin system of the streptococcal plasmid pSM19035. *J. Bacteriol.* 187(17):6094-105
151. Zinchenko У V, Piven V, Melnik VA & Shestakov S V (1999) Vectors for the Complementation Analysis of Cyanobacterial Mutants. *Russ. J. Genet.* 35(3):228-232

Details of research paper published

1. **Afshan S**, Pilla S.K, Dokku S, Kopfmann S, Wolfgang R. Hess, Musti J. Swamy, Sue Lin-Chao, J.S.S. Prakash (2017). The Ssl2245-Sll1130 toxin-antitoxin system mediates heat-induced programmed cell death in *Synechocystis* sp. PCC6803. Published in Journal of Biological Chemistry, 292(10) : 4222-4234

Details of research work presented in conferences

1. **Afshan S**, Pilla S.K, Dokku S, Kopfmann S, Wolfgang R. Hess, Musti J. Swamy, Sue Lin-Chao, J.S.S. Prakash,(2017), "Heat induced programmed cell death is mediated by Ssl2245-Sll1130 TA system in *Synechocystis* sp. PCC6803" Poster presentation at "PRS-2017" International conference on photosynthetic research at the University of Hyderabad, Hyderabad India. (International)

2. **Afshan S**, J.S.S. Prakash (2017), "Heat induced programmed cell death is mediated by Toxin-Antitoxin system in the cyanobacterium, *Synechocystis* sp. PCC6803" Oral presentation at "Bioquest-2017" at University of Hyderabad, Hyderabad India. (National)

3. **Afshan S**, J.S.S. Prakash, (2015) "Heat induced programmed cell death is mediated by Ssl2245-Sll1130 TA system in *Synechocystis* sp. PCC6803" Oral presentation at "Plastid Preview -2015" at University of Essex, Colchester, UK. (International)

4. **Afshan S**, Pilla S.K, Dokku S, Kopfmann S, Wolfgang R. Hess, Musti J. Swamy, Sue Lin-Chao, J.S.S. Prakash, (2015) "Heat induced programmed cell death is mediated by a Toxin-Antitoxin system, Ssl2245-Sll1130 in *Synechocystis* sp. PCC6803" Poster presentation at International conference "All India microbiologists association-2015" at JNU, Delhi, India. (International)

THE JOURNAL OF BIOLOGICAL CHEMISTRY VOL. 292, NO. 10, pp. 4222–4234, March 10, 2017

The Ssl2245-Sll1130 Toxin-Antitoxin System Mediates Heat-induced Programmed Cell Death in *Synechocystis* sp. PCC6803*[S]

Received for publication, July 13, 2016, and in revised form, January 17, 2017 Published, JBC Papers in Press, January 19, 2017, DOI 10.1074/jbc.M116.748178

Afshan Srikumar[‡], Pilla Sankara Krishna[‡1], Dokku Sivaramakrishna[§2], Stefan Kopfmann[¶], Wolfgang R. Hess[¶], Musti J. Swamy[§], Sue Lin-Chao[‖], and Jogadhenu S. S. Prakash[‡3]

From the [‡]Department of Biotechnology and Bioinformatics, School of Life Sciences and [§]School of Chemistry, University of Hyderabad, Hyderabad 500046, India, [¶]Genetics and Experimental Bioinformatics, Faculty of Biology, University of Freiburg, D-79104 Freiburg, Germany, and [‖]Institute of Molecular Biology, Academia Sinica, Taipei 115, Taiwan

Edited by Charles E. Samuel

Two putative heat-responsive genes, *ssl2245* and *sll1130*, constitute an operon that also has characteristics of a toxin-antitoxin system, thus joining several enigmatic features. Closely related orthologs of Ssl2245 and Sll1130 exist in widely different bacteria, which thrive under environments with large fluctuations in temperature and salinity, among which some are thermo-epilithic biofilm-forming cyanobacteria. Transcriptome analyses revealed that the clustered regularly interspaced short palindromic repeats (CRISPR) genes as well as several hypothetical genes were commonly up-regulated in Δ*ssl2245* and Δ*sll1130* mutants. Genes coding for heat shock proteins and pilins were also induced in Δ*sll1130*. We observed that the majority of cells in a Δ*sll1130* mutant strain remained unicellular and viable after prolonged incubation at high temperature (50 °C). In contrast, the wild type formed large cell clumps of dead and live cells, indicating the attempt to form biofilms under harsh conditions. Furthermore, we observed that Sll1130 is a heat-stable ribonuclease whose activity was inhibited by Ssl2245 at optimal temperatures but not at high temperatures. In addition, we demonstrated that Ssl2245 is physically associated with Sll1130 by electrostatic interactions, thereby inhibiting its activity at optimal growth temperature. This association is lost upon exposure to heat, leaving Sll1130 to exhibit its ribonuclease activity. Thus, the activation of Sll1130 leads to the degradation of cellular RNA and thereby heat-induced programmed cell death that in turn supports the formation of a more resistant biofilm for the surviving cells. We suggest to designate Ssl2245 and Sll1130 as MazE and MazF, respectively.

Microorganisms are constantly exposed to various kinds of biotic and abiotic environmental challenges that can threaten their very survival. Therefore, various acclimative mechanisms have evolved to cope with such unfavorable conditions. These mechanisms make them tolerant to the stress, letting them survive until the return of favorable conditions. One such response is the ability to alternate from unicellular to multicellular organization like microbial colonies, aggregates, and biofilms (1, 2). In such microbial colonies, a subpopulation of cells can be genetically determined to undergo programmed cell death (PCD).[4] Thus, a bacterial population, upon being subjected to stress, utilizes PCD to sacrifice a portion of their population for survival of the remaining cells (3). Thus, based on the various strategies reviewed so far, it can be hypothesized that by utilizing the essential nutrients from the cells that are programmed to die, the surviving cells (persisters) are sustained until the return of favorable conditions after which they can resume reproduction and replenish their population (4–6). Autocatalytic PCD has been reported in certain cyanobacteria with possible implications for the export of carbon and nitrogen (7, 8), and metacaspases appear to be mechanistically involved in PCD in the marine cyanobacterium *Trichodesmium* (9) of which many molecular details are unknown.

Bacterial PCD is frequently mediated by specialized genetic systems known as the toxin-antitoxin (TA) modules (10). There are at least six major types of TA systems from which type II TA systems are the best characterized (11). The TA gene pair consists of a stable toxin and a labile antitoxin. The toxic properties of the toxin are masked by the antitoxin either by binding to it or by inhibiting its translation (12). In *Escherichia coli*, some of the well characterized TA systems are *mazEF* (13, 14), *relBE* (15, 16), *chpAB* (17), and *yefM-yoeB* (18). These systems are found on plasmid as well as chromosomal loci but were first identified in *E. coli* on low copy number plasmids (19). Several TA systems have been reported to trigger PCD under various conditions like amino acid starvation, exposure to antibiotics, plasmid segregation during cell division, phage infection, and high temperature (13, 15, 19–22).

* This work was supported in part by Council of Scientific and Industrial Research (CSIR) Grant 38(1405)/15/EMR-II and Department of Science and Technology Grant SR/SO/PS-47/09) (to J. S. S. P) and Deutsche Forschungsgemeinschaft, Bonn, Grants HE 2544/6-1 and HE 2544/8-2 (to W. R. H.). The authors declare that they have no conflicts of interest with the contents of this article.

[S] This article contains supplemental Figs. S1–S4 and Tables S1 and S2.

[1] Present address: Molecular Biomimetics, Dept. of Chemistry, Angstrom Laboratory, Uppsala University, 752 36 Uppsala, Sweden.

[2] Supported by a senior research fellowship from the CSIR (India).

[3] To whom correspondence should be addressed. E-mail: syamsunderp@yahoo.com.

[4] The abbreviations used are: PCD, programmed cell death; TA, toxin-antitoxin; CRISPR, clustered regularly interspaced short palindromic repeats; ITC, isothermal titration calorimetry; qRT-PCR, quantitative RT-PCR; AFM, atomic force microscopy; DSC, differential scanning calorimetry; Sp^R, Ω-spectinomycin gene cassette.

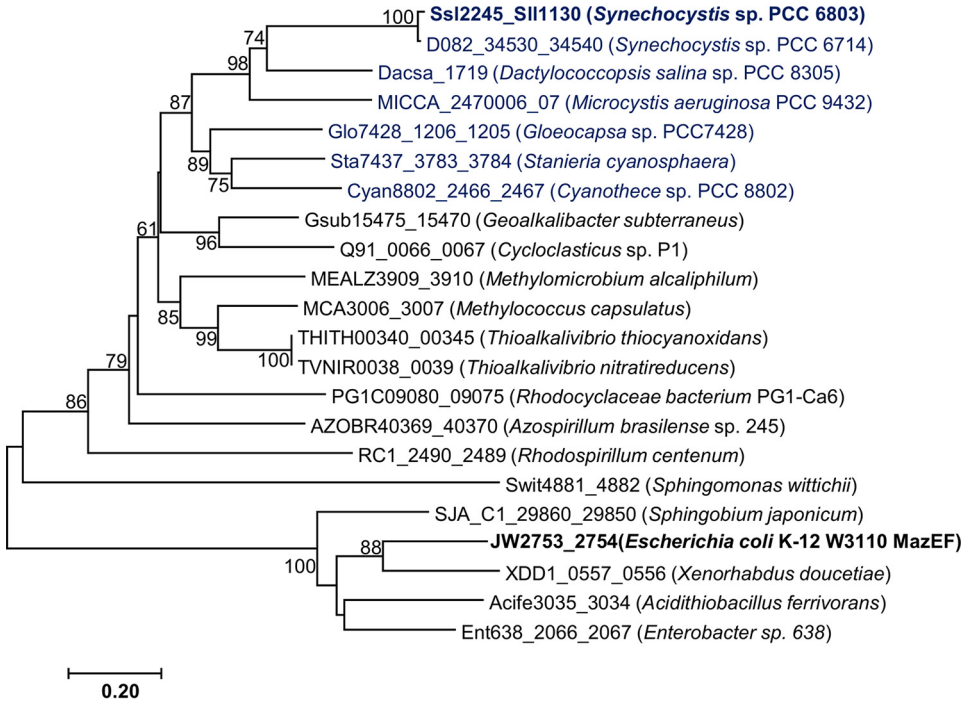

FIGURE 1. **Phylogenetic relationship of Ssl2245 and Sll1130 with their closely related orthologs.** The complete amino acids sequences of Ssl2245 and Sll1130 were concatenated and aligned with their putative orthologs using ClustalW (45), yielding a multiple sequence alignment of 208 positions. All cyanobacterial proteins are highlighted in *blue*, and the here investigated *Synechocystis* proteins, Ssl2245 and Sll1130, are in *bold font*. The archetypical *E. coli* K-12 MazEF (*black boldface*) and four proteins more closely related to it were also included. Phylogenetic relationships were inferred by Minimum Evolution (48) as implemented in MEGA 7.0 (49) using the pairwise deletion option. The optimal tree with the sum of branch length = 7.90605607 is shown. The percentage of replicate trees in which the associated taxa clustered together in the bootstrap test (1,000 replicates) is shown next to the branches when ≥60. The tree is drawn to scale with branch lengths in the same units as those of the evolutionary distances used to infer the phylogenetic tree. The evolutionary distances are given in the number of amino acid substitutions per site as indicated by the *scale bar* representing 0.2 substitutions per amino acid. The compared protein sequences were retrieved from the KEGG and NCBI databases.

A well known example is the CcdAB TA system that triggers PCD during bacterial cell division. The purpose of PCD in this case is to ensure plasmid partitioning during cell division (22). When the daughter cell fails to receive the plasmid harboring the TA operon, it is selectively killed by the toxin as the labile antitoxin, unable to replenish itself, is degraded faster. The toxin is released from the TA complex and targets DNA gyrase, triggering cell death (19, 22). Another TA system, *relBE*, is involved in PCD during amino acid starvation. The RelB antitoxin levels fall due to a decrease in translation and Lon-dependent proteolysis, freeing the RelE toxin to inhibit translation, thereby arresting growth until the return of favorable conditions (15). Upon exposure to antibiotics, the MazEF induced-PCD is activated due to a decrease in the amount of the antitoxin MazE (and its degradation by cellular proteases), leading to an increase in levels of the free MazF toxin (5, 6, 10). Under lethal concentrations of antibiotics, a small portion of the cells can even manage to survive until they experience favorable conditions (23).

MazEF also prevents the spread of infective phages to healthy individuals by initiating PCD in the infected cell. The lysogenic phage contains a gene that encodes a repressor that lets them replicate in the host cells without entering the lytic cycle (24). Inactivation of *mazEF* led to higher heat tolerance in *E. coli*, suggesting a possible role in the heat stress response. However, the mechanism of heat-induced cell death has not been reported (13). MazEF TA systems are known for their autoregulation by conditional cooperativity (14), and TA systems in general may function as global regulators (25–27). A role in the regulation of several hypothetical, pilin, and heat shock genes has been reported for the MazF-type transcriptional modulator Sll1130 in the cyanobacterium *Synechocystis* (28). In this study, we identified Ssl2245-Sll1130 as a pair of putative heat-responsive TA-like transcriptional regulators encoded by a dicistronic operon. We report the mechanism of heat-induced PCD mediated by this TA system as a survival strategy under high temperature.

Results

Phylogenetic Analysis—Ssl2245 and Sll1130 are encoded by two overlapping genes in the genome of *Synechocystis*. Ssl2245 is an unknown protein with similarity to AbrB-like transcriptional regulators. The second gene, *sll1130*, codes for a putative PemK-like MazF transcriptional modulator, consistent with its earlier reported regulatory function (28). The best BlastP hits of these two proteins were observed mainly from bacteria that thrive under high temperature and high salt environments. Interestingly, some of these cyanobacteria are thermo-epilithic biofilm-forming species (29, 30). Phylogenetic analysis of Ssl2245 and Sll1130 demonstrated that both are related more closely to putative TA proteins of organisms that thrive in high temperature and high salt environments, whereas MazE and MazF of *E. coli* and other related species formed a separate clade (Fig. 1). In fact, Ssl2245 and Sll1130 possess only 21.2 and 35.3% sequence identity with MazE and MazF of *E. coli* but 59 and 74.1% with homologs from *Dactylococcopsis salina* sp. PCC

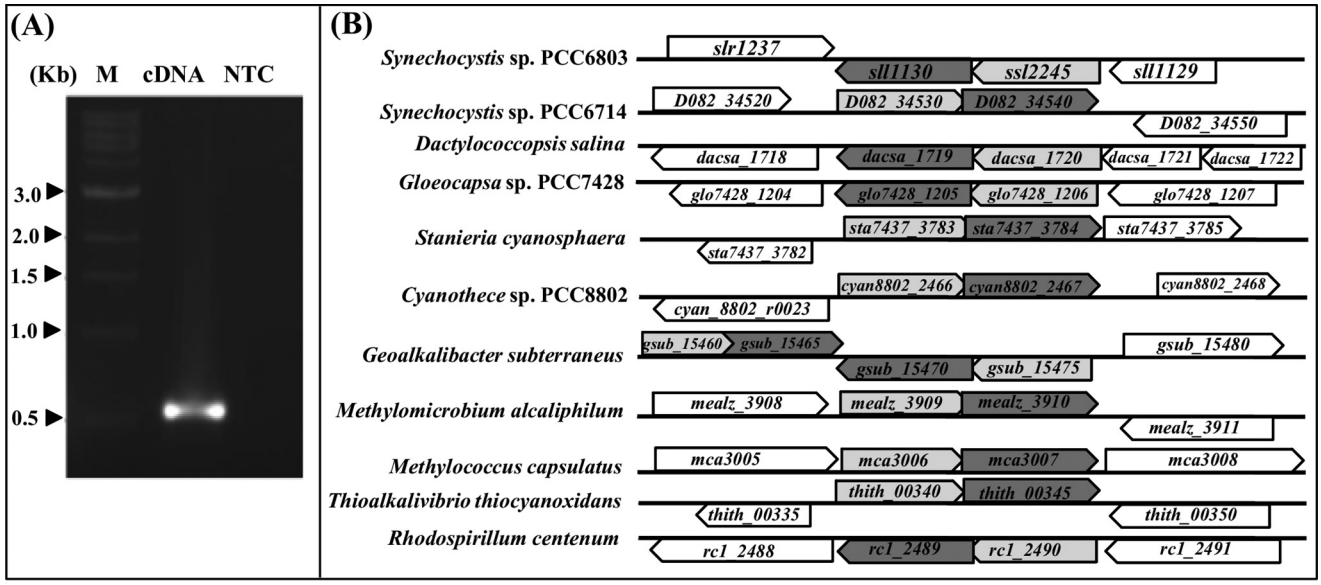

FIGURE 2. ***ssl2245* and *sll1130* are structural genes of a dicistronic operon.** *A*, agarose gel image confirming the transcription of *ssl2245* and *sll1130* as a single mRNA species from the dicistronic operon. cDNA was used as template for amplification with the primers covering both *ssl2245* and *sll1130* ORFs. *NTC*, non-template control; *M*, 1-kb DNA ladder (catalog number SM0313, Thermo Scientific); *cDNA*, PCR-amplified product using cDNA as template. *B*, graphical representation of the orientation of the operon *ssl2245-sll1130* along with its closely related orthologs obtained from gene clusters of the KEGG database. The putative antitoxin and toxin genes are represented with *gray* and *dark gray arrows*, respectively.

8305 isolated from a heliothermal saline pool (31) and 50 and 70.3% identity with those from *Microcystis aeruginosa* sp. PCC 9432, respectively (32). Because homologs of the *ssl2245-sll1130* operon appear well conserved among thermophilic bacteria, it appeared likely that the two proteins might be antagonistic to each other and play a key role in heat stress response.

Ssl2245 and Sll1130 Are Conserved Proteins Encoded by a Dicistronic Operon—The open reading frames (ORFs) *ssl2245* and *sll1130* have a four-nucleotide overlap where the stop codon of *ssl2245* overlaps with the start codon of *sll1130*. To validate whether both belong to a single operon controlled by the same promoter, cDNA made from total RNA by reverse transcription was used as template for PCR. Amplification using the primers *ssl2245*-F and *sll1130*-R specifically annealing to *ssl2245* and *sll1130*, respectively, gave a product of ~600 bp, which corresponds to the size of the entire operon. No amplification was obtained without the cDNA (non-template control). This result confirms co-transcription and dicistronic organization of *ssl2245* and *sll1130* (Fig. 2*A*), originating from a single transcriptional start site found in the genome-wide mapping of the primary transcriptome at position 1049139 on the reverse strand of the chromosome (33). Overlap between the stop codon of the first and the start codon of the second gene has been described in many other dicistronic TA systems (34). Such overlaps probably are required for stringent regulation of genes involved in common physiological or cellular roles. We found this as a common feature among the homologs of *ssl2245-sll1130* with overlaps ranging from 4 to 26 bp (Fig. 2*B*). The thermo-epilithic biofilm-forming cyanobacterium *Stanieria cyanosphaera* has a 26-bp overlap between *sta7437_3783* and *sta7437_3784*.

The Δsll1130 Mutant Can Survive Prolonged Incubation at High Temperature—In our previous study with this mutant, we observed that, upon heat exposure of wild type and Δ*sll1130* mutant at 50 °C for 30 min followed by recovery at 34 °C, Δ*sll1130* mutant cells recovered relatively faster from heat shock than the wild type cells (28). In this study, we observed that a relatively greater number of Δ*sll1130* mutant cells than wild type cells remained viable during prolonged incubation at 50 °C. Fig. 3 shows the heat tolerance of Δ*sll1130* mutant in comparison with wild type cells. Before incubation of cells at high temperature, both wild type and Δ*sll1130* cells appeared as bright red fluorescent cells, indicating that the cells were equally viable at the optimal growth temperature (34 °C) (Fig. 3, *A* and *E*). When the exponentially growing cells were shifted to 50 °C for 8 h, although only 25–30% of the total wild type cells were viable (cells emitting red fluorescence over green fluorescence) (Fig. 3, *C* and *I*), almost 70–80% of the Δ*sll1130* cells remained viable (Fig. 3, *G* and *I*). Interestingly, we also observed that the wild type cells showed a tendency to form clumps during prolonged incubation at 50 °C, although some of the cells continued to exist individually (Fig. 3*D*). In contrast, mutant cells always existed as individual entities throughout the period of incubation at 50 °C (Fig. 3*H*). This result indicates that disruption of *sll1130* leads to a higher thermotolerance in *Synechocystis.* In addition, we also observed that introduction of an extra copy of this operon into the wild type *Synechocystis* cells led to the slow growth phenotype (supplemental Fig. S1).

Genes Whose Expression Was Altered Due to Mutations in ssl2245 and sll1130 Genes—In our previous work, the DNA microarray used for gene expression profiling of Δ*sll1130* contained only probes for chromosomal genes; therefore no differential expression was observed in plasmid genes (28). In the current study, a new custom made chip was designed that included probes covering genes located in the genome as well as all seven *Synechocystis* plasmids. We analyzed the changes in gene expression in both Δ*ssl2245* and Δ*sll1130.* Supplemental Table S1 shows the list of genes that were significantly either

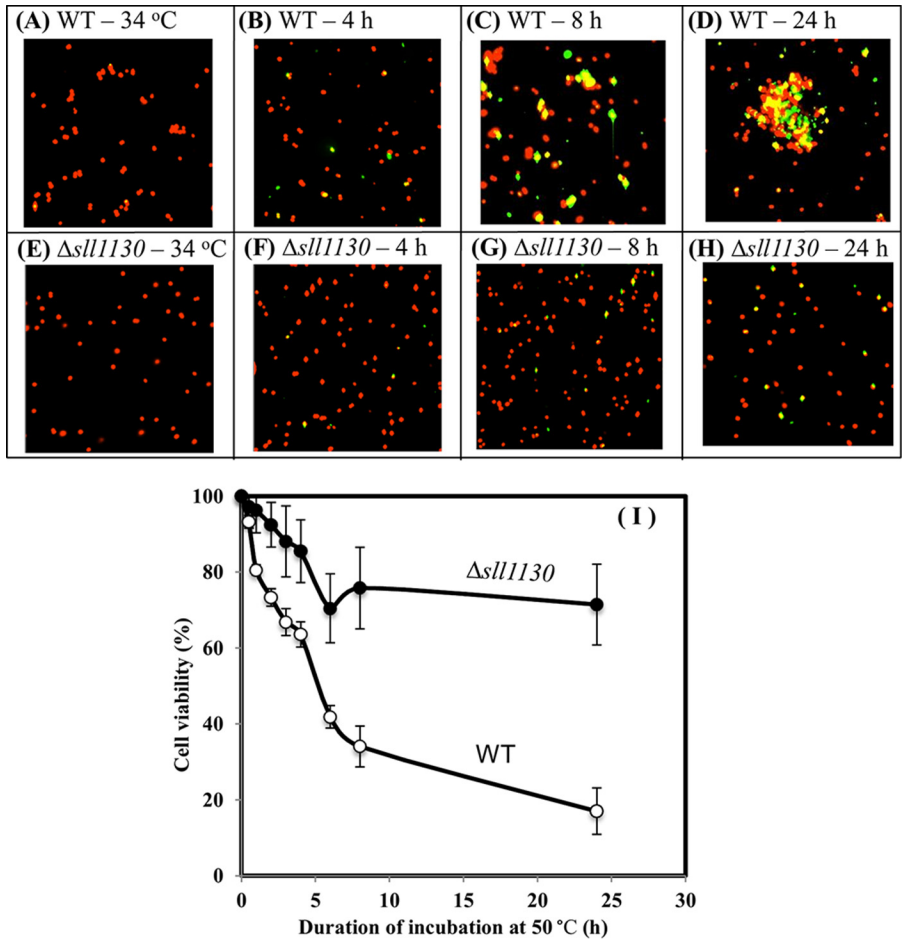

FIGURE 3. **Survival rate of *Synechocystis* wild type and Δ*sll1130* cells during incubation at high temperature.** Wild type and Δ*sll1130* cells were grown at 34 °C for 16 h (*A*, WT-34 °C cells; *E*, Δ*sll1130*-34 °C). Wild type and Δ*sll1130* cells that were grown at 34 °C for 16 h were subjected to heat treatment at 50 °C for 4, 8, and 24 h (*B*, WT-4 h; *C*, WT-8 h; *D*, WT-24 h; *F*, Δ*sll1130*-4 h; *G*, Δ*sll1130*-8 h; *H*, Δ*sll1130*-24 h). *Scale bar*, 10 μm. Cells were stained with SYTOX Green dye, and the percentage of viable cells (*red*) and dead cells (*green*) in the wild type and Δ*sll1130* mutant before and during the course of incubation at 50 °C was determined (*I*) by counting under 40× *magnification* using a confocal microscope. *Open circles*, wild type cells; *closed circles*, Δ*sll1130* mutant cells. Data represent the mean ± S.D. (*error bars*) for three independent experiments.

up- or down-regulated in the Δ*ssl2245* and Δ*sll1130* mutants in comparison with wild type cells. Genes whose mean induction was greater than 2.0 at least in one of the two mutants are listed as up-regulated, and those with an induction ratio below 0.3 in the Δ*ssl2245* and Δ*sll1130* mutants are listed as down-regulated (supplemental Fig. S2). We observed up-regulation of several genes located on the large plasmids pSYSA, pSYSX, and pSYSM in Δ*ssl2245* as well as Δ*sll1130* (supplemental Table S1). Most of the up-regulated genes on plasmid pSYSA encoded parts of the clustered regularly interspaced short palindromic repeats (CRISPR) system. CRISPR systems provide adaptive immunity against phage invasion. Plasmid pSYSA harbors three separate CRISPR-Cas systems called CRISPR1, CRISPR2, and CRISPR3 (35). These were classified as subtype I-D, subtype III-D, and subtype III-B according to Makarova *et al.* (36). The genes up-regulated in Δ*ssl2245* and Δ*sll1130* belong to CRISPR2 (genes *sll7062–sll7067*) and CRISPR3 (genes *sll7085–sll7090*), whereas expression of the CRISPR1 cassette remained unaffected. Plasmid pSYSA also harbors several other TA systems (37). However, expression of these TA systems was not affected, similar to the unchanged expression of CRISPR1 genes. Thus, the higher expression of the pSYSA-located CRISPR2 and CRISPR3 genes in the two mutants is not a consequence of a higher pSYSA plasmid copy number but points to a specific regulatory effect. The up-regulation of CRISPR-associated genes in Δ*ssl2245* and Δ*sll1130* suggests that they might function as master regulators of these plasmid-located viral defense genes. Indeed, repression of CRISPR arrays by a global transcriptional repressor, the heat-stable nucleoid-structuring (H-NS) protein, has been described in some *E. coli* strains (38). Alternatively, Ssl2245 and Sll1130 could control a process that leads indirectly to their activation, *e.g.* as part of a lifestyle change. Certain TA systems were reported previously to be involved in virus defense (24). Thus, the Ssl2245-Sll1130 system could act in a multifunctional way like *E. coli* MazEF, which exhibits multiple stress responses (13). The genes of the *slr1788-slr1789* dicistronic operon, heat-responsive *frpC*, and pilin genes that were previously confirmed to be up-regulated in the Δ*sll1130* mutant were also commonly up-regulated (28).

qRT-PCR Analysis Confirms DNA Microarray Expression Changes—We chose the first gene of selected plasmid-localized operons, which were differentially expressed due to mutation in both *ssl2245* and *sll1130* for qRT-PCR validation of their expression changes as observed in the DNA microarray analysis

(supplemental Table S1, ORF numbers in bold letters). These genes were *sll7064*, *sll7067*, *sll7085*, *sll7090*, *slr7091*, *sll5097*, and *sll6010*. In addition, we chose two chromosome-located genes, *slr0909* and *sll1396* (supplemental Table S2). The gene expression changes observed by both DNA microarray and qRT-PCR analyses were consistent (Fig. 4) and indeed suggested the direct or indirect involvement of Ssl2245 and Sll1130 in the regulation of expression of CRISPR2 and CRISPR3 as well as of certain chromosomal genes.

Enhanced Formation of Pili in Δsll1130—As we observed up-regulation of pilin genes due to mutation in Δ*sll1130*, we compared the pilus formation in wild type and Δ*sll1130* cells using atomic force microscopy (AFM). Wild type and Δ*sll1130* cells deposited onto the mica were around 1–1.5 μm in diameter. The surface of the wild type cells appeared to have very few appendages or pili (Fig. 5*A*). In contrast, the Δ*sll1130* cells were distinctly surrounded with multiple threadlike appendages (Fig. 5*B*), suggesting a possible role of Sll1130 in regulating pilin expression and pilus formation in *Synechocystis*.

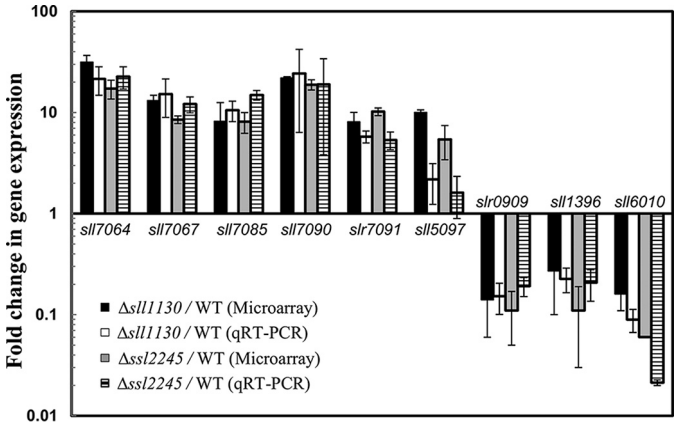

FIGURE 4. **Confirmation of DNA microarray gene expression changes by qRT-PCR.** Genes whose expression was up-regulated (*slr7064*, *sll7067*, *sll7085*, *sll7090*, *slr7091*, and *sll5097*) and the genes whose expression was down-regulated (*slr0909*, *sll1396*, and *sll6010*) due to mutation in Δ*sll1130* as well as in Δ*ssl2245* cells were selected for qRT-PCR analysis. *Black* and *gray bars* represent -fold changes observed by DNA microarray analysis; *white* and *striped bars* represent -fold changes observed by qRT-PCR analysis due to the mutation in Δ*sll1130* and Δ*ssl2245*, respectively. Similar results were obtained in two independent experiments; data are presented as mean ratios ± S.D. (*error bars*).

Ssl2245 and Sll1130 Interact with Each Other and Form a Stable Complex—Because Ssl2245 and Sll1130 showed similarity to TA systems of other bacteria, we addressed their possible interaction. A bacterial two-hybrid system involving two plasmids, pT25 and pT18, harboring the ORFs *sll1130* and *ssl2245*, respectively, was utilized (39). Simultaneously, the interaction of thioredoxin B (Slr1139) with Ssl2245 as well as Sll1130 was tested because Ssl2245 was reported as a possible target of this thioredoxin (40). As expected, the DHP1 cells harboring empty plasmids, pT25 and pT18 (as a negative control) without any DNA inserts, did not change their color upon incubation of cells at 30 °C even after 48 h (Fig. 6*A*, *a*). The DHP1 cells harboring pT25-RhlB and pPNP-T18 (as a positive control) turned a dark pink color upon plating onto MacConkey agar (41) (Fig. 6*A*, *b*). We observed a dark pink color formation on plating the DHP1 cells co-transformed with pT25-Sll1130 and pSsl2245-T18, demonstrating the strong interaction between Ssl2245 and Sll1130 (Fig. 6*A*, *c*). Color change was not observed with the cells harboring pT25-Slr1139 and pSsl2245-T18 or pT25-Slr1139 and pSll1130-T18, suggesting that Slr1139 interacts with neither Ssl2245 nor Sll1130 (Fig. 6*A*, *d* and *e*). To verify the possible physical association between Ssl2245 and Sll1130, they were expressed together in such a way that both proteins were expressed from the same plasmid upon induction, and only one protein contained the His_6 tag. Thus, only Ssl2245 was expressed with an N-terminal His_6 tag (His-Ssl2245). SDS-PAGE analysis of the eluates revealed the presence of Sll1130 along with the His-tagged Ssl2245 despite lacking a purification tag (Fig. 6*B*, *lanes 5–10*). The mass spectrometric analysis showed the masses of Ssl2245 and Sll1130 to be 9.20 and 12.925 kDa, respectively. These results indicated a stable and strong physical interaction between Ssl2245 and Sll1130. Their physical association could be mainly due to electrostatic interactions as Ssl2245 is acidic with a pI of 4.2 and Sll1130 is basic with a calculated pI of 8.8.

Thermal Stability of Ssl2245 and Sll1130 Proteins—To characterize the thermal stability of Ssl2245 and Sll1130, we

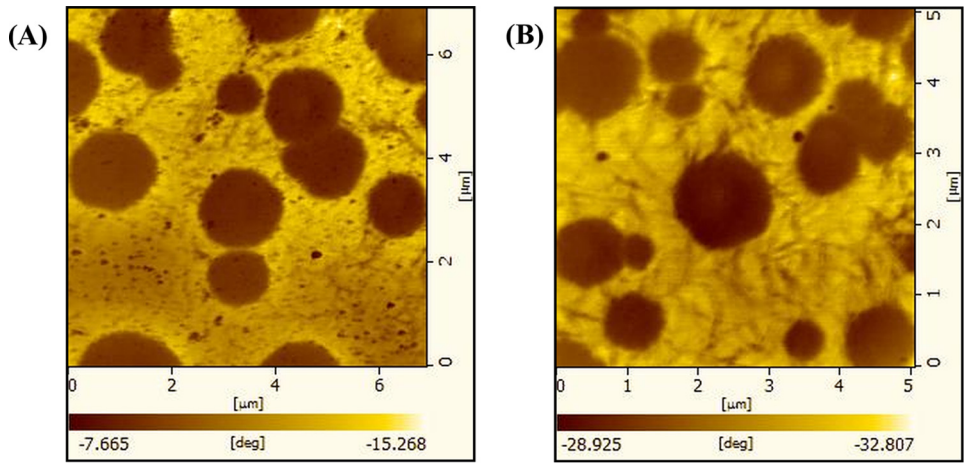

FIGURE 5. **Atomic force microscopic images of air-dried wild type and Δ*sll1130 Synechocystis* cells.** *A*, wild type cells grown in liquid BG11 medium observed with very few appendages with relatively smooth surfaces. *B*, Δ*sll1130* mutant cells grown in liquid BG11 medium observed with numerous hairlike appendages. Cells were scanned and imaged with a scanning probe microscope (SPA400) using the tapping mode at a scan rate of 1–2 Hz and a resonance frequency of 110–150 kHz.

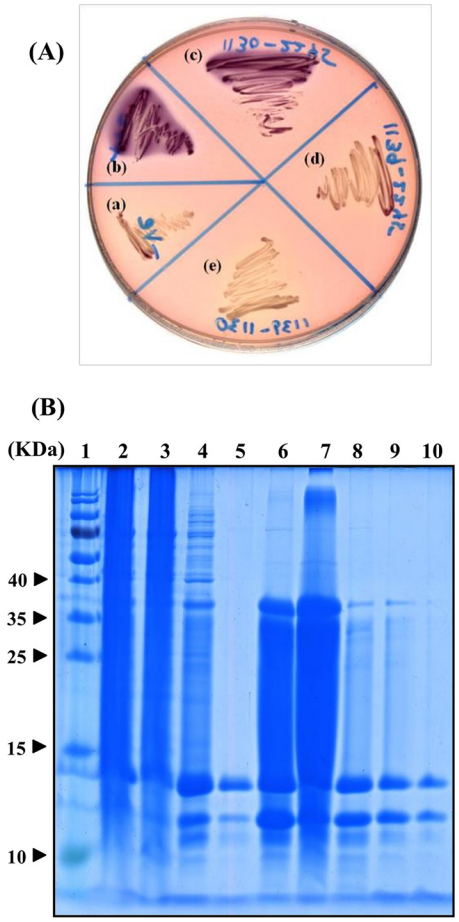

FIGURE 6. **Ssl2245 and Sll1130 proteins are physically associated.** *A*, demonstration of interaction between Ssl2245 and Sll1130 using a bacterial two-hybrid system. The *E. coli* strain DHP1 carrying the plasmids encoding different proteins was plated on a MacConkey/maltose plate as indicated to visualize protein-protein interactions. The cells carrying pT25 and pT18 were negative controls (*a*). The cells carrying pT25-RhlB and pPNP-T18 were positive controls (*b*). *a–c*, cells harboring pT25-Sll1130 along with pSsl2245-T18 (*c*), pT25-Slr1139 with pSsl2245-T18 (*d*), and pT25-Slr1139 with pSll1130-T18 (*e*). *B*, SDS-PAGE analysis of co-expressed and purified His-tagged Ssl2245 and Sll1130 recombinant proteins in *E. coli* BL21 (DE3). *Lane 1*, protein molecular mass standards (catalog number 26616, Thermo Scientific); *lane 2*, whole cell lysate of induced *E. coli* harboring plasmid pET-*ssl2245-sll1130*; *lane 3*, flow-through collected from nickel-nitrilotriacetic acid column; *lanes 4* and *5*, protein washes of nickel-nitrilotriacetic acid column with 40 mM imidazole used for eluting nonspecifically bound proteins; *lanes 6–10*, proteins eluted with increasing concentrations of imidazole of 100, 200, 300, and 400 mM. The molecular masses of standards are shown in the *left margin*.

performed high sensitivity differential scanning calorimetry (DSC). Typical DSC thermograms of Ssl2245 and Sll1130 are shown in Fig. 7, *A* and *B*. From these thermograms, the obtained temperatures corresponding to the unfolding transition of Ssl2245 and Sll1130 proteins were 60.6 and 62.8 °C, respectively.

Temperature-dependent Association of Ssl2245 and Sll1130—Thermodynamic parameters characterizing the interaction between Ssl2245 and Sll1130 were determined by isothermal titration calorimetry (ITC) at various temperatures. Fig. 7, *C* and *D*, show typical ITC profiles for the binding of Ssl2245 to Sll1130 at 25 and 50 °C, respectively. These titration profiles indicated that injection of small aliquots of Ssl2245 into Sll1130 gives large exothermic heat of binding, which decreased in magnitude with subsequent injections, showing saturation behavior. The data obtained at all temperatures could be best fitted by a non-linear least square approach to the "one set of sites" binding model, which yielded the association constant (K_a), stoichiometry of binding (n), and the thermodynamic parameters, enthalpy of binding (ΔH) and entropy of binding (ΔS). These values are listed in Table 1. At 25 °C, the stoichiometry, n, was found to be 0.46, indicating that each molecule of Ssl2245 binds to two molecules of Sll1130; *i.e.* the two proteins form a complex with a 1:2 (Ssl2245:Sll1130) stoichiometry. Table 1 clearly indicates that although the binding constant K_a did not change significantly between 25 and 50 °C, the stoichiometry of interaction decreased quite dramatically from 0.46 at 25 °C to 0.16 at 50 °C. Because the thermal unfolding temperature of both proteins is clearly well above 50 °C, it is unlikely that the steep decrease in the stoichiometry is due to the significant thermal inactivation of one of the proteins. Instead, it is likely that at the elevated temperature one of the two proteins undergoes some conformational changes but not complete unfolding due to which its interaction with the second protein is altered. To investigate this in more detail, we performed circular dichroism (CD) spectroscopic studies. CD spectra of Sll1130 and Ssl2245 recorded at various temperatures between 25 and 60 °C are shown in Fig. 8. The far-UV CD spectra of Sll1130 and Sll2245 in Fig. 8, *A* and *C*, respectively, show that the secondary structure of the two proteins remains essentially unaltered between 25 and 60 °C, which is consistent with the results of DSC studies presented above. Interestingly, although the near-UV CD spectra of Ssl2245 were largely unchanged in the temperature range of 25 and 60 °C, the molar ellipticity in the corresponding spectra of Sll1130 exhibited a significant decrease at and above 40 °C. These results are consistent with the formation of a molten globule-like structure by Sll1130 at temperatures above 40 °C (42, 43). The apparent decrease in stoichiometry then suggests that only a fraction of Sll1130 (which is still in the native form) complexes with Ssl2245, whereas the fraction that is in the molten globule-like structure does not bind to it. Because Sll1130 exhibits ribonuclease activity up to 60 °C (as shown below), these observations suggest that the molten globule-like form is functionally active and acts as an RNase.

Sll1130 Is a Ribonuclease, and Its Function Is Masked by Ssl2245—In vitro synthesized partial 16S rRNA and *slr1788*/*slr1789* mRNA substrates were incubated with purified Sll1130, purified Ssl2245, or both. Addition of Sll1130 alone resulted in the cleavage of the RNA, whereas the incubation with Ssl2245 alone had no effect on the RNA integrity. The simultaneous addition of both Sll1130 and Ssl2245 also had no effect on the RNA integrity (Fig. 9, *A* and *B*). Significantly high decay of both tested RNA substrates by Sll1130 suggests that Sll1130 functions as ribonuclease, and such an RNA degradation by Sll1130 was inhibited by Ssl2245. Thus, Sll1130 in its free form can degrade RNA, and this function seems to be lost while it is associated with Ssl2245. Because a decreased association of Sll1130 and Ssl2245 at high temperature using ITC analysis was demonstrated, we examined the ribonuclease activity of Sll1130 alone and in the presence of Ssl2245 at 37, 50, and 60 °C on the *in vitro* synthesized *slr1788*/*slr1789* mRNA. Irrespective of the temperature of incubation, Sll1130 degraded the mRNA

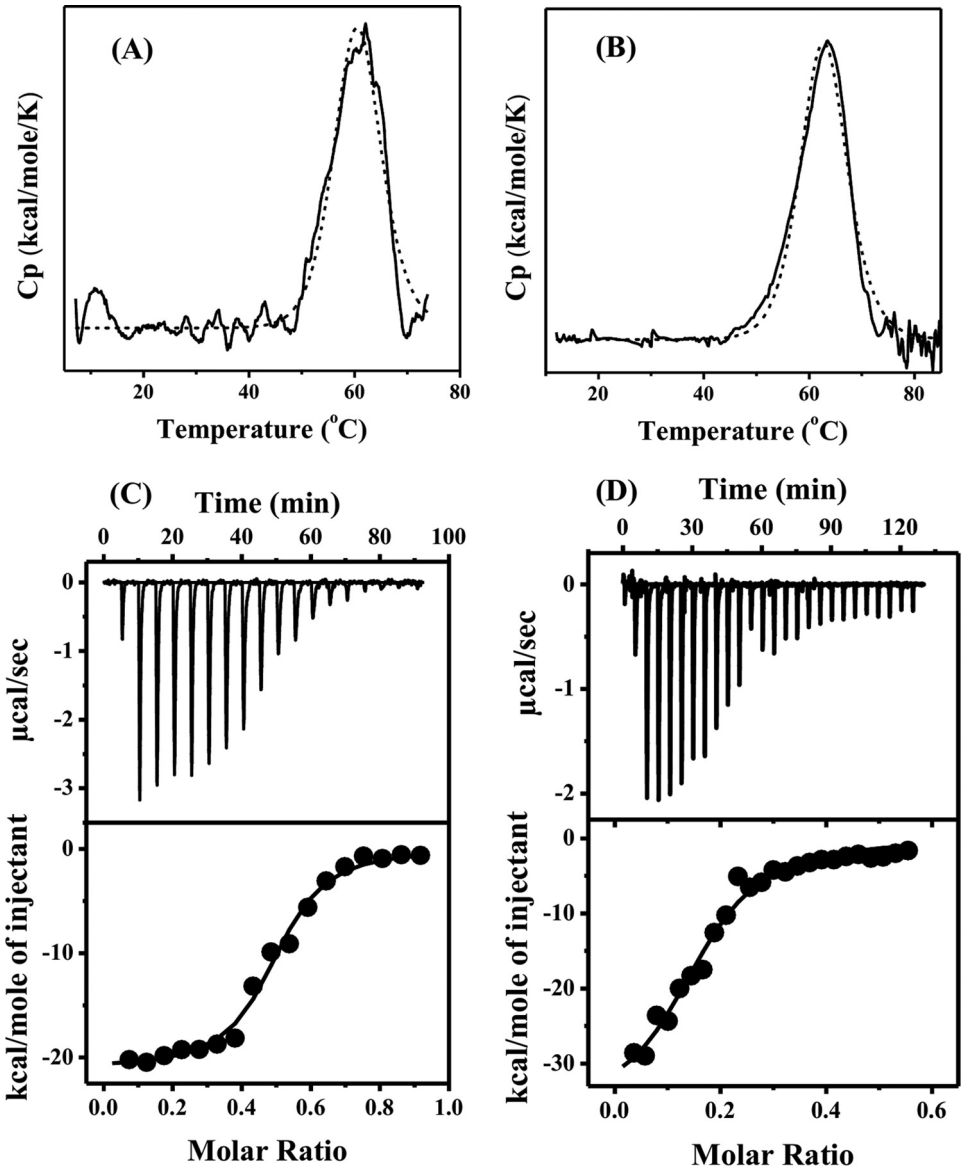

FIGURE 7. **Thermal stability and temperature-dependent analysis of interactions between Ssl2245 and Sll1130 proteins.** *A* and *B* show DSC thermograms of Ssl2245 and Sll1130, respectively. The data points are shown as *black lines*, and the *dotted lines* are the best fits of the DSC data to a non-two-state transition model. Concentrations of Ssl2245 and Sll1130 used were 149 and 81 μM, respectively. ITC profiles corresponding to the binding of Ssl2245 to Sll1130 at 25 (*C*) and 50 °C (*D*) are shown. *Upper panels* show the raw data for the titration of the two proteins, and *lower panels* show the integrated heats of binding obtained from the raw data after subtracting the heat of dilution. The *solid lines* in the *bottom panels* represent the best fits of the experimental data to the one set of sites binding model in the MicroCal Origin ITC data analysis software.

TABLE 1

Thermodynamic parameters obtained from isothermal titration calorimetric studies on the interaction between Ssl2245 and Sll1130 at different temperatures

Average values obtained from two independent titrations are shown with standard deviations.

T	Stoichiometry (n)	$K_a \times 10^5$	ΔH	ΔS
°C		M^{-1}	$kcal \cdot mol^{-1}$	$cal \cdot mol^{-1} \cdot K^{-1}$
25	0.46 ± 0.03	8.7 ± 4.8	−19.9 ± 1.8	−39.5 ± 4.8
34	0.39 ± 0.2	12.4 ± 3.0	−28.0 ± 5.5	−63.2 ± 17.5
50	0.16 ± 0.01	7.45 ± 2.54	−37.6 ± 6.8	−89.7 ± 21.0

substrates efficiently, whereas Ssl2245 alone had no effect on integrity of mRNA at all tested temperatures. Degradation of RNA was observed at both 50 and 60 °C when the RNA was incubated together with Ssl2245 and Sll1130. Conformational change in Sll1130 within the Ssl2245-Sll1130 complex probably released the free molten globule-like form of Sll1130, leading to the observed mRNA cleavage (Fig. 9, *C*, *D*, and *E*). Consistent with this result, we found that mRNA isolated from Δ*sll1130* cells was relatively more stable than that from wild type cells during prolonged incubation of cells at high temperature (data not shown).

Discussion

Synechocystis contains multiple putative TA systems, but only a very few of them have been experimentally addressed thus far. The *Synechocystis* TA system initially identified was the chromosomally located *relNE* (*ssr1114-slr0664*) that is proteolytically regulated by ATP-dependent proteases (44). At least seven TA systems are located on the plasmid pSYSA of which only *sll7003-ssl7004* has been biochemically character-

ized (37). The Sll7003 toxin acts as Mg^{2+}-dependent RNase whose activity is inhibited in the presence of Sll7004, demonstrating its antitoxin property (37). Recently, there have been several reports on the role of TA systems in PCD and persistence (4–6, 45). To the best of our knowledge, this is the first detailed report of a cyanobacterial TA system and its role in survival of *Synechocystis* under high temperature conditions. Ssl2245 and Sll1130 are similar to putative MazEF proteins from thermophilic bacteria (Fig. 1). Therefore, the Ssl2245-Sll1130 TA system might have evolved for high temperature adaptation in *Synechocystis*. In almost all type II TA systems, the antitoxin gene is located upstream of the toxin gene and in the same operon. Similarly, in *Synechocystis*, the *ssl2245* gene is located upstream of *sll1130* with a four-nucleotide overlap. Being in a dicistronic operon, these are transcribed together as a single mRNA perhaps for stringent regulation of these two genes as the function of one protein is masked by the other (Fig. 2). Previous studies from our laboratory revealed Sll1130 as a negative regulator of several heat shock genes and demonstrated a faster recovery of the Δ*sll1130* mutant in comparison with the wild type cells upon heat shock (28). Furthermore, we noticed that Δ*sll1130* is highly tolerant to heat even under continuous incubation at high temperature (Fig. 3). The genes in a TA system are frequently functionally antagonistic to each other. Hence, we anticipated that Sll1130 might function as a toxin whose function is masked by Ssl2245 under optimal temperature by binding to it. Therefore, we expected a physical association between Ssl2245 and Sll1130. Indeed, bacterial two-hybrid screening and co-elution studies revealed a strong physical association (Figs. 6 and 10*A*).

The DNA microarray- and qRT-PCR-based gene expression profiling of mutants revealed the role of this TA system in the regulation of expression of plasmid genes (Fig. 4 and supplemental Table S1). The gene expression changes observed in both cases were found to be similar. Especially, we observed inducible expression of CRISPR-associated genes, which are pivotal for defense (35). There is a report demonstrating roles of TA systems in viral defense in *E. coli* (24). Our results based on the AFM imaging showed a large number of distinct pili in the Δ*sll1130* mutant, but the wild type cells were found to have a comparatively smoother cell membrane (Fig. 5). Hence, the Ssl2245-Sll1130 TA system could be multifunctional, analogous to *e.g. E. coli* MazE-MazF. The detailed mechanism of regulation of plasmid genes and their role in formation of pili need to be further elucidated.

Some TA systems induce PCD under various stress conditions whereby a portion of the bacterial population is sacrificed, aiding the survival of the rest of the cells (persisters) (21). In some cases, the bacterial populations form biofilms upon induction of PCD in which the persisters reduce their metabolic activities and survive on the nutrients obtained from the surrounding dead cells until the return of favorable conditions. High temperature is one such harsh condition that can induce biofilm formation in cyanobacteria (2). Interestingly, the more closely related orthologs of these two proteins were identified in *Dactylococcopsis salina* from a heliothermal saline pool; *Microcystis aeruginosa*; *Stanieria cyanosphaera*, a thermo-epilithic biofilm-forming cyanobacteria; and several other colony-forming cyanobacteria. *M. aeruginosa* shows colony size distribution in its population as an adaptive strategy to disturbances

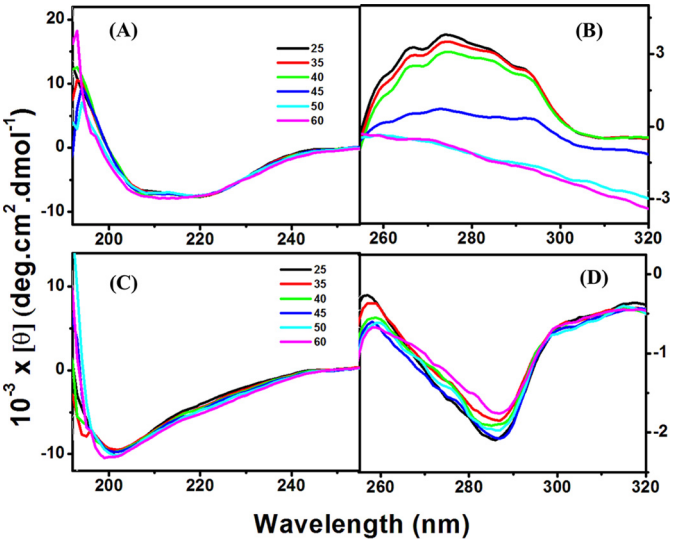

FIGURE 8. **Circular dichroism spectra of Sll1130 and Ssl2245 recorded at various temperatures.** Far- and near-UV CD spectra, respectively, of Sll1130 (*A* and *B*) and far- and near-UV CD spectra, respectively, of Ssl2245 (*C* and *D*) are shown. Spectra recorded at various temperatures are identified by different colors as indicated in the figure. *deg*, degrees.

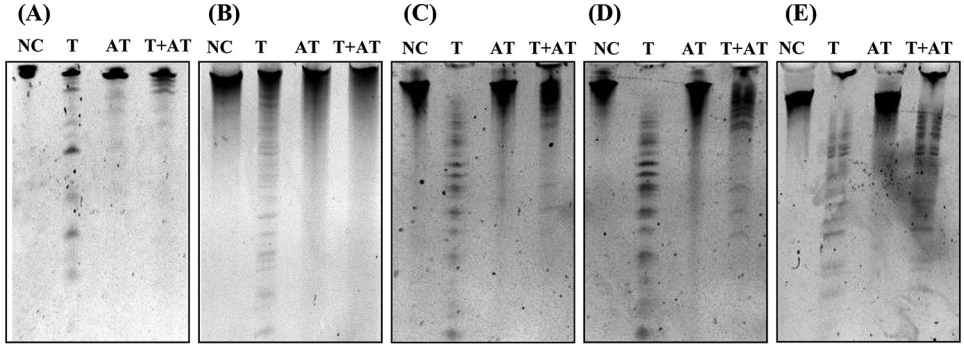

FIGURE 9. **Sll1130 possesses endoribonuclease activity that is counteracted by Ssl2245.** *In vitro* synthesized partial *Synechocystis* 16S rRNA fragment (*A*) and *slr1788-slr1789* mRNA (*B*) were incubated for 30 min with Sll1130 (*T*), Ssl2245 (*AT*), or both Sll1130 and Ssl2245 (*T*+*AT*), respectively. The addition of Sll1130 resulted in degradation of the RNA, which was prevented by concurrent addition of Sll1130 and Ssl2245 together. The effect of temperature on endoribonuclease activity of Sll1130 in the presence or absence of Ssl2245 was determined. *In vitro* synthesized *slr1788-slr1789* mRNA was incubated with Sll1130, Ssl2245, or both Sll1130 and Ssl2245 at 37 (*C*), 50 (*D*), and 60 °C (*E*), respectively. Sll1130 degrades RNA at high temperature even in the presence of Ssl2245. *NC*, negative control in which RNA was incubated for 30 min in the elution buffer without any protein.

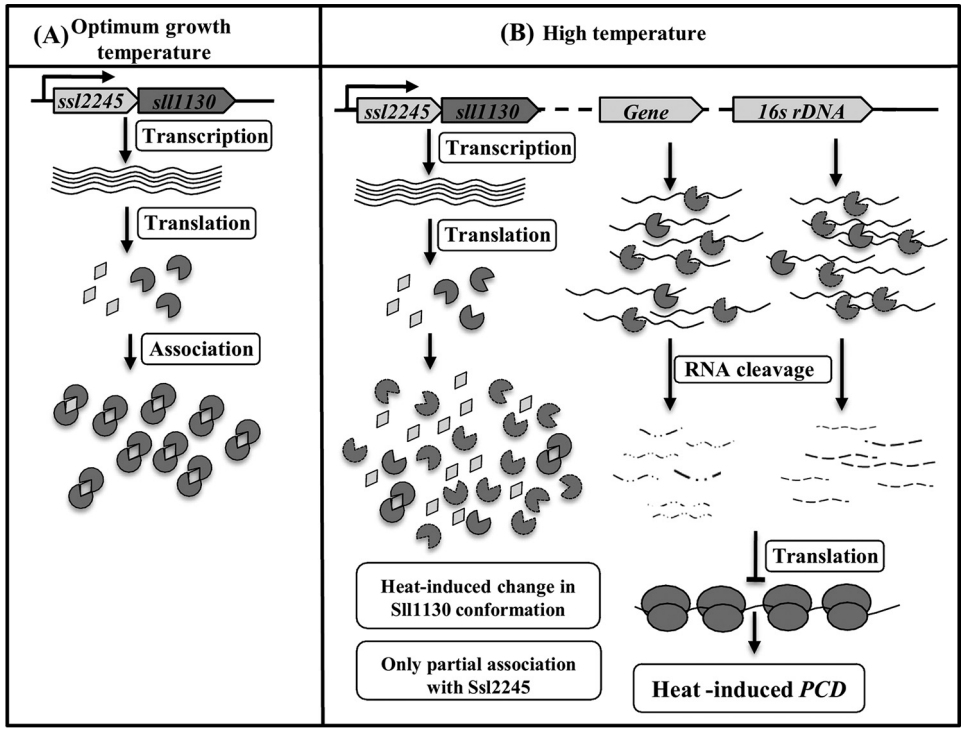

FIGURE 10. **Schematic representation of heat-induced programmed cell death mediated by MazE and MazF.** *A*, *ssl2245* and *sll1130* genes constitute a dicistronic operon and are co-transcribed. The Ssl2245 and Sll1130 form a complex under optimal growth conditions. Two molecules of Sll1130 are associated with one molecule of Ssl2245. Sll1130 is a ribonuclease whose function is masked by Ssl2245 under optimal growth conditions. *B*, at high temperature, Sll1130 undergoes a transition to a molten globule-like form, the association between Ssl2245 and Sll1130 is significantly decreased, and only a fraction of the molecules (which are in the native state) complex with Ssl2245, whereas those in the molten globule state are free. Because Sll1130 is a stable ribonuclease, the free molecules degrade 16S rRNA and several other mRNA species. Degradation of 16SrRNA leads to inhibition of translation, causing growth arrest, and eventually induces PCD of the bacterial cells. *Open diamonds*, Ssl2245; *gray three-quarter circles*, Sll1130; *gray three-quarter dotted circles*, molten-globule form of Sll1130.

in its surroundings and in which PCD-related orthocaspase and TA genes are physically linked (46). These examples strongly support the role of this TA system in PCD under heat and the switch between a free living planktonic unicellular lifestyle and a colonial/biofilm sessile lifestyle (29–32). We noticed clumps of the wild type cells upon incubation at high temperature, hence resembling biofilm formation, and the population seemed to undergo PCD, sacrificing a portion of the cells and letting the rest of the cells survive through the stress (Fig. 3).

For the toxin and antitoxin proteins to induce PCD, they have to separate from each other to free the toxin protein to function and kill the cells. Therefore, under heat stress, we expected the dissociation of these two proteins from each other such that the toxin Sll1130 would be free to function. This hypothesis was tested using ITC, which demonstrated that the stoichiometry of interaction decreased between Ssl2245 and Sll1130 at high temperatures (Fig. 7). Because at such high temperature most proteins are unstable, we verified the stability of the two proteins by DSC, which confirmed the thermal stability of these proteins to be quite high with unfolding temperatures above 60 °C (Fig. 7), which was well above the temperature where the decrease in association of these proteins was observed. CD spectroscopic studies revealed that Sll1130 exists predominantly in a molten globule-like structure above 40 °C, whereas the structure of Ssl2245 is essentially unaltered up to 60 °C.

One of the mechanisms by which the toxin of the TA system induces cell death is by endoribonuclease activity. Sll1130 is indeed a stable ribonuclease that degrades RNA (Fig. 9). At optimal growth temperature, Ssl2245 inhibits the ribonuclease activity of Sll1130. When cells experience high temperature, Sll1130 undergoes conformational changes, leading to the formation of the molten globule-like structure, which does not interact with Ssl2245. The free form of Sll1130 (not associated with Ssl2245) degrades cellular RNA, thus inducing PCD (Fig. 10*B*). Thus, we report for the first time a putative TA system involving heat-responsive antitoxin (MazE) and toxin (MazF) encoded by the ORFs *ssl2245* and *sll1130*, respectively, which mediate heat-induced PCD in *Synechocystis*, when cells are exposed to high temperature. In conclusion, based on the experimental evidence obtained, we have designated these two proteins, Ssl2245 and Sll1130, as MazE and MazF, respectively.

Experimental Procedures

Bacterial Strains and Culture Conditions—Synechocystis, a glucose-tolerant strain that was originally obtained from Dr. J. G. K. Williams (Dupont de Nemours, Wilmington, DE) served as the wild type. Wild type cells were grown photoautotrophically at 34 °C in a specialized cyanobacterial BG11 medium buffered with 20 mM HEPES/NaOH (pH 7.5) under continuous illumination at 70 μmol of photons/m^2/s as described previously (28). The Δ*sll1130* and Δ*ssl2245* cultures in which the *sll1130* and *ssl2245* genes were disrupted by inserting a kanamycin resistance gene cassette and Ω-spectinomycin gene cassette (Sp^R) were grown under the same conditions as described above with the exception that the culture medium

contained kanamycin at 25 μg/ml and spectinomycin at 20 μg/ml, respectively, in the precultures. Density of the cells in the culture was measured by optical density at 730 nm using a spectrophotometer (Thermo Scientific Nanodrop 2000c). For heat treatment, wild type culture was grown to midexponential phase (an absorbance of ~0.6 at 730 nm) at 34 °C and then shifted to a water bath maintained at 50 °C with continuous illumination (70 μmol of photons/m^2/s). For the viability test, wild type and Δ*sll1130* mutant cultures were grown at 34 °C to midexponential phase (~0.6 OD at 730 nm) and then incubated at 50 °C over a course of time in a water bath. Cells were harvested before and during heat treatment for the viability test.

Phylogenetic Analysis of Ssl2245 and Sll1130—Orthologs of Ssl2245 and Sll1130 were downloaded from the Kyoto Encyclopedia of Genes and Genomes (KEGG) and NCBI databases. The amino acid sequences of Ssl2245 and Sll1130 or of the respective two homologs from other bacteria were concatenated and aligned using ClustalW (47). Phylogenetic relationships were inferred by Minimum Evolution (48) as implemented in MEGA 7.0 (49). Bootstrap values were obtained through 1,000 repetitions.

Targeted Mutagenesis of ssl2245 (Δssl2245)—We generated a Δ*ssl2245* mutant by insertional inactivation of the *ssl2245* gene. A DNA fragment containing the *ssl2245* and *sll1130* ORFs was amplified by PCR using primers *ssl2245*-F (5′-ATG TCT ATC AAT GCT TAC AAA CTA GCT ACG-3′) and *sll1130*-R (5′-GCG AAG CTT ACC GAG TTT AAA AAC ATG GGG-3′). The resulting 615-bp fragment was ligated to a linear T vector (GeNei™ INSTANT Cloning kit, catalog number 107416, Bangalore Genie Pvt. Ltd., Bangalore, India) to generate pT2245-1130. Then *ssl2245* was inactivated by EcoRI digestion and blunting by T4 DNA polymerase followed by ligation with the Ω-spectinomycin cassette, yielding pT*ssl2245*::Sp^R. This construct was used to transform wild type *Synechocystis*. Developing mutant colonies were re-plated on BG11 with increasing concentrations of spectinomycin and finally maintained on BG11 plates with 20 μg/ml final concentration of spectinomycin. Genomic DNA of the Δ*ssl2245* mutant cells grown for several rounds in BG11 medium was prepared and the extent of *ssl2245* replacement by *ssl2245*::Sp^R was checked by PCR using primers *ssl2245*-F and *sll1130*-R. The mutant thus generated was named Δ*ssl2245*.Segregation analysis of this mutant by comparing the size of amplified PCR products showed that *ssl2245* gene copies were replaced by the disrupted version *ssl2245*::Sp^R after several generations of antibiotic selection pressure. When the genomic DNA of wild type cells was used as template, a PCR product of 615 bp corresponding to the uninterrupted *ssl2245-sll1130* genes was amplified (supplemental Fig. S3 in supplemental material). In contrast, when the genomic DNA of Δ*ssl2245* cells was used as template with the same set of primers, a 2698 bp DNA fragment was obtained, corresponding to the wild type fragment (615 bp) including the inserted Ω-spectinomycin gene cassette (2083 bp) (supplemental Fig. S3).

Preparation of cDNA for DNA Microarray Analysis—Fifty milliliters each of wild type, Δ*sll1130*, and Δ*ssl2245* cells grown at 70 μmol of photons/m^2/s were killed instantaneously by the addition of 50 ml of ice-cold 5% phenol in ethanol (w/v), and then total RNA was extracted as described previously in Prakash *et al.* (50). The RNA was treated with DNase I (catalog number EN0521, Thermo Fisher Scientific Inc.) to remove any contaminating DNA. The cDNA was prepared from 10 μg of total RNA and labeled using FairPlay III microarray labeling kit (catalog number 252012-5, Agilent Technologies Inc., La Jolla, CA) according to the manufacturer's instructions. For labeling cDNA, monoreactive Cy3 and Cy5 fluorescent dyes (catalog numbers PA23001 and PA25001, GE Healthcare) were used.

DNA Microarray Analysis—Genome-wide analysis of transcript levels was performed with custom made DNA microarray chips (*Synechocystis* microarray chip with 8 × 15,000 format, Agilent Technologies Inc.) that covered 3611 genes including the genes of all native plasmids of *Synechocystis*. Dye-coupled cDNA was purified using microspin columns and hybridized to the DNA microarray chip according to the manufacturer's recommendations (gene expression hybridization kit, catalog number 5188-5281, Agilent Technologies Inc.). A total of 45 μl of the hybridization mixture with Cy3- and Cy5-labeled DNA was allowed to hybridize at 65 °C for 16 h in a hybridization chamber. The chip was scanned using an Agilent Technologies Inc. microarray chip scanner (G2505B microarray scanner). Feature extraction was done using Agilent Technologies Inc. feature extraction (FE) software version 9.5.1 according to the manufacturer's protocol. The signal from each gene on the microarray was normalized by reference to the total intensity of signals from all genes, and then the change in the level of the transcript of each gene relative to the total amount of mRNA was calculated.

Quantitative Real Time PCR Analysis—RNA isolated from wild type, Δ*ssl2245*, and Δ*sll1130* cells was used for cDNA synthesis with the Affinity Script cDNA synthesis kit following the manufacturer's protocol (catalog number 600559, Agilent Technologies Inc.). qRT-PCR was carried out using the Power SYBR Green Master Mix kit (catalog number 4368708, Applied Biosystems). Each reaction was carried out in a 25-μl volume containing 12.5 μl of SYBR Green Master Mix, a 0.2 μM concentration of each of the forward and reverse primers, and 5 μl of diluted cDNA (35 ng). All reactions were run in duplicates using a qRT-PCR instrument (Mx3005P, Agilent Technologies Inc.). The instrument was programmed for 95 °C for 10 min, 40 cycles of 30 s at 95 °C, 60 s at 60 °C, and 60 s at 72 °C. For each reaction, the melting curve was analyzed to check the specific amplification of the target gene by corresponding primers. Expression levels were normalized using the *gap1* gene as an internal reference. Primers used for qRT-PCR are listed in supplemental Table S2.

Overexpression and Co-elution of Ssl2245 and Sll1130—A DNA fragment covering the *ssl2245* and *sll1130* ORFs was amplified from *Synechocystis* genomic DNA by PCR using the primer set His2245-1130-F (5′-GGA CAT ATG TCT ATC AAT GCT TAC AAA CTA GC-3′ and His2245-1130-R (5′-CTC AAG CTT CTA ACC GAG TTT AAA AAC ATG GG-3′). The amplified fragment was digested with NdeI and HindIII and then ligated to pET28a(+) vector (catalog number 69864-3, Novagen), which had also been digested with the same enzymes, to generate the HisSsl2245-Sll1130-pET28a construct. The N-terminal His_6-tagged Ssl2245 and untagged

Sll1130 proteins were transformed and expressed in the BL21(DE3) pLysS *E. coli* host strain and purified using nickel affinity gel (His60 Ni Superflow Resin, catalog number 635660, Clontech). Expression of these proteins was induced by addition of a 1 mM final concentration of isopropyl 1-thio-β-D-galactopyranoside. Bacterial cells were collected 3 h after induction by centrifugation at 10,000 rpm for 10 min at 4 °C. Cell pellets were resuspended in lysis buffer (20 mM Tris-HCl (pH 7.5), 500 mM NaCl, and 1 mM PMSF), lysed by French press thrice at a pressure of 1,000 p.s.i., and centrifuged at 10,000 rpm for 10 min at 4 °C. The supernatant was filtered through a 0.45-μm filter to remove unlysed cells and then loaded onto the nickel affinity column. The column was washed twice with 20 mM Tris-HCl (pH 7.5), 500 mM NaCl, and 40 mM imidazole, and sequentially the His-tagged Ssl2245-Sll1130 was eluted with 20 mM Tris-HCl (pH 7.5), 500 mM NaCl, and 100, 200, 300, and 400 mM imidazole, respectively. The purity of each fraction was examined by SDS gel electrophoresis. The fractions that gave a single band at the expected region on the gel were combined and dialyzed against 20 mM Tris-HCl (pH 7.5) and 150 mM NaCl.

Viability Test—Synechocystis wild type and Δ*sll1130* cells were stained with ViaGram™ Red$^+$ Bacterial Gram Stain and Viability kit according to the manufacturer's instructions (catalog number V-7023, Molecular Probes, Invitrogen). Sixty microliters of water was added to dilute 3 μl of the SYTOX Green stain. To 50 μl of the cell suspension, 2.5 μl of the diluted SYTOX Green stain was added and incubated for 15 min at room temperature (28 °C). Thereafter, 10 μl of the stained cell suspension was examined with an inverted fluorescence microscope (model 1X71, Olympus, Tokyo, Japan).

Sample Preparation for AFM—Synechocystis wild type and Δ*sll1130* cells were cultivated in liquid BG11 until an optical density at 730 nm of around 1.0 was reached. Twenty microliters of this bacterial suspension was placed onto freshly cleaved mica surface and dried in airflow for 30 min for adsorption. The samples were then imaged with a scanning probe microscope (SPA400, Seiko, Japan) using the tapping mode at a scan rate of 1–2 Hz and a resonance frequency of 110–150 kHz.

Bacterial Two-hybrid System—Constructs carrying *sll1130* and *slr1139* were cloned into plasmid pT25 following PstI and BamHI digestion. Constructs carrying *ssl2245* and *sll1130* were cloned into plasmid pT18 following XhoI and HindIII digestion. The plasmid combinations pT25-Sll1130 and pSsl2245-T18, pT25-Slr1139 and pSsl2245-T18, pT25-Slr1139 and pSll1130-T18, and positive control pT25-RhlB and pPNP-T18, respectively, were co-transformed into DHP1 to screen for protein-protein interaction as described and plated onto MacConkey agar plates (39). Color changes on the MacConkey agar due to the interactions between the proteins were monitored.

Expression and Purification of Ssl2245 and Sll1130 Proteins for Isothermal Titration Calorimetry, Ribonuclease Assays, and CD Spectroscopic Measurements—Individual pET28a constructs carrying the His-tagged *ssl2245* and *sll1130*, respectively, were generated. DNA fragment covering the *ssl2245* and *sll1130* ORFs were amplified from *Synechocystis* genomic DNA by PCR using the specific primer sets Ssl2245-Exp-FP (5′-CGG CAT ATG TCT TAT CAA TGC TTA CAA ACT AGC TAC G-3′) and Ssl2245-Exp-RP (5′-GGC AAG CTT TCA TAG GTG TCG GTA TGC CAG AAT TAT CAG C-3′) and Sll1130-Exp-FP (5′-GCA GGC ATA TGA ATA CAA TTT ACG AAC-3′) and Sll1130-Exp-RP (5′-CGT CGA ATT CCT AAC CGA GTT TAA AAA CAT GG-3′), respectively. The amplified *ssl2245* fragment was digested with NdeI and HindIII, and *sll1130* fragment was digested with NdeI and EcoRI, respectively, and then ligated to pET28a(+) vector, which had also been digested with the same enzymes, to generate the HisSsl2245-pET28a and HisSll1130-pET28a constructs, respectively. These constructs were transformed and expressed in the BL21(DE3) pLysS *E. coli* host strain and purified using nickel affinity gel (His60 Ni Superflow Resin). Expression of these proteins was induced by addition of a 1 mM final concentration of isopropyl 1-thio-β-D-galactopyranoside. Bacterial cells were collected 3 h after induction by centrifugation at 10,000 rpm for 10 min at 4 °C. Cell pellets were resuspended in lysis buffer, lysed by French press thrice at a pressure of 1,000 p.s.i., and centrifuged at 10,000 rpm for 10 min at 4 °C. The supernatant was filtered through a 0.45-μm filter to remove unlysed cells and then loaded onto the nickel affinity column. The column was washed twice with 20 mM Tris-HCl (pH 6.5), 500 mM NaCl, and 40 mM imidazole, and sequentially the His-tagged Ssl2245-Sll1130 was eluted with 20 mM Tris-HCl (pH 6.5), 500 mM NaCl, and 100, 200, 300, and 400 mM imidazole, respectively. The fractions that gave a single band at the expected region on the gel were combined and dialyzed against 20 mM Tris-HCl (pH 6.5) and 150 mM NaCl. The purified and dialyzed proteins were then concentrated using Amicon Ultra centrifugal filters with a 3-kDa cutoff. The purity of both the proteins was examined by SDS gel electrophoresis (supplemental Fig. S4). These proteins were further used for ITC experiments, ribonuclease assays, and CD spectroscopic measurements.

Isothermal Titration Calorimetric Studies—Thermodynamics governing the interaction between Ssl2245 and Sll1130 proteins was investigated by ITC measurements using a MicroCal VP-ITC instrument (MicroCal LLC, Northampton, MA) (51). The purified protein solutions were first degassed under vacuum before use in the ITC experiments. Typically, 15–25 consecutive injections of 5-μl aliquots of Ssl2245 at a concentration of 500–900 μM were added with the help of a rotator stirrer-syringe into the 1.445-ml-volume calorimeter cell filled with Sll1130 protein at a final concentration of 70–100 μM. To minimize the contribution of heat of dilution to the measured heat change, the protein solutions were prepared in the same buffer. Injections were made at intervals of 5 min for all titrations. To ensure proper mixing after each injection, a constant stirring speed of 300 rpm was maintained throughout the experiment. Control experiments were performed by injecting Ssl2245 into the buffer solution in an identical manner, and the resulting heat changes were subtracted from the measured heats of binding. Because the first injection is often inaccurate, the first data point was deleted before the remaining data were analyzed. The data obtained from these calorimetric titrations were analyzed using the one set of sites binding model available in the Origin ITC data analysis software (51, 52) supplied by the instrument manufacturer.

Differential Scanning Calorimetric Studies—The thermal stability of Ssl2245 and Sll1130 proteins was investigated by DSC studies using a MicroCal VP-DSC microcalorimeter (MicroCal LLC) equipped with fixed reference and sample cells (0.545 ml each) (53). Protein solutions were dialyzed extensively against large volumes of 20 mM Tris buffer (pH 6.5) containing 150 mM NaCl, thoroughly degassed under vacuum for 5 min at room temperature, and then carefully loaded in the calorimeter cells. DSC thermograms were recorded at a scan rate of 60 °C/h. A background scan collected with buffer in both cells was subtracted from each scan. The temperature dependence of the molar heat capacity of the protein was further analyzed using the Origin DSC analysis software supplied by the manufacturer.

Circular Dichroism Spectroscopy—Circular dichroism measurements were carried out in a Jasco-J1500 CD spectrometer at a scan rate of 50 nm/min with a 1-nm data pitch and 2-s response using a 2-mm bandwidth. Temperature was varied by means of a Peltier thermostat supplied by the manufacturer. Spectra in the far-UV region (260–190 nm) were recorded with samples taken in a 1.0-mm quartz cell, whereas for measurements in the near-UV region (320–250 nm) a 10-mm-path length cell was used. For measurements in the far-UV region, the concentrations of Sll1130 and Ssl2245 used were 10 and 8.5 μM, respectively, whereas the corresponding concentrations used for measurements in the near-UV region were 66 and 285 μM, respectively.

In Vitro Transcription and Ribonuclease Activity of the Sll1130—In vitro transcription for all RNAs was performed with the MEGAscript or MAXIscript kit (Invitrogen). PCR products containing a T7 RNA polymerase promoter sequence were used as templates, and transcription was carried out according to the manufacturer's instructions including the optional DNase treatment and phenol/chloroform extraction. Purified Sll1130 and Ssl2245 (100–250 ng of each) were incubated with 50–400 ng of target *in vitro* transcripts at 30 or 37 °C for 30–120 min in 25 mM Tris-HCl (pH 7.5), 60 mM KCl, 100 mM NH_4Cl, 5 mM $MgCl_2$, and 0.1 mM DTT, respectively. Duplex RNA formation was achieved as described previously (54) with the following modification. The reaction mixture was complemented with 25 mM Tris-HCl (pH 7.5), 60 mM KCl, 5 mM $MgCl_2$, 100 mM NH_4Cl, and 0.1 mM DTT. Purified Sll1130, Ssl224, and controls were also incubated with target transcripts at 37, 50, and 60 °C to test temperature dependence on the toxic activity-masking property of the Ssl2245. Reactions were stopped by adding 1 volume of RNA loading buffer (New England Biolabs or Fermentas). Samples were heated for 5 min at 95 °C prior to electrophoretic separation on 6–10% 7 M urea polyacrylamide gels (6 mA, 1.5–2.5 h).

Author Contributions—A. S. performed the majority of the experiments and wrote the paper. P. S. K. generated the mutant strains and performed DNA microarray experiment with Δ*sll1130*. S. K. performed ribonuclease assays. D. S. and A. S. performed ITC and DSC experiments together. M. J. S. analyzed the ITC, DSC, and CD spectroscopic results and edited the paper. S. L.-C. and W. R. H. advised on experiments and edited the paper. J. S. S. P. conceived the idea for the project and wrote the paper with A. S.

Acknowledgments—We acknowledge the Department of Biotechnology-Centre for Research and Education in Biology and Biotechnology program of the School of Life Sciences, University of Hyderabad for providing genomics facility. We acknowledge Taiwan International Graduate Program, Academia Sinica, Taiwan for the summer internship to A. S. The MicroCal VP-ITC and VP-DSC equipment used in this study were obtained from the funds made available to the University of Hyderabad through the Universities with Potential for Excellence program of the University Grants Commission (India). We acknowledge the University Grants Commission (India) for support through the Centre for Advanced Studies program to the School of Chemistry.

References

1. Claessen, D., Rozen, D. E., Kuipers, O. P., Søgaard-Andersen, L., and van Wezel, G. P. (2014) Bacterial solutions to multicellularity: a tale of biofilms, filaments and fruiting bodies. *Nat. Rev. Microbiol.* **12,** 115–124
2. Johnson, L. R. (2008) Microcolony and biofilm formation as a survival strategy for bacteria. *J. Theor. Biol.* **251,** 24–34
3. Tanouchi, Y., Lee, A. J., Meredith, H., and You, L. (2013) Programmed cell death in bacteria and implications for antibiotic therapy. *Trends Microbiol.* **21,** 265–270
4. Rice, K. C., and Bayles, K. W. (2008) Molecular control of bacterial death and lysis. *Microbiol. Mol. Biol. Rev.* **72,** 85–109
5. Maisonneuve, E., and Gerdes, K. (2014) Molecular mechanisms underlying bacterial persisters. *Cell* **157,** 539–548
6. Wen, Y., Behiels, E., and Devreese, B. (2014) Toxin-antitoxin systems: their role in persistence, biofilm formation and pathogenicity. *Pathog. Dis.* **70,** 240–249
7. Bar-Zeev, E., Avishay, I., Bidle, K. D., and Berman-Frank, I. (2013) Programmed cell death in the marine cyanobacterium *Trichodesmium* mediates carbon and nitrogen export. *ISME J.* **7,** 2340–2348
8. Berman-Frank, I., Bidle, K., Haramaty, L., and Falkowski, P. G. (2004) The demise of the marine cyanobacterium, *Trichodesmium* spp., via an autocatalyzed cell death pathway. *Limnol. Oceanogr.* **49,** 997–1005
9. Spungin, D., Pfreundt, U., Berthelot, H., Bonnet, S., Al Roumi, D., Natale, F., Hess, W. R., Bidle, K. D., and Berman-Frank, I. (2016) Mechanisms of *Trichodesmium* demise within the New Caledonia lagoon during VAHINE mesocosm experiment. *Biogeosciences* **13,** 4187–4203
10. Engelberg-Kulka, H., Amitai, S., Kolodkin-Gal, I., and Hazan, R. (2006) Bacterial programmed cell death and multicellular behavior in bacteria. *PLoS. Genet.* **2,** e135
11. Chan, W. T., Espinosa, M., and Yeo, C. C. (2016) Keeping the wolves at bay: antitoxins of prokaryotic type II toxin-antitoxin systems. *Front. Mol. Biosci.* **3,** 9
12. Schuster, C. F., and Bertram, R. (2013) Toxin-antitoxin systems are ubiquitous and versatile modulators of prokaryotic cell fate. *FEMS Microbiol. Lett.* **340,** 73–85
13. Hazan, R., Sat, B., and Engelberg-Kulka, H. (2004) *Escherichia coli* mediated mazEF-mediated cell death is triggered by various stressful conditions. *J. Bacteriol.* **186,** 3663–3669
14. Zorzini, V., Buts, L., Schrank, E., Sterckx, Y. G., Respondek, M., Engelberg-Kulka, H., Loris, R., Zangger, K., and van Nuland, N. A. (2015) *Escherichia coli* antitoxin MazE as transcription factor: insights into MazE-DNA binding. *Nucleic Acids Res.* **43,** 1241–1256
15. Christensen, S. K., Mikkelsen, M., Pedersen, K., and Gerdes, K. (2001) RelE, a global inhibitor of translation, is activated during nutritional stress. *Proc. Natl. Acad. Sci. U.S.A.* **98,** 14328–14333
16. Gotfredsen, M., and Gerdes, K. (1998) The *E. coli* relBE genes belong to a new toxin-antitoxin gene family. *Mol. Microbiol.* **29,** 1065–1076
17. Masuda, Y., Miyakawa, K., Nishimura, Y., and Ohtsubo, E. (1993) *chpA* and *chpB*, *Escherichia coli* chromosomal homologs of the *pem* locus responsible for stable maintenance of plasmid R100. *J. Bacteriol.* **175,** 6850–6856

18. Grady, R., and Hayes, F. (2003) Axe-Txe, a broad-spectrum protein toxin-antitoxin system specified by a multidrug-resistant, clinical isolate of *Enterococcus faecium*. *Mol. Microbiol.* **47,** 1419–1432
19. Hayes, F. (2003) Toxins-antitoxins: plasmid maintenance, programmed cell death, and cell cycle arrest. *Science* **301,** 1496–1499
20. Sat, B., Hazan, R., Fisher, T., Khaner, H., Glaser, G., and Engelberg-Kulka, H. (2001) Programmed cell death in *Escherichia coli*: some antibiotics can trigger mazEF lethality. *J. Bacteriol.* **183,** 2041–2045
21. Allocati, N., Masulli, M., Di Ilio, C., and De Laurenzi, V. (2015) Die for the community: an overview of programmed cell death in bacteria. *Cell Death Dis.* **6,** e1609
22. Ogura, T., and Hiraga, S. (1983) Partition mechanism of F plasmid: two plasmid gene-encoded products and a cis-acting region are involved in partition. *Cell* **32,** 351–360
23. Lewis, K. (2008) Multidrug tolerance of biofilms and persister cells. *Curr. Top. Microbiol. Immunol.* **322,** 107–131
24. Hazan, R., and Engelberg-Kulka, H. (2004) *Escherichia coli* mazEF-mediated cell death as a defense mechanism that inhibits the spread of phage P1. *Mol. Genet. Genomics.* **272,** 227–234
25. Soo, V. W., and Wood, T. K. (2013) Antitoxin MqsA represses curli formation through the master biofilm regulator CsgD. *Sci. Rep.* **3,** 3186
26. Hu, Y., Benedik, M. J., and Wood, T. K. (2012) Antitoxin DinJ influences the general stress response through transcript stabilizer CspE. *Environ. Microbiol.* **14,** 669–679
27. Kim, Y., Wang, X., Zhang, X. S., Grigoriu, S., Page, R., Peti, W., and Wood, T. K. (2010) *Escherichia coli* toxin/antitoxin pair MqsR/MqsA regulate toxin CspD. *Environ. Microbiol.* **12,** 1105–1121
28. Krishna, P. S., Rani, B. R., Mohan, M. K., Suzuki, I., Shivaji, S., and Prakash, J. S. (2013) A novel transcriptional regulator, Sll1130, negatively regulates heat-responsive genes in *Synechocystis* sp. PCC 6803. *Biochem. J.* **449,** 751–760
29. Foster, J. S., Green, S. J., Ahrendt, S. R., Golubic, S., Reid, R. P., Hetherington, K. L., and Bebout, L. (2009) Molecular and morphological characterization of cyanobacterial diversity in the stromatolites of Highbone Cay, Bahamas. *ISME. J.* **3,** 573–587
30. Pandey, V. D. (2013) Rock-dwelling cyanobacteria: survival strategies and biodeterioration of monuments. *Int. J. Curr. Microbiol. Appl. Sci.* **2,** 519–524
31. Walsby, A. E., Van Rijin, J., and Cohen, Y. (1983) The biology of new gas-vacuolate cyanobacterium, *Dactylococcopsis salina* sp.nov., in Solar Lake. *Proc. R. Soc. Lond. B Biol. Sci.* **217,** 417–447
32. Sabart, M., Misson, B., Descroix, A., Duffaud, E., Combourieu, B., Salençon, M. J., and Latour, D. (2013) The importance of small colonies in sustaining *Microcystis* population exposed to mixing conditions: an exploration through colony size, genotypic composition and toxic potential. *Environ. Microbiol. Rep.* **5,** 747–756
33. Kopf, M., Klähn, S., Scholz, I., Matthiessen, J. K., Hess, W. R., and Voß, B. (2014) Comparative analysis of the primary transcriptome of *Synechocystis* sp. PCC6803. *DNA Res.* **21,** 527–539
34. Pandey, D. P., and Gerdes, K. (2005) Toxin-antitoxin loci are highly abundant in free-living but lost from host-associated prokaryotes. *Nucleic Acids Res.* **33,** 966–976
35. Scholz, I., Lange, S. J., Hein, S., Hess, W. R., and Backofen, R. (2013) CRISPR-Cas systems in the cyanobacterium *Synechocystis* sp. PCC6803 exhibit distinct processing pathways involving at least two Cas6 and a Cmr2 protein. *PLoS One* **8,** e56470
36. Makarova, K. S., Wolf, Y. I., Alkhnbashi, O. S., Costa, F., Shah, S. A., Saunders, S. J., Barrangou, R., Brouns, S. J., Charpentier, E., Haft, D. H., Horvath, P., Moineau, S., Mojica, F. J., Terns, R. M., Terns, M. P., *et al.* (2015) An updated evolutionary classification of CRISPR-Cas systems. *Nat. Rev. Microbiol.* **13,** 722–736
37. Kopfmann, S., and Hess, W. R. (2013) Toxin-antitoxin systems on the large defense plasmid pSYSA of *Synechocystis* sp. PCC 6803. *J. Biol. Chem.* **288,** 7399–7409
38. Westra, E. R., Pul, U., Heidrich, N., Jore, M. M., Lundgren, M., Stratmann, T., Wurm, R., Raine, A., Mescher, M., Van Heereveld, L., Mastop, M., Wagner, E. G., Schnetz, K., Van Der Oost, J., Wagner, R., *et al.* (2010) H-NS-mediated repression of CRISPR-based immunity in *Escherichia coli* K12 can be relieved by the transcription activator LeuO. *Mol. Microbiol.* **77,** 1380–1393
39. Karimova, G., Pidoux, J., Ullmann, A., and Ladant, D. (1998) A bacterial two-hybrid system based on a reconstituted signal transduction pathway. *Proc. Natl. Acad. Sci. U.S.A.* **95**, 5752–5756
40. Hosoya-Matsuda, N., Motohashi, K., Yoshimura, H., Nozaki, A., Inoue, K., Ohmori, M., and Hisabori, T. (2005) Anti-oxidative stress system in cyanobacteria: significance of type II peroxiredoxin and the role of 1-Cys peroxiredoxin in *Synechocystis* sp. PCC 6803. *J. Biol. Chem.* **280,** 840–846
41. Tseng, Y. T., Chiou, N. T., Gogiraju, R., and Lin-Chao, S. (2015) The protein interaction of RNA helicase B (RhlB) and polynucleotide phosphorylase (PNPase) contributes to the homeostatic control of cysteine in *Escherichia coli*. *J. Biol. Chem.* **290,** 29953–29963
42. Arai, M., and Kuwajima, K. (2000) Role of the molten globule state in protein folding. *Adv. Protein Chem.* **53,** 209–282
43. Polverino de Laureto, P., Frare, E., Gottardo, R., and Fontana, A. (2002) Molten globule of α-lactalbumin at neutral pH induced by heat, trifluoroethanol, and oleic acid: a comparative analysis by circular dichroism spectroscopy and limited proteolysis. *Proteins* **49,** 385–397
44. Ning, D., Ye, S., Liu, B., and Chang, J. (2011) The proteolytic activation of the relNEs (ssr1114/slr0664) toxin-antitoxin system by both proteases Lons and Clp2s/Xs of *Synechocystis* sp. PCC 6803. *Curr. Microbiol.* **63,** 496–502
45. Hu, M. X., Zhang, X., Li, E. L., and Feng, Y. J. (2010) Recent advancements in toxin and antitoxin systems involved in bacterial programmed cell death. *Int. J. Microbiol.* **2010,** 781430
46. Klemenčič, M., and Dolinar, M. (2016) Orthocaspase and toxin-antitoxin loci rubbing shoulders in the genome of *Microcystis aeruginosa* PCC 7806. *Curr. Genet.* **62,** 669–675
47. Chenna, R., Sugawara, H., Koike, T., Lopez, R., Gibson, T. J., Higgins, D. G., and Thompson, J. D. (2003) Multiples sequence alignment with the Clustal series of programs. *Nucleic Acids Res.* **31,** 3497–3500
48. Rzhetsky, A., and Nei, M. (1992) A simple method for estimating and testing minimum evolution trees. *Mol. Biol. Evol.* **9,** 945–967
49. Kumar, S., Stecher, G., and Tamura, K. (2016) MEGA7: Molecular Evolutionary Genetics Analysis version 7.0 for bigger datasets. *Mol. Biol. Evol.* **33,** 1870–1874
50. Prakash, J. S., Krishna, P. S., Sirisha, K., Kanesaki, Y., Suzuki, I., Shivaji, S., and Murata, N. (2010) An RNA helicase, CrhR, regulated the low-temperature-inducible expression of heat-shock genes *groES*, *groEL1* and *groEL2* in *Synechocystis* sp. PCC 6803. *Microbiology* **156,** 442–451
51. Narahari, A., Singla, H., Nareddy, P. K., Bulusu, G., Surolia, A., and Swamy, M. J. (2011) Isothermal titration calorimetric and computational studies on the binding of chitooligosaccharides to pumpkin (*Cucurbita maxima*) phloem exudate lectin. *J. Phys. Chem. B* **115,** 4110–4117
52. Wiseman, T., Williston, S., Brandts, J. F., and Lin, L. N. (1989) Rapid measurement of binding constants and heats of binding using a new titration calorimeter. *Anal. Biochem.* **179,** 131–137
53. Kavitha, M., Bobbili, K. B., and Swamy, M. J. (2010) Differential scanning calorimetric and spectroscopic studies on the unfolding of *Momordica charantia* lectin. Similar modes of thermal and chemical denaturation. *Biochimie* **92,** 58–64
54. Stazic, D., Lindell, D., and Steglich, C. (2011) Antisense RNA protects mRNA from RNase E degradation by RNA-RNA duplex formation during phage infection. *Nucleic Acids Res.* **39,** 4890–4899

Investigations on the mechanism of heat-induced programmed cell death mediated by a MazE-MazF like type II toxin-antitoxin system in the cyanobacterium, Synechocystis sp. PCC 6803

by Afshan Srikumar

Submission date: 28-Jun-2019 10:42AM (UTC+0530)
Submission ID: 1147645344
File name: Afshan_thesis_27-6-19-plagiarism.pdf (4.62M)
Word count: 24145
Character count: 121427

Investigations on the mechanism of heat-induced programmed cell death mediated by a MazE-MazF like type II toxin-antitoxin system in the cyanobacterium, Synechocystis sp. PCC 6803

ORIGINALITY REPORT

29%	25%	28%	8%
SIMILARITY INDEX	INTERNET SOURCES	PUBLICATIONS	STUDENT PAPERS

PRIMARY SOURCES

1	www.jbc.org Internet Source	21%
2	www.biochemj.org Internet Source	1%
3	Afshan Srikumar, Pilla Sankara Krishna, Dokku Sivaramakrishna, Stefan Kopfmann et al. " The Ssl2245-Sll1130 Toxin-Antitoxin System Mediates Heat-induced Programmed Cell Death in sp. PCC6803 ", Journal of Biological Chemistry, 2017 Publication	1%
4	genome.annotation.jp Internet Source	<1%
5	J. S. S. Prakash. "An RNA helicase, CrhR, regulates the low-temperature-inducible expression of three genes for molecular chaperones in Synechocystis sp. PCC 6803",	<1%